# NASA Technical Memorandum 78818

NASA-TM-78818 19790015717

# CHARACTERISTICS OF THE ADVANCED SUPERSONIC TECHNOLOGY AST-105-1 CONFIGURED FOR TRANSPACIFIC RANGE WITH PRATT AND WHITNEY AIRCRAFT VARIABLE STREAM CONTROL ENGINES



HAL T. BABER, JR.



MARCH 1979

NASA
National Aeronautics and
Space Administration

**Langley Research Center**
Hampton, Virginia 23665

# CHARACTERISTICS OF THE ADVANCED SUPERSONIC TECHNOLOGY AST-105-1 CONFIGURED FOR TRANSPACIFIC RANGE WITH PRATT AND WHITNEY AIRCRAFT VARIABLE STREAM CONTROL ENGINES

Hal T. Baber, Jr.
NASA Langley Research Center
Hampton, Virginia 23665

## SUMMARY

The AST-105-1, a new Advanced Supersonic Technology configuration, is defined by application of: an expanded aerodynamic data base; a recently developed aircraft sizing and performance computer program; a new noise prediction program; and a new engine concept by Pratt and Whitney Aircraft. This engine concept has the potential for noise reduction, which is provided by a dual (primary and secondary) exhaust stream through a coannular nozzle.

Range of the AST-105-1, cruising at Mach number 2.62 (hot day), is essentially transpacific with 273 passengers. Aerodynamic efficiency (in cruise) as measured by lift-to-drag ratio, is slightly higher for the present configuration than for previous AST configurations; about four percent higher, at the start of cruise, than the last transatlantic-range AST concept.

The aircraft can be trimmed over a center-of-gravity range from 42.55 to 60.10 percent of the reference mean aerodynamic chord or 4.7m (15.5 ft.). Due to inherently high positive effective dihedral of arrow-wing configurations in high-lift approach, the AST-105-1 operating crosswind limit would be 11.6 m/sec (22.4 kt) with application of 75 percent of available lateral control. Crosswind landing gear would permit operation in crosswinds of greater magnitude. An increase in roll control power to meet lateral trim requirements would also improve lateral response as measured by Pilot Rating.

Noise from normal power takeoff with cutback, although in excess of the Federal Aviation Regulation Part 36 limit, is less than for conventional (without power cutback) takeoff procedure. Results from preliminary studies of advanced (noncertificated) programmed throttle takeoff and approach operating procedures, not yet optimized, indicate that such can be an important additional method of noise reduction.

## INTRODUCTION

The Langley Research Center has, since 1972, been actively engaged in, and contractually supporting, work in advanced supersonic technology for potential

application to future U.S. transport aircraft. Technology advances since 1972 have prompted several advanced supersonic technology (AST) vehicle integration studies, for example references 1 and 2.

Subsequent to these studies, a number of significant advances have occurred. These are: (1) development of an expanded data base for aerodynamic concerns such as low-speed trim, longitudinal stability and control (ref. 3) and lateral-directional stability and control (ref. 4) for a low aspect ratio wing configuration; (2) development of an aircraft sizing and performance program (ref. 5), an unpublished Langley takeoff performance program, and a noise prediction program (ref. 6); and, (3) a new engine concept by Pratt and Whitney Aircraft, which is a duct burning turbofan variable stream control engine. This engine has the potential of lower noise operation than conventional turbojets with the improvement attributed to coannular nozzle noise relief.

The objective of the study reported herein was to apply this new technology to the conceptual design of an AST transport for transpacific range comparable to a San Francisco-Tokyo flight and then subject the concept to the latest analytical techniques for performance, noise, and economic evaluations. In addition, this detailed systems integration study supports a recent Langley noise sensitivity tradeoff study by giving: (1) credence to the systems weights used therein; (2) assurance that the noise study AST concept could be balanced, and (3) hence, confidence that the noise study was based on a reasonable AST aircraft concept.

Basic criteria for the study were as follows:

- Five abreast seating of 273 passengers, all tourist class with seat pitch of 0.864 m (34 in.)
- Standard day cruise at M = 2.7
- Range of 8334 km (4500 n.mi.) on a standard day + $8^{o}C$* at M = 2.62
- Engine sized to meet the design takeoff thrust-to-weight ratio
- Land on existing runways with tire footprint no greater than that of DC-8-50
- Stability and control - More detail can be found in the appropriate section, but generally stated the criteria were:
  - Configuration to be trimmed, for minimum trim drag, throughout the flight envelope
  - No significant pitch-up in the takeoff or landing modes
  - Satisfactory short-period characteristics at approach speed

* Hot day as used herein is a so-called "simple hot day." That is, the temperature at any altitude as found in the U.S. Standard Atmosphere, 1962 tables

is increased by the hot day increment ($8^{o}C$ for mission analysis and $10^{o}C$ for noise analysis) and the speed of sound is calculated for the increased temperature, whereas other state variables are assumed to be the same as for a standard day.

## SYMBOLS

Computations in the course of this study were performed in U.S. Customary (English) Units. Results were converted to the International System of Units (SI) by using conversion factors given in reference 7 and are presented in this report along with the Customary Units.

| | |
|---|---|
| AR | wing reference aspect ratio |
| ac | aerodynamic center, percent $\bar{c}_{ref}$ |
| $a_y$ | lateral acceleration, g units |
| b | wing span, m (ft) |
| $\bar{c}_{ref}$ | reference mean aerodynamic chord, m (ft) |
| $C_D$ | drag coefficient, $\frac{\text{Drag}}{q\ S_{ref}}$ |
| $C_{D_{min}}$ | minimum drag coefficient |
| $C_{D_o}$ | drag coefficient at zero lift |
| $C_{D_{po}}$ | profile drag coefficient associated with camber, proturbances, interference, and separated flow |
| CG, c.g. | center-of-gravity |
| $C_L$ | lift coefficient, $\frac{\text{Lift}}{q\ S_{ref}}$ |
| $C_{L_\alpha}$ | lift curve slope per unit angle of attack, per radian |
| $C_l$ | rolling moment coefficient, $\frac{\text{Rolling Moment}}{q\ S_{ref}\ b}$ |
| $C_{l_\beta}$ | dihedral effect derivative, $deg^{-1}$ |
| $C_{l_{\delta_a}}$ | aileron control power derivative, $deg^{-1}$ |
| $C_{l_{\delta_r}}$ | rolling moment coefficient due to rudder deflection cross derivative, $deg^{-1}$ |
| $C_{l_{fl_i}}$ | inboard flaperon power derivative, $deg^{-1}$ |

$C_{l_{fl_o}}$ outboard flaperon power derivative, $deg^{-1}$

$C_{l_p}$ damping in roll derivative, $rad^{-1}$

$C_{l_r}$ rolling moment coefficient due to yawing cross derivative, $rad^{-1}$

$C_{m_{\dot{\alpha}}}$ rate of change of pitching moment coefficient with rate of change of angle of attack with respect to nondimensional time, $rad^{-1}$

$C_{m_q}$ damping in pitch derivative, $rad^{-1}$

$C_n$ yawing moment coefficient

$C_{n_\beta}$ static directional stability derivative, $deg^{-1}$ (or $rad^{-1}$ in fig. 30)

$C_{n_{\delta a}}$ yawing moment coefficient due to aileron deflection cross derivative, $deg^{-1}$

$C_{n_{\delta r}}$ rudder control power derivative, $deg^{-1}$

$C_{n_p}$ yawing moment coefficient due to rolling cross derivative, $rad^{-1}$

$C_{n_r}$ damping in yaw derivative, $rad^{-1}$

$C_{n_{fl_i}}$ rate of change of yawing moment coefficient with inboard flaperon deflection, $deg^{-1}$

$C_{n_{fl_o}}$ rate of change of yawing moment coefficient with outboard flaperon deflection, $deg^{-1}$

$C_{Y_\beta}$ side force derivative, $deg^{-1}$ (or $rad^{-1}$ in fig. 30)

$C_{Y_{\delta a}}$ side force coefficient due to aileron deflection cross derivative, $deg^{-1}$

$C_{Y_{\delta r}}$ rudder side force derivative, $deg^{-1}$

$C_{Y_{fl_i}}$ rate of change of side force coefficient with inboard flaperon deflection, $deg^{-1}$

$C_{Y_{fl_o}}$ rate of change of side force coefficient with inboard flaperon deflection, $deg^{-1}$

$C_{Y_p}$ side force coefficient due to roll rate cross derivative, $rad^{-1}$

$C_{Y_r}$ side force coefficient due to yaw rate derivative, $rad^{-1}$

DGW Design Gross Weight, Newton (pounds)

| | |
|---|---|
| dB | decibel |
| EAS | equivalent airspeed, m/sec (knots) |
| $F_n$ | net engine thrust - N (lbf) |
| g | acceleration due to gravity, meters/sec$^2$ (ft/sec$^2$) |
| HP | horsepower |
| h | height of center-of-gravity above ground |
| $I_X$, $I_Y$, $I_Z$ | moments of inertia about X, Y, and Z body axes, respectively, kilogram-meters$^2$ (slug-ft$^2$) |
| $I_{XZ}$ | product of inertia, kilogram-meters$^2$ (slug-ft$^2$) |
| $K_1$ | directional control flexibility factor |
| kw | kilowatts |
| $L_{1,2,6}$ | wing leading-edge flap designations |
| $L_\alpha$ | lift per unit angle of attack per unit of momentum, $\frac{1}{mV}\left(\frac{\partial C_L}{\partial \alpha}\right)$ per second |
| LRC | Langley Research Center |
| $l_t$ | distance from wing $.25\bar{c}_{ref}$ to horizontal tail $.25\bar{c}$ (mean aerodynamic chord), m (ft) |
| M | Mach number |
| N | Newtons |
| $n/\alpha$ | incremental load-factor per unit angle of attack |
| OGE | out of ground effect |
| P | period of longitudinal short period oscillation, sec |
| $P_d$ | period of Dutch roll oscillation, sec |
| RAH | roll attitude hold mode on |
| $\overline{\text{RAH}}$ | roll attitude hold mode off |
| PR | pilot rating |
| PSP | polar shape parameter |

| | |
|---|---|
| $q$ | dynamic pressure, Pa ($lbf/ft^2$) |
| SFC | specific fuel consumption, kg/hr/N (lb/hr/lb) |
| $S_{ref}$ | wing reference area, $m^2$ ($ft^2$) |
| $S_{an}$ | static normal acceleration gust sensitivity, g/(m/sec) (g/ft/sec) |
| STW | structural weight, N (lbf) |
| s | wing leading edge suction |
| TOGW | takeoff gross weight, N (lbf) |
| T/W | thrust/weight ratio |
| t/c | wing thickness to chord ratio, percent |
| $t_{1,2,3,4}$ | wing trailing edge flap designations (see fig. 3) |
| $t_2$ | time to double amplitude, sec |
| $t_{1/2}$ | time to damp to one-half amplitude, sec |
| $t_{\phi = 30^o}$ | time required to roll $30^o$, sec |
| V | airspeed, m/sec (ft/sec) |
| $\bar{V}$ | horizontal tail volume coefficient, based on $S_{ref}$ and $l_t$ as defined herein |
| W | airplane weight, N (lbf) |
| Wa | engine airflow kg/sec (lbm/sec) |
| WAT2 | corrected compressor inlet airflow WA $\sqrt{\theta_{t2}/\delta_{t2}}$ ~ kg/sec (lbm/sec) |
| WE | weight empty, N (lbf) |
| $\bar{x}$ | longitudinal distance from the airplane center-of-gravity to the pilot station, m (ft) |
| $\bar{z}$ | vertical distance from the airplane center-of-gravity to the pilot station, positive when below center-of-gravity, m (ft) |
| ZFW | zero fuel weight, N (lbf) |
| WL | wings leveler mode on |
| $\overline{WL}$ | wings leveler mode off |

$\alpha_{wrp}$ angle of attack of wing reference plane, deg.

$\alpha_0$ angle of attack for zero lift relative to wing reference plane

$\beta$ angle of sideslip, deg.

$\Delta$ increment

$\delta$ ratio of local pressure to sea level standard pressure

$\delta_a$ aileron deflection, positive for right roll command, deg.

$\delta_c$ control-column deflection, positive for pull force, deg.

$\delta_f$ flap deflection, deg.

$\delta_{fl_i}=fl_i$ inboard flaperon deflection, deg.

$\delta_{fl_o}=fl_o$ outboard flaperon deflection, deg.

$\delta_r$ rudder deflection, deg.

$\delta_t$ horizontal-tail deflection, positive when leading-edge is deflected up, deg.

$\zeta_d$ Dutch roll damping ratio

$\zeta_{SP}$ longitudinal short period damping ratio

$\zeta_\phi$ damping ratio of numerator quadratic of $\phi/\delta_a$ transfer function

$\theta$ pitch angle, deg.

$\dot{\theta}$ pitch rate, deg/sec

$\ddot{\theta}$ pitch acceleration, rad/sec$^2$

$\phi$ roll angle, deg.

$\dot{\phi}$ roll rate, deg/sec

$\dot{\phi}_1, \dot{\phi}_2$ rolling angular velocities at the first and second peaks of a roll rate oscillation, deg/sec

$\ddot{\phi}$ roll acceleration, rad/sec$^2$

$\psi$ yaw angle, deg.

$\psi_\beta$ phase angle expressed as a lag for a cosine representation of the Dutch roll oscillation in sideslip, deg.

| | |
|---|---|
| $\dot{\psi}$ | yaw rate, deg/sec |
| $\ddot{\psi}$ | yaw acceleration, rad/sec$^2$ |
| $\rho$ | air density, kilograms/meter$^3$ (slugs/ft$^3$) |
| $\tau_R$ | time constant of roll mode, sec |
| $\omega_d$ | undamped natural frequency of Dutch roll mode, rad/sec |
| $\omega_{SP}$ | longitudinal short-period undamped natural frequency, $\frac{2\pi}{P}$, rad/sec |
| $\omega_\phi$ | undamped natural frequency appearing in numerator quadratic of $\phi/\delta_a$ transfer function, rad/sec |

Subscripts:

| | |
|---|---|
| app | approach |
| av | average |
| b | baseline |
| CG | center-of-gravity |
| f | friction |
| fm | form |
| gi | gaps and irregulataries |
| LG | landing gear |
| max | maximum |
| min | minimum |
| osc | oscillation |
| P.S. | pilot station |
| r | required (in PROPULSION Section), or roughness (in LOW-SPEED AERODYNAMICS Section) |
| ss | steady state |
| sym | symmetrical (untwisted and uncambered wing) |
| 1 | entrance to engine inlet |
| 2 | entrance to fan inlet |

## CONFIGURATION DEVELOPMENT

Since publication of the AST-100 configuration study, (ref. 2), additional low speed wind tunnel testing and design analyses have been conducted. Results of these tests and analyses along with improvements in engine technology have prompted the development of an improved configuration concept. This new configuration is designated AST-105-1.

The arrow-wing planform of the AST-100 has been retained. However, it has been adjusted for the AST-105-1 wing loading of 3.926 kPa (82 psf) at a design point gross weight of 3.051 MN (686,000 lbf) (see MISSION ANALYSIS). A plot of wing thickness distribution as a function of semispan is shown in figure 1. A thickness map of the selected wing configuration is shown in figure 2. Wing control surfaces are essentially the same as those the the AST-100 with the exception that the outboard leading-edge flap ($L_6$ in fig. 3) is a Krueger instead of a plain flap. These are also adjusted due to reduced wing area and are shown in figure 3. The outboard trailing edge flap, $t_3$, is used for additional roll control and the spoiler slot deflector of the AST-100 has been deleted.

General arrangement and inboard profile are presented in figures 4 and 5. Geometric characteristics are given in table I. Fuselage length is 92.96 m (305 ft) with provisions for 273 passengers seated five abreast with a seat pitch of 0.86 m (34 in). Passenger baggage and cargo volume is provided under the floor forward of the wing structural box. In previous configuration studies, all mission fuel was carried in the wing with the exception of the combined reserve/balance tank located in the fuselage aft of the wing. For the AST-105-1, two fuel tanks were added in the center wing section below the cabin floor. This permits additional fuel capacity for extended range with reduced payload. Figure 6 shows the fuel tank arrangement and capacity. The latter should not be taken as synonymous with mission fuel plus reserves requirements.

Nacelles for the Pratt and Whitney Aircraft VSCE-516 duct burning turbofan engines are located under the wing in essentially the same positions as for the AST-100 with the small differences attributable to the reduction in AST-105-1 wing dimensions. Nacelle shape is based on that developed by The Boeing Company (ref. 8) for the Pratt and Whitney Aircraft VSCE-502 engine and was scaled for the Pratt and Whitney Aircraft VSCE-516 engine as sized for AST-105-1 mission requirements (see PROPULSION).

The main landing gear, which retracts forward into the wing, is a two strut arrangement with 12 wheels per strut. Tires were sized at 0.80 m x 0.28 m (31.5 in x11 in) with the appropriate ply rating to satisfy the equivalent single wheel (0.41 m (16 in) dia)) load and the flotation criteria for landing on a runway of 0.61 m (24 in) flexible pavement with a subsoil California Bearing Ratio (CBR) of 15. Strut location provides for a 13° flare angle from the static ground line and a 14.5° flare angle with the gear fully extended. These flare angles provide nominal clearance on the order of 0.305 m (1 ft) for the nacelle, wing tip, and horizontal tail (whichever is at the minimum) in the normal landing attitude at an acceptable sink rate. Wing tip deflection could, however, negate these clearances depending upon landing sink rate and combined roll and flare angles. Additional study is needed to evaluate wing stiffness

combined with operational approach conditions to determine their effect on wing tip deflection, clearances, and consequently, required landing gear length.

The nose gear is a single strut, two wheel arrangement that retracts aft into the fusleage. Tire size is 0.69 m x 0.19 m (27 in x 7.5 in) with the required ply rating to comply with loading and flotation requirements.

A Mach number 1.0 area distribution curve of the AST-105-1 showing the volume utilization of the aircraft by subsystem is presented in figure 7.

## LOW-SPEED AERODYNAMICS

The low-speed aerodynamics presented in this report are based on (1) wind-tunnel test determined lift and drag increments attributable to high-lift devices (ref. 3); (2) a new technique for determining full-scale drag polar shape, and (3) conventional methods for estimating minimum drag.

Previous low-speed aerodynamic analyses corrected wind-tunnel model measured leading edge suction values to full scale through the use of unpublished test results from the NASA-Ames Research Center 12-foot Pressure Tunnel. Since, at present, these data remain unpublished, a different approach, based primarily on low speed test results (ref. 3) obtained with a large scale model of a supersonic cruise transport concept, was taken in determining full scale drag polars. Details of the methods used for development of the AST-105-1 low speed aerodynamic characteristics are given in the following paragraphs.

### Methods

To determine the effect of Reynolds number on leading-edge suction, data from four wind tunnel runs at different tunnel wind speeds (dynamic pressures, (ref. 3)), were analyzed. Leading edge suction is algebraically defined as,

$$s = \frac{C_L \tan \alpha' \, (C_D - C_{D_{sym}})}{C_L \tan \alpha' - C_L^2/\pi AR}$$

where $\alpha' = \alpha - \alpha_o$ (see SYMBOLS) and $C_{D_{sym}}$ in this instance was taken as the basic configuration $C_{Dmin}$ with nondeflected high-lift devices and without the horizontal tail. Wind tunnel test determined values of $C_{D_{min}}$ used to calculate leading-edge suction are tabulated as follows (values in English units rounded to nearest whole number):

| Tunnel operating dynamic pressure, Pa (lbf/ft$^2$) | 143.64 (3.) | 335.16 (7.) | 526.68 (11.) | 1244.89 (26.) |
|---|---|---|---|---|
| $C_{D_{min}}$, basic configuration without horizontal tail | .0198 | .0185 | .0180 | .0175 |

Plots of s as a function of $C_L$ were made for the various tunnel operating conditions. The computed values of s presented in figure 8 clearly show that leading-edge suction is a function of both lift coefficient and tunnel dynamic pressure, and hence of Reynolds number. Further, it shows that at a given lift coefficient, the value of leading-edge suction for this configuration becomes a maximum at and above a dynamic pressure of approximatley 526.68 Pa (11 lb/ft$^2$). All aerodynamic performance computations were, therefore, based on tunnnel data recorded at a nominal dynamic pressure of 526.68 Pa (11 lbf/ft$^2$).

A method, which defines the drag polar shape as calculated about the minimum drag level, was used to relate wind-tunnel results to full scale. The polar shape parameter (PSP) is defined as follows:

$$PSP = \frac{C_L' \tan \alpha' - (C_D - C_{D_{min}})}{C_L' \tan \alpha' - (C_L)^2/\pi AR}$$

where $C_L' = C_L - \Delta C_L$. The $\Delta C_L$ term is the polar offset due to camber effect. The effect of high-lift devices on the measured value of PSP is shown on figure 9 as a function of $C_L'$ from the data of reference 3. To determine full-scale configuration drag the following relationship, obtained by algebraic rearrangement and substitution, was used:

$$(C_D - C_{D_{min}})_{full\text{-}scale} = (1 - PSP)\ \Delta C_D + (C_L')^2/\pi AR,$$

where $\Delta C_D$ is equivalent to $C_L' \tan \alpha' - (C_L')^2/\pi AR$ with $C_L'$ and $\alpha'$ being determined from test data (ref. 3). Full-scale friction, form, roughness, gaps, and irregularities and trim drag estimates were added to the value for $(C_D - C_{D_{min}})_{fullscale}$.

Full-scale friction drag was estimated by the use of the NASA T' method (ref. 9). Friction drag was computed by representing various configuration components by appropriate wetted areas and reference lengths. Components such as wing and tails, with significant variations in reference lengths, were subdivided into several strips for improved accuracy of friction drag estimates. Assumed conditions were smooth flat plate, and turbulent boundary layer with transition fixed at the leading edge of each component. Reynolds number computations required for skin friction drag estimates were based on a free stream Mach number of 0.3 at sea level since the aerodynamics in this section are applicable to the takeoff and approach flight modes, which are at low Mach number and are assumed to be at low elevation.

Form drag was computed for each component by multiplying the flat plate friction drag level of the component by the respective form factor. These form factors, which are a function of thickness-to-chord ratio for lifting surfaces and fineness ratio for bodies, are assumed for the AST-105-1 as follows:

| Component: | Wing | Wing Fins | Vertical Tail | Horizontal Tail | Fuselage | Nacelles |
|---|---|---|---|---|---|---|
| Form Factor: | 1.0375 | 1.0451 | 1.0451 | 1.0451 | 1.0198 | 1.0148 |

Roughness drag was accounted for by a three-percent increase in friction drag with an additional five-percent assumed for gaps and irregularities.

Trim drag was obtained from wind tunnel test results of reference 3 corrected to account for horizontal tail size and wing reference area differences.

Lift and drag displacements of the drag polars attributable to the high-lift devices were also taken from reference 3 as increments from the basic (without horizontal tail) configuration test data. These increments are as follows:

$$L_{1,2} = 30^{o},\ L_6 = 45^{o};\ t_3 = t_4 = 5^{o}$$

| $t_1 = t_2$, deg | 0 | 10 | 20 | 30 |
|---|---|---|---|---|
| $\Delta C_L$ | .0730 | .0853 | .1000 | .1166 |
| $\Delta C_{Dmin}$ | .0066 | .0110 | .0178 | .0268 |
| $\Delta C_{D_o}$ | .0087 | .0145 | .0226 | .0339 |

The landing gear drag increments, which were previously estimated for the configuration of reference 10, were adjusted to account for a 25.4 cm (10 in) increase in main gear strut length. These increments of $C_D$ are presented in figure 10 as a function of lift coefficient.

Equations for modification of out-of-ground effect $C_L$ and $C_D$ to obtain in-ground-effect coefficients were taken from reference 1. The computing procedure for the AST-105-1, which was internal to the unpublished Langley computer program for takeoff performance, was tailored to yield maximum ground effect at takeoff and linearly diminish, with increasing altitude, to zero at a point in initial climb where the altitude-to-wing span ratio, h/b, equals unity.

## Lift and Drag

Results from application of the methods just described in preceding paragraphs to estimation of drag from sources which contribute to the minimum drag buildup are as follows:

| $C_{D_f}$ | $C_{D_{fm}}$ | $C_{D_r}$ | $C_{D_{gi}}$ | $C_{D_{min}}$ |
|---|---|---|---|---|
| 0.00639 | 0.00020 | 0.00019 | 0.00032 | 0.00710 |

Lift and drag coefficients, with the aircraft trimmed at the aft center-of-gravity limit of 0.6010 $\bar{c}_{ref}$, are presented in table II as a function of angle of attack and flap deflection. Trimmed lift curves and lift drag polars, out-of-ground effect with landing gear retracted, are presented in figures 11 and 12, respectively, for flap deflections through $30^{o}$ in $10^{o}$ increments.

### Lift-to-Drag Ratios

Lift-to-drag ratios (out-of-ground effect) were computed using the data from table II. Trimmed lift-to-drag ratio, with the landing gear extended, is shown in figure 13(a) as a function of lift coefficient and flap deflection. Ratios for the landing gear retracted condition are plotted in figure 13(b).

## HIGH SPEED AERODYNAMICS

The procedure used to determine high speed drag values for the AST-105-1 was similar to the techniques used in references 1 and 2. A common data base was used throughout these analyses and was again employed in the present study. The approach to drag "buildup" for the AST-105-1 for Mach numbers from 0.5 to 2.62 is illustrated in figure 14. These drag items are discussed in the paragraphs which follow.

### Wave Drag

Zero-lift wave drag coefficients for the AST-105-1 were computed using the supersonic area rule technique of reference 11. Equivalent area distributions, at a Mach number of 2.62, developed by the area rule for both the fuselage and complete configuration are shown in figure 15. Wave drag variation with Mach number for the total configuration is presented in figure 16.

### Skin Friction and Roughness Drag

Skin friction drag was computed using the reference 9 computer program which is based on the T' method described in reference 12. Configuration friction drag for a particular Mach number-altitude combination was computed by representing the various components by appropriate wetted areas and reference lengths. Smooth flat plate, adiabatic wall, and turbulent boundary layer conditions were assumed. Transition to turbulent flow was assumed to occur at the leading edge of each component. Components which have significant variation in reference length depending upon spanwise position, such as the wing and tail, were subdivided into strips to improve the accuracy of friction drag computation. Results of the analysis are shown in figure 17 for both climb and cruise conditions.

The total roughness drag increment was assumed to be six percent of the friction drag for the M = 2.62 cruise condition. For lower Mach numbers, the

ratios of roughness drag to skin friction developed previously in reference 1 were used. Roughness drag variation with Mach number so determined can also be seen in figure 17.

For subsonic speeds ($0.50 \leq M \leq 0.95$) empirical methods from reference 13 were used to compute form factors. These form factors, which relate the pressure, or form drag, of the lifting surface or body to the associated skin friction, were computed as a function of thickness ratio for lifting surfaces and of fineness ratio for fuselage and nacelles.

## Profile Drag

The final increment of zero-lift drag to be accounted for is profile drag, the coefficient of which is denoted herein as $C_{D_{Po}}$. In this instance it includes drag due to camber, protuberances, and interference as well as locally separated flow effects. This increment was taken from the analysis presented in reference 1 and is shown in figure 18 as a function of Mach number.

## Minimum Drag

The various drag contributions, identified in preceding paragraphs along with determinative procedures, were combined to obtain total configuration minimum drag coefficient for $M = 0.5$ to 2.62. These data are presented in figure 19.

## Lifting Horizontal Tail Drag

Horizontal tail incidence angles required for maximum configuration aerodynamic performance were calculated at various Mach numbers from 0.5 to 2.62. The procedure employed for determination of the required tail incidence and the associated $\Delta C_{D_{i,tail}}$ increments for a particular Mach number is illustrated in figure 20. Theoretical drag due-to-lift of the AST-105-1 was calculated for several tail incidence angles. For subsonic Mach numbers the method of reference 14 was used, with the technique of reference 15 being used for supersonic cases. Maximum values of L/D corresponding to the combining of calculated zero-lift drag coefficients (skin friction, roughness, pressure, profile, and wave) with the theoretical drag due-to-lift coefficients were then plotted as a function of tail incidence angle (see fig. 20). This approach made possible the selection of a tail incidence angle which will maximize the aerodynamic efficiency of the complete configuration.

Drag-due-to-lift characteristics of the configuration over a range of lift coefficients were then calculated for this optimum tail incidence angle and also for the configuration with the tail off. The $\Delta C_{D_{i,tail}}$ values over the range of lift coefficients for a particular Mach number were equal to the differences in these results.

Baseline drag polars, as presented in reference 1 and based on experimental data, are for a similar arrow-wing configuration with horizontal tail on, but always at zero tail lift. The $\Delta C_{D_{i,tail}}$ increments obtained as just described were then added to the baseline polars to obtain the AST-105-1 drag due-to-lift characteristics.

## Configuration Aerodynamic Characteristics

Drag polars were developed by combining the $C_{D_{min}}$ values (fig. 19) calculated specifically for the AST-105-1 with the drag due-to-lift characteristics obtained as described in the preceding subsection. Drag polars for three representative (subsonic, transonic, and supersonic) Mach numbers are shown in figure 21. Typical operating points are also identified.

Detailed polar data for the mid-subsonic through cruise Mach number range are provided in table III. The data of table III are plotted in figure 21 for three representative Mach numbers.

Maximum lift-to-drag ratios were calculated and the results are presented as a function of Mach number in figure 22. It should be noted that the operating lift-to-drag ratio at the start of cruise is 9.23 whereas the $(L/D)_{max}$ value is 9.39. Throughout cruise, the operating L/D values closely approximate the maximum achievable.

# STABILITY AND CONTROL

This section presents the design stability and control criteria, the aerodynamic data base, stability and control analyses, and the aerodynamically-constrained center-of-gravity limits.

## Criteria

Longitudinal stability and control.-

Takeoff: Forward center-of-gravity set at a position for neutral stability; center-of-gravity range of 66.04 cm (26 in); main landing gear struts located at 0.06 $c_{ref}$ aft of the aft center-of-gravity limit: control to the geometry limit in ground effect, and no significant pitchup.

Landing: Aft center-of-gravity limit based on the ability to provide a nosedown pitching acceleration of 0.08 rad/sec$^2$ at the minimum demonstrated speed, at normal landing weight; acceptable dynamic short-period characteristics at the approach speed with the hardened stability augmentation system, HSAS, operative, and no significant pitchup. (Minimum demonstrated speed is defined at a lift coefficient consistent with a 0.5g incremental pull-up maneuver from trim at the approach speed of 81.3 m/sec (158 kts)).

Supersonic cruise: A positive static margin $\geq$ three percent at cruise to compensate for loss of stability due to structural flexibility at the required 2.5g pull-up maneuver condition.

Lateral-directional stability and control.-

General: Negative roll due to positive sideslip (positive dihedral effect).

Takeoff: Directional control sufficient to trim the airplane in a 15.4 m/sec (30kt) $90^{o}$ crosswind. Directional control shall be sufficient, following application of "full" power from three engines, to counteract an outboard engine failure with failure occurring at, or beyond, critical (balanced) field length.

Taxiing: For crosswind taxiing, minimum control speed shall be sufficiently low such that nose wheel steering can be used.

Landing: Lateral control, at or above the normal approach speed, shall be sufficient to produce a $30^{o}$ roll response in 2.5 seconds after initiation of a rapid full control input; lateral and directional control, in a 15.4 m/sec (30 kt) $90^{o}$ crosswind, adequate to trim the airplane at $\psi = 0^{o}$ with not more than 75 percent of full lateral control; the airplane shall possess inherent Dutch roll stability with acceptable levels of undamped natural frequency ($\omega_d \geq 0.4$ rad/sec).

Supersonic cruise: Directional stability of $C_{n_\beta} \geq 0$ for the 2.5g maneuver at cruise speed.

## Data Base

Low speed, high lift longitudinal stability and control data were obtained from reference 3. These experimental data included the effects of leading and trailing edge flap deflections and horizontal tail incidence/elevator deflection. Transonic and supersonic longitudinal data were obtained from references 4 and 16, respectively. These data were corrected for horizontal tail volume differences and based on AST-105-1 reference dimensions by the method given in reference 1.

Low speed, high lift lateral directional stability and control were taken from reference 4, and recent unpublished wind tunnel test results, corrected for vertical tail volume differences and based on AST-105-1 reference dimensions. Supersonic lateral-directional data were taken from reference 16 and also corrected in the manner just indicated.

Wing flexibility associated with lateral control deflections was taken from estimates given in reference 17, whereas fuselage transverse bending due to vertical tail deflection was taken from reference 18.

## Lift and Control Devices

Longitudinal high lift devices along with longitudinal, lateral and directional controls were considered to be as follows:

| Longitudinal | Lateral | Directional |
|---|---|---|
| Leading-edge flaps ⑨, ⑪, ⑬ | Outboard ailerons ⑦ | *All movable vertical tail |
| Trailing-edge flaps ①, ③ | *Outboard flaperons ⑤ | |
| *All-movable horizontal tail/geared elevator | Inboard flaperons ③ ** | |

*These surfaces also used for control in transonic and supersonic flight
**See figure 3 for location as identified by encircled numbers

The high-lift configuration is herein defined with the wing apex flaps deflected $30^{o}$ ($L_{1,2,} = 30^{o}$) and the outboard wing panel leading-edge Krueger flaps deflect $45^{o}$ ($L_6 = 45^{o}$). The two inboard trailing edge flaps, $t_1$ and $t_2$, were (in wind tunnel test) deflected in $10^{o}$ increments through the range of $0^{o}$ to $40^{o}$ with the outboard flaperon ($t_3$) and aileron ($t_4$) deflected $5^{o}$.

## Longitudinal and Lateral-Directional Control

Longitudinal.- Longitudinal control power was established by the use of data from reference 3 where pitching moment is presented as a function of trailing-edge flap deflection, angle of attack, and horizontal tail deflection, with and without elevator deflections. Based on the tail incidence to elevator gearing assumed for the AST-100 (and shown in fig. 23), longitudinal control capability was determined for the tested (ref. 3) horizontal tail volume coefficient, $\bar{V}$. Since test data indicated tail lift coefficients as high as 1.9, full-scale Reynolds number effect correction to these pitching moment data were not made. Application of the stability and control criteria resulted in the smallest horizontal tail size for the largest trailing edge flap deflection, and the largest required tail for the condition of zero flap deflection.

The L/D is a maximum for the high-lift configuration at approximately $20^{o}$ trailing edge flap ($t_1$ and $t_2$) deflection for the takeoff and approach speeds considered. Since $20^{o}$ flap deflection provides adequate lift for operation within field length constraints, it was selected for the remainder of the analysis.

Approach angle of attack was assumed to be $8^{o}$ at 81.3 m/sec (158/kt) EAS. This, in conjunction with the assumption that the AST-105-1 could be flown on the approach with a static margin of approximately 4 percent negative, influenced establishment of the most rearward center-of-gravity position at $0.601\ \bar{c}_{ref}$. The nose-down pitch acceleration criterion of 0.08 rad/sec$^2$ at minimum demonstrated speed has been found to be mandatory based on approach simulation studies reported in reference 10. This necessitates a horizontal tail of 57.6 m$^2$ (620 ft$^2$), projected exposed area.

With the landing gear positioned 0.06 $\bar{c}_{ref}$ aft of 0.601 $\bar{c}_{ref}$, the minimum nose-wheel lift-off speed is approximately 77.2 m/sec (150 kt) EAS. Normal nose-wheel lift-off speed, based on takeoff performance considerations, is approximately 95.2 m/sec (185 kt) EAS.

Table IV presents low-speed force coefficients and derivatives, as a function of angle of attack, for flap deflection $t_1 = t_2 = 0^o$, $10^o$, $20^o$, and $30^o$. Pitching moment coefficients as a function of angle of attack, and horizontal tail deflection for the aforementioned flap deflections are given in table V.

It should be noted that values presented in tables IV and V are not test data, since, for example, the arrow wing model was not tested precisely at flap deflections of $t_1 = t_2 = 20^o$ and $t_3 = t_4 = 5^o$, but are representative of aerodynamic force and moment characteristics for the AST-105-1, which were derived from 102 tunnel "runs" reported in reference 3.

Lateral.- Lateral control capability was determined utilizing the results of the aileron, and inboard and outboard flaperon deflection tests. These data, for a rigid airframe, are presented in table VI. Lateral control flexibility factors for each surface, which are presented in figure 24, were established by the use of data from reference 17 and represent results based on a stiffness sized (flutter free) wing design.

Figure 25 illustrates the steady state sideslip, bank angle, rudder deflection, and lateral control required for approaches at $\psi = 0^o$ in a 15.4 m/sec (30 kt) $90^o$ crosswind at an airspeed of 81.3 m/sec (158 kt). It can be seen that 75 percent of available lateral control was required for a crosswind component of 11.6 m/sec (22.5 kt). To achieve trim capability in a 15.4 m/sec (30 kt) crosswind with no more than 75 percent lateral control capability would require a reduction of about 25 percent in positive dihedral effect.

In light of the results of wind tunnel tests (ref. 4), it does not appear that additional control capability is available using aerodynamic surfaces. Consequently, acceptable crosswind landing capability can only be achieved by the use of a crosswind landing gear or by a significant reduction in positive dihedral effect. Wind tunnel data from reference 19 show a reduction in positive dihedral effect by incorporating wing geometric anhedral. Models used in the tests reported in references 3 and 4 did not incorporate this additional wing geometric anhedral. Further, these models were tested in the high-lift configuration, flap-wise, combined with the supersonic cruise wing shape. Reference 17 indicates significant geometric anhedral for the calculated low-speed wing shape. This would, of course, reduce the adverse dihedral effect but necessitate longer main landing gear struts.

Directional.- Directional control tests (ref. 4) were conducted using an all-movable vertical tail. Results indicate that the directional control derivative, $C_{n_{\delta_r}}$, for the vertical tail in the presence of the horizontal tail, was lower than the determined value of $C_{n_\beta}$ (see table VI) assuming that a degree of sideslip is equivalent to a degree of vertical tail deflection. The study of reference 10 recommended an increase in directional control capability to

meet the crosswind requirement. A 30-percent increase in directional control results in a vertical tail of 33.3$m^2$ (358 $ft^2$) for the AST-105-1. Rudder flexibility was accounted for by application of the appropriate value of the directional control flexibility factor, $K_1$, taken from figure 26.

Applying the rationale that since the AST-105-1, in the approach mode, is limited to crosswinds $\leq$11.6 m/sec (22.5 kt), rather than the goal of 15.4 m/sec (30 kt) the crosswind criterion for ground roll was taken to be the former value for consistency with the approach crosswind constraint. Directional control requirements, in terms of rudder deflections, for various ground roll speeds, were determined by equating yawing moment, $C_{n_{\delta r}} \delta_r$ (due to rudder deflection) to airplane yawing moment (due to sideslip) expressed as $C_{n_\beta}$ and using the relationship $V_{cw} = V\tan\beta$. Results are shown in figure 27. It can be seen that, in the aforementioned crosswind, directional control cannot be maintained at ground roll speeds less than approximately 43.8 m/sec (85.0 kt). The implication here is that, in higher crosswind, nose wheel steering, and/or differential thrust would have to be used during the initial segment of the takeoff ground roll.

## Longitudinal and Lateral-Directional Static Stability

Longitudinal.- Low-speed longitudinal static stability analysis is based on wind tunnel measured lift and pitching moment characteristics given in reference 3. These tests were conducted on a tenth-scale model of the configuration in reference 1. However, the AST-105-1 fuselage is 3.05 m (10 ft) shorter than that of the reference 1 configuration. Therefore, small corrections were made to the test data to account for the effect of the change in fuselage contribution on the zero-lift pitching moment coefficient and aerodynamic center location. The change in zero-lift pitching moment was determined to be -0.0002 and the forward shift in aerodynamnic center, a.c., was calculated to be 0.0015 $\bar{c}_{ref}$. Test data were transferred to a new moment reference center shifted forward by an amount corresponding to the a.c. shift. The horizontal tail contribution to trim and stability, at zero tail incidence, was established for the AST-105-1 in the high-lift configuration with trailing edge flap deflection ($t_1$ and $t_2$) of $0^o$, $10^o$, $20^o$, and $30^o$. Deflection of the wing apex leading edge flaps, $L_{1,2} = 30^o$, suppressed vortex lift and produced improved pitching moment characteristics compared to earlier AST versions. Further improvement in pitching moment was obtained by deflecting the outboard wing leading edge flap, $L_6$, to $45^o$. There is, however, gradual pitch-up present within the operating angle of attack range.

Figure 28 presents stability and trimmed lift curves for forward and aft center-of-gravity limits with trailing edge flap deflection $t_1 = t_2 = 20^o$. Rationale for selecting this flap deflection is given in Longitudinal Control. In performance computations, the horizontal tail/elevator was considered to be operating to maximize the complete configuration lift-to-drag ratio (tail upload, minimum trim drag) for climb, acceleration to cruise and deceleration and descent from cruise. From the data presented, it can be seen that the trimmable center-of-gravity range, is from 42.55 to 60.10 percent of the reference mean aerodynamic chord.

Supersonic longitudinal static stability was estimated from aerodynamic center data of reference 2 (fig. 25). These data were adjusted to account for the difference in fuselage and horizontal tail contributions between the AST-100 and AST-105-1.

The flexible airplane aerodynamic center location over the operating Mach number range is shown in figure 29.

Lateral-directional.- Low speed static lateral-directional stability analyses are based on wind tunnel measured data presented in reference 4. These tunnel tests were performed with a 0.045 scale free-flight model of an arrow wing supersonic transport configuration. Due to the shorter fuselage of the AST-105-1, a small correction was applied to the test determined values of $C_{n_\beta}$, for the model without vertical tail. This correction was estimated to be -0.00004/degree, based on methods described in reference 20. When end-plated by the horizontal tail, the vertical tail contribution to body axis directional stability was stabilizing, as shown in reference 4, up to an angle of attack of about $16^0$ beyond which the configuration was unstable through the tested angle of attack of $23^0$. Lateral-directional stability for the AST-105-1 includes the strong stabilizing effect of the tested fuselage forebody strakes (ref. 4). The fuselage ventral fin was found to have no contribution to stability below $25^0$ angle of attack. Hence. it is not included in the present configuration concept. Low-speed lateral and directional moment derivatives are presented in table VI.

Supersonic cruise static lateral-directional stability characteristics for the flexible AST-105-1 are presented in figure 30 as a function of lift coefficient. These data were estimated by the use of data from reference 2 (fig. 30). The data were corrected due to the difference in vertical tail contribution because of the differences in fuselage length and tail size between the configuration of reference 2 and the AST-105-1. It can be seen in figure 30 that there is barely sufficient directional stability to meet the criterion of $C_{n_\beta} \geq 0$ in a 2.5g pull-up maneuver.

## Stability Augmentation

Since the AST-105-1 concept is quite similar to the configuration evaluated in reference 10, the same stability and control augmentation systems were assumed applicable.

The Hardened Stability Augmentation System, HSAS, included the following features: longitudinally, a filtered pitch rate feedback signal acting through a relatively high gain was used to reduce the unstable mode and to enhance the short period characteristics; laterally, a simple roll damper provided rapid damping of the roll mode and increased Dutch roll damping; directionally, roll-rate feedback was used to provide improved turn-entry coordination, reduction in Dutch roll coupling during rolling maneuvers (i.e. increased $\omega_\phi/\omega_d$) and further increased Dutch roll damping.

The Stability and Control Augmentation System, SCAS, provided pitch rate proportional to control column deflection with attitude hold, which stabilizes the inherently unstable mode; rapid, well damped responses to pilot input; and, minimization of the disturbances due to engine coupling effects and turbulence. Laterally, a rate command system provided a roll rate proportional to control wheel position plus roll attitude hold. Directionally, three trim coordination features were included as rudder-control wheel interconnect, rudder-roll rate feedback, and rudder-bank angle feedback.

These lateral-directional features provided rapid, uniform response to pilot input, improved Dutch roll characteristics, minimal Dutch roll excitation during roll maneuvers, neutral spiral stability and minimization of atmospheric turbulence effects. Block diagrams of the HSAS and SCAS are shown in figures 31 and 32, respectively.

An autothrottle to maintain airspeed throughout the approach and landing was part of the normal operational augmentation. Since the simulated engine dynamics produced rapid thrust response (see ref. 10, fig. 3), the autothrottle essentially maintained approach speed within approximatley (+ 3 kt). The airplane of the reference 10 study was "flown" well on the "backside" of the thrust required curve at the approach speed of 78.7 m/sec (153 kt), $\partial(T/W)/\partial V$ = -0.0045/m/sec (-0.0023/kt), where the pilot would normally use thrust for glide path control and pitch attitude for airspeed control. However, the simulated rapid engine response permitted the use of thrust for airspeed control and pitch attitude for glide path control which is a natural "front side" technique. The AST-105-1 was also "flown" well on the "back side" of the thrust required curve at the approach speed of 81.3 m/sec (158 kt) at $\partial(t/w)\partial V$ = -0.0033/m/sec (-0.0017/kt). As a consequence, speed control for the AST-105-1 should be similar to that for the configuration of reference 10.

## Dynamic Stability Criteria and Results

The AST-105-1 was "flown" on the Langley ground simulator for evaluation of low-speed handling characteristics. Inputs such as physical characteristics and dynamic stability derivatives utilized in simulation and for calculating dynamic stability characteristics, are presented in tables VII, and VIII, respectively. Control surface deflections and deflection rates can also be found in table VII.

Dymamic stability characteristics of the AST-105-1 are presented in table IX where results for the reference 10 (and 25) aircraft are also shown for comparison. Control response is given in table X.

Pilot-in-the-loop handling quality evaluations were not performed for the AST-105-1. Hence, the Pilot Ratings (PR) of reference 10 mentioned in the discussion that follows can only be related by inference to the AST-105-1, which is similar to the conceptual aircraft of reference 10. The PR system is presented in table XI.

In smooth air, the longitudinal and lateral-directional handling qualities of the unaugmented configuration of reference 10 were assigned a Pilot Rating

of 7, when evaluated separately. However, the combination of poor characteristics resulted in an overall PR of 10. With the beneficial influence of the HSAS, the PR was 4 in smooth air and 5 in heavy turbulence where the root mean square value of the turbulence was 2.7 m/sec (9 ft/sec). With the SCAS, the PR was 2 in smooth air and 3 in heavy turbulence.

Two of the conventionally used longitudinal handling qualities criteria are presented in figure 33. Short period frequency requirement of reference 21 is presented in figure 33(a), along with results obtained for the AST-105-1 and the reference 10 concept from flight simulation. The often used Shomber-Gertsen longitudinal handling qualities criterion of reference 22 is shown in figure 33(b). Current airplane experience and the results of both the present and the reference 10 studies correlate reasonably well with this criterion. The low-speed pitch rate response criterion shown in figure 34 was taken from reference 23 and is based on the Shomber-Gertsen criterion. Constraints applicable to the boundary plot of this figure are given in reference 23.

Lateral response criteria are presented in figure 35. Roll control power criterion, from reference 24, is shown in figure 35(a) as a function of roll mode time constant. From the reference 10 (and 25) and AST-105-1 results, it would appear that the unaugmented aircraft exhibits better characteristics, in terms of roll acceleration, than the augmented. However, reference 25 indicated that handling qualities of the unaugmented aircraft were unacceptable. Actually, more roll control power, which is needed to comply with lateral trim requirements, would improve the relationship between the HSAS and SCAS points and the criterion boundaries with attendant improvement in PR. Roll rate response criterion, as taken from reference 26, is shown in figure 35(b). The results for the AST-105-1 and for the reference concept agree fairly well with the criterion, especially with SCAS.

Time histories of the lateral-directional motions produced by a roll control step input with a modified SCAS are compared, in figure 36, with motions resulting from a like input with the initial SCAS. Modification of the lateral-directional SCAS was achieved by: (1) slowing the initial roll rate command signal, (2) reducing the control-wheel roll rate command sensitivity, and (3) substantially reducing the aileron-to-rudder interconnect gain. The block diagram of the modified SCAS is shown in figure 37.

In the reference 25 study, lateral accelerations at the aircraft center-of-gravity were considered acceptable for ride quality. However, the evaluation pilots who sat (in simulation) approximately 44.2 m (145 ft) ahead of and 4.8 m (15.7 ft) above the center-of-gravity rated ride quality unacceptable with the initial SCAS. This was due to the large moment arm combined with the high yaw acceleration associated with good turn coordination provided by the SCAS. Modification of the SCAS, as just described, changed the ride quality rating at the pilot station to acceptable. This change in the SCAS did result, however, in a slight degradation in Pilot Rating of handling qualities, going from a Pilot Rating of 2. to 3.

To more precisely define high-lift, low-speed characteristics of AST configurations and subsequently determine handling and ride qualities, wind tunnel testing of a model with the arrow wing in the low speed (rather than cruise)

shape is required. In addition, a more extensive investigation of the effects of forebody strakes as "chin fins" should be undertaken since the limited data available indicate that they have potential for reducing lateral accelerations at the pilot station without diminishing lateral-directional handling qualities.

## PROPULSION

### Background

The Pratt and Whitney Aircraft variable stream control engine concept, (ref. 27), was selected for this study. The particular version is designated VSCE-516. It was designed for cruise at a Mach number of 2.62 (std. day + $8^{o}$C) and has been sized to meet the following airplane requirements:

Takeoff gross weight - 3.051 MN (686000 lbf)

Wing Loading - 3.926 kPa (82 lbf/ft$^2$)

Installed thrust-to-weight ratio on a standard day +$8^{o}$C - 0.254

Payload - 273 passengers plus baggage

Nominal range - 8334 km (4500 n.mi.)

Presented herein are installed VSCE-516 performance data for a standard +$8^{o}$C hot day adequate for mission analysis. Standard +$10^{o}$C hot day data were used for noise analysis. Nacelle geometric data necessary to estimate nacelle drag and engine weight data required for mass properties calculations are also provided.

### Description

Engine.- The JP-4 fueled VSCE-516 engine is a two spool, duct-burning turbofan which utilizes a coordinated throttle schedule. Through the use of a variable fan and compressor along with selective ducting, burning and throttling of the engine airflow, performance of the VSCE can be tailored to the changing flight environment encountered by a supersonic transport. The coordinated throttle scheduling permits the engine to be operated with a fixed exhaust jet velocity ratio (fan stream to primary stream) to achieve maximum benefit of coannular noise suppression. Primary and fan stream nozzles are of the variable throat type and the combined stream exit area is also variable. These variable-area nozzles are integrated with ejectors and thrust reversers (see fig 38).

Sea level standard day baseline engine static characteristics are as follows:

Fan pressure ratio - 3.1:1

Bypass ratio - 1.3:1

Overall pressure ratio - 16.0:1

Total corrected airflow - 408.2 kg/sec (900 lbm/sec)

Maximum combustion exit temperature

Primary burner - 1810.9°K (3259.7°R)

Duct burner - 1644.3°K (2959.7°R)

The engine was scaled from a sea level standard day +8°C static net thrust of 286630N (64,437 lbf) to a sea level standard day +8°C static net thrust of 193769N (43,561 lbf) to meet the takeoff design thrust-to-weight, T/W, ratio of 0.254. This latter thrust value requires an airflow of 276.0 kg/sec (608.4 lbm/sec). The required engine is somewhat smaller than the baseline VSCE-516 engine. Size and weight were reduced to that required, based on relative engine size and the scaling data provided by Pratt and Whitney Aircraft which is shown in figure 39. Here relative size is the ratio of the required thrust level, $F_{n_r}$, to the corresponding baseline VSCE-516 thrust level, $F_{n_b}$. Gross thrust, ram drag, and fuel flow were also scaled based on relative size.

The weight of the VSCE-516 engine scaled to AST-105-1 requirements is 39.3 kN (8835 lbf) and includes the following:

Gas generator

Nozzle/thrust reverser

Ignition system for burner and augmenter

Augmenter hardware including flame holder, liners, case and fuel manifold

Fuel-oil cooler, oil tank and filter

Engine instrumentation

Engine accessory gear box

Fire seals

Primary stream tail cone

Blade containment

Nacelle and inlet.- After the baseline VSCE-516 engine was reduced to a size consistent with the thrust requirements of the AST-105-1, by application of the aforementioned scaling data, a nacelle concept layout, based on a Boeing design (ref. 8) was prepared. A sketch of the resultant nacelle is shown in figure 40. The nozzle is canted so that the thrust line will pass through the airplane center of gravity during takeoff and landing. The cant angle is 8° downward with the nozzle being fixed in this position. Location of nacelles on the aircraft is shown in figure 41. The inlet selected is the NASA-Ames "P" inlet which is detailed in reference 28 for the VSCE-502 engine. This inlet is an axisymmetric, mixed compression design with a translating center body with bleed on both the centerbody and cowl. The inlet is sized for the cruise Mach

number and altitude. An additional two-percent airflow is included for cooling and ventilation of the nacelle. Inlet performance is presented in figures 42(a) and (b).

### Engine Operation and Performance

During takeoff, the engine fuel flow and nozzle areas are under the control of a coordinated throttle schedule designed to maintain a ratio of fan jet exit velocity to primary jet exit velocity of approximately 1.7. This velocity ratio is maintained during takeoff to optimize the coannular noise reduction.

In the climb/acceleration phase the throttle setting is varied between maximum augmented power and maximum nonaugmented power to minimize fuel burned during this segment of the mission.

The engine inlet is designed to match the airflow requirements at supersonic cruise. The capability of varying fan speed and stator angle has permitted the engine airflow to be tailored to match the maximum inlet airflow at all operating Mach numbers as shown in figure 42(b). Optimum power setting for supersonic cruise is usually at a slightly augmented power condition.

For subsonic cruise, the nozzles and fuel flow are varied to maintain, as near as possible, constant airflow as the power setting is reduced to match the aircraft required thrust.

Engine performance presented in this report is based on a technology readiness consistent with a late 1980's certification date. Installed performance of the VSCE-516 engine includes installation effects of the NASA-Ames "P" inlet, nozzle, thrust reverser, 0.8 kg/sec (1.76 lbm/sec) service airbleed, 149 kw (200 HP) power extraction and propulsion drag effects. Propulsion drag includes inlet "spillage," bypass, and nozzle boattail drags. Nacelle skin friction, interference and wave drags are accounted for in the airplane drag polars.

Engine performance data generated by Pratt and Whitney Aircraft (contract NAS3-19540) was provided to the Langley Research Center in the form of an unpublished data package. This data, scaled to AST-105-1 requirements, are presented for maximum climb, maximum cruise, and part power cruise in figures 43 through 45 at standard day +8$^{o}$C conditions for mission analysis. Engine performance at standard day +10$^{o}$C conditions, which was included in the aforementioned data package, was used for takeoff and landing analysis and the related noise analysis.

## MASS CHARACTERISTICS

### Criteria and Methods

Configuration selection and sizing was influenced by the mission performance criteria stated in the PROPULSION section plus an approach speed

constraint of 81.3 m/sec (158 kts). Structural weight analysis was based on all titanium primary structure. Design features and fabrication techniques for major components were assumed to be as follows:

- o Wing and Aerodynamic Surfaces: Stress-skin titanium skin/core sandwich panels
- o Fuselage: Titanium skin/stringer/frame construction
- o Landing Gear: Two-strut main gear and single-strut nose gear structure of high strength steel alloy
- o Engines: Duct burning turbofan variable stream control engines with dimensions, weight, and airflow scaled down (see PROPULSION) from the Pratt and Whitney Aircraft VSCE-516 engine

Initial selection and sizing of the AST-105-1 was accomplished through the use of the NASA-Langley developed Aircraft Sizing and Performance program (ref. 5). Results from this program were used to generate the plots commonly referred to as "thumbprints" (see MISSION ANALYSIS). The sizing and configuration selection syntheses was performed by producing a matrix of potential aircraft with an array of design gross weights ranging from 3.047 to 3.670 MN (685,000 to 825,000 lbf) with sea level, standard day $+8^{o}C$ installed thrust-to-weight ratios varying from 0.20 to 0.40. Wing loading was varied from 3.351 to 4.788 kPa (70 to 100 $lb/ft^2$). These candidate aircraft were then subjected to mission performance evaluations within the same program. The aircraft with the best match of the aforementioned three parameters and which had the range capability within the criteria constraints was selected for more refined analysis.

Characteristics which roughly define the aircraft selected for further study are as follows:

Design Gross Weight - 3.051 MN (686,000 lbf)

Wing Loading ($W/S_{ref}$) - 3.926 kPa (82 $lb/ft^2$)

Thrust-to-Weight Ratio (T/W) - 0.254 installed, sea level, standard day $+8^{o}C$

After initial sizing of the study aircraft was accomplished by use of the program of reference 5, semidetailed mass characteristics of the selected configuration were determined through the use of the Vought Corporation - Hampton Technical Center developed computerized Statistical Mass Properties Estimating Program. This program, designed to predict mass values for multiengine commercial transports, is the same as that used in previous NASA-Langley AST studies. It is statistically based with empirical modifications, and contains a supersonic prediction portion. Data so generated has shown good correlation with airframe contractors' data. Application of an advanced structural/aeroelastic analytical method (ref. 17) to an earlier, similar AST configuration resulted in a takeoff gross weight approximately 17.79 kN (4000 lbf) less than predicted by the aforementioned mass properties program, which was used in the AST-105-1 study. Hence, structural weights generated for the AST-105-1 by use of the

latter are more than adequate for a viable flutter-free design, based on titanium technology. Use of advanced composite technology would make possible a significant reduction in structural weight.

## Weight, Balance, and Inertia

After the three principal parameters, namely design gross weight, wing loading and thrust-to-weight ratio were fixed, the weight analysis consisted of using the configuration geometry, which was dictated by sizing, as input and performing a semidetailed allocation of weight by system/flight condition. A tabular summary of the weight allocation is given in table XII. The tabulated data are also presented in bar chart form, along with the major components as a percentage of the total in figure 46. A more detailed weight breakdown under these major components is provided in table XIII.

The AST-105-1 was configured in a way to insure that the balance characteristics would be such that the takeoff, cruise, and landing centers-of-gravity lie within limits prescribed by stability and control criteria. These limits are:

Percent $\bar{c}_{ref}$

| Flight Condition | Forward Limit | Aft Limit | For Minimum Trim Drag |
|---|---|---|---|
| Takeoff | 42.55 | 60.10 | |
| Landing | 42.55 | 60.10 | |
| Begin cruise | | | 50.00 |
| End cruise | | | 50.00 |

Combinations of fuel utilization transfer sequencing were investigated to determine the most forward and aft attainable center-of-gravity (c.g.) boundaries. These limiting boundaries, along with the desired c.g. trace during a typical mission, are presented in figure 47. With the wing apex at fuselage station 15.24 m (50 ft), all points along the stability and trim constrainted c.g. path lie within the limit boundaries and are attainable by proper fuel management.

It should be noted that the attainable aft c.g. exceeds the 0.6010 $\bar{c}_{ref}$ aft stability limit. The region aft of this point must, therefore, be "out of bounds" for flight operation. Although increases in horizontal tail area would extend the operational c.g. into this region, it is inappropriate to do so since the desired region of minimum trim drag exists nearer the forward boundary. Consequently, the region rearward of the aft stability limit is of scant importance other than for payload and fuel loading limit considerations.

Inertia characteristics were computed for two of the flight conditions considered to be of importance in stability and control analyses. These conditions are gross takeoff weight and normal landing weight. Inertias of the individual components were computed about the respective centroids of each, transferred to the aircraft overall c.g. locations for these two conditions (within limits required for stability and control) and then summed. Inertia data generated for the AST-105-1 are summarized in table XIV.

## ENVIRONMENTAL FACTORS

### Noise

Noise characteristics of the AST-105-1 at the three measuring stations prescribed in reference 29 have been calculated for both takeoff and approach. Relative location of these stations is shown in figure 48.

Engine noise was calculated using the NASA Aircraft Noise Prediction Program (ANOPP), which is described in reference 6. Both centerline and sideline noise during takeoff and centerline noise in approach were determined using the ANOPP method. Takeoff and approach trajectory data required as input for the ANOPP were generated by using an unpublished Langley performance computer program.

Standard procedure operation.- Computed noise (jet only) for the VSCE with coannular nozzle is presented in table XV for three takeoff procedures designated as cases 1, 2, and 3. Descriptions of the cases can be found in this table where it can be seen that case 1 is quasi-standard (no power cutback) whereas the other two cases can be considered to be standard procedure. Neither procedure results in compliance with FAR 36 (ref. 29). However, it can be seen that the case 3 procedure would provide a reduction in sideline maximum noise of 2.2 EPNdB and 6.4 EPNdB in centerline noise compared to case 1 (no cutback).

Although results are not presented here, takeoffs with oversized engines operating at derated thrust (92 percent of maximum power) were also analyzed. For the case with cutback comparable to the aforementioned case 3 procedure, it was found that the derated thrust takeoff resulted in a reduction in maximum sideline noise of 0.8 EPNdB but in an increase in centerline noise of 6.8 EPNdB.

Jet noise at the approach measurement point was computed to be 106.6 EPNdB for a standard approach, 3-degree glide slope and constant speed of 81.3 m/sec (158 kt).

Ground contours ("footprint") of constant EPNL provide a graphical representation of the benefit possible by changing climb operational procedure from case 1 to case 3. Accordingly, noise contours were generated using an unpublished computer program, developed by the Hampton Technical Center (HTC), which uses jet noise characteristics as predicted by the reference 6 program. The HTC program calculates single point EPNdB levels, for jet exhaust noise only, as distributed over a grid of psuedo observer stations. In this instance, the 400 observer-station grid, situated only on one side of the runway centerline due to contour symmetry, was defined as follows: at each of 40 downrange positions in the interval from 1524 m (5000 ft) to 13,716 m (45,000 ft) from brake release there was a linear array of ten sideline stations transverse to the runway centerline beginning at 304.8 m (1000 ft) and going out to 3048 m (10,000 ft). From this grid, points of constant EPNL were selected to plot noise contours as shown in figures 49 and 50. Since these contours were developed by meshing the ANOPP predicted results with the HTC simplfied noise

prediction program, which does not account for ground reflection, it should be understood that these plots show trends rather than absolute values. Data for the 108 EPNdB contour for climb without cutback was generated but was of such magnitude relative to the 115 EPNdB contour as to be off the normal page-size plot.

Results from measurement of the area contained within the 115 EPNdB contours for climb without and with cutback (figs. 49 and 50, respectively) provide relative, though not absolute, measure of the merit of the two procedures. For climb without cutback, the area enclosed in the 115 EPNdB contour, measured from 1.52 km (5000 ft) from brake release, is 7.74 $km^2$ (2.99 $mi^2$) whereas it is 3.68 $km^2$ (1.42 $mi^2$) for accelerating climb followed by cutback.

Airframe noise at the takeoff flyover measuring station and the approach measuring station was also computed by using the ANOPP method. In takeoff, with trajectory parameters as previously determined for the full-power without "cutback" climb, the airframe contribution to noise at the monitor is about 68 EPNdB. In the conventional approach mode ($3^o$ glide slope) airframe noise is approximately 90 EPNdB.

Advanced procedure operation.- Since sideline noise peaks well downrange from brake release, a potential procedure is to allow the noise level to increase during ground roll and lift off while achieving higher speed, better climb, and increased L/D. This will permit greater power cutback resulting in lower community noise. Therefore, preliminary studies of advanced (noncertificated) procedures as applied to the AST-105-1 were performed. These included takeoff with higher thrust level, prior to cutback, and decelerating approaches with higher glide slope than normal, standard procedures. Results from application of advanced procedures for noise reduction during takeoff and approach for the AST-105-1 are presented in figures 51 through 53. The takeoff advanced procedure is illustrated in figure 51 which shows the variation of flight altitude and throttle setting with distance from brake release. For a standard takeoff, the throttle remains at the normal takeoff setting throughout the ground roll and climbout. At 5944 m (19500 ft) horizontal distance from brake release, cutback is initiated. In the normal procedure, the aircraft is at an altitude of 282 m (925 ft). For the advanced procedure takeoff, a higher level of thrust is used during the ground roll and liftoff to the 10 m (35 ft) obstacle. By operating the engines at maximum allowable turbine inlet temperature, thrust is increased approximately 16 percent over that for normal procedure. The obstacle is reached in 488 m (1600 ft) less distance and with a 2 m/s (4 kt) increase in speed. Between the obstacle and the point where the aircraft reaches an altitude of 61 m (200 ft), the throttle is reduced to 105 percent of the normal thrust level and maintained until cutback is initiated. The higher thrust level and increased speed result in improved climbout performance. Altitude at the cutback point is 415 m (1360 ft), or 133 m (435 ft) higher than that of the standard procedure profile.

Several advanced procedures for approach along with the standard procedure are illustrated in figure 52, which shows the variation in altitude, speed and throttle with distance to the 15 m (50 ft) obstacle threshold point at the end of the runway. Variations are shown for the standard, constant speed approach

on a 3 degree glide slope and for two decelerating approaches on 3 and 6 degree glide slopes. All approaches are with flap deflections as cited in STABILITY AND CONTROL, and for each approach the aircraft reaches the obstacle with a speed of 81 m/s (158 kt). For decelerating approaches, the initial speed above a point 11.1 km (6 n.mi.) from the obstacle is limited by the minimum thrust level of the engines (approximately 21 percent of normal power). Deceleration continues to a point, arbitrarily selected as being 305 m (1000 ft) prior to the obstacle, in order to maintain the low thrust level inbound from the 1.8 km (1 n.mi.) noise measuring station.

A synopsis of results from the initial effort to apply advanced operating procedures to alleviate noise is presented in figure 53 as jet noise (EPNL values) only at the three noise monitoring stations. At the "flyover" station, advanced procedure using programmed throttle reduced the centerline (community) noise level by 2.6 dB, due primarily to the higher flight profile. Maximum sideline noise increased by 1.5 dB as a result of higher jet velocities associated with the higher thrust levels. The optimum procedure, in terms of reduction of both flyover and sideline noise, has not been identified at present and will require more detailed studies. Decelerating approaches significantly reduced jet noise at the 1.85 (1 n.mi.) station to such levels that other noise sources (fan, core, airframe, etc.) may become important in the noise predictions.

Although preliminary, these results indicate that advanced operating procedures can be an important additional method for noise reduction in the continuing effort to make the supersonic transport a more welcome visitor in the airport community.

## Sonic Boom

Equivalent area distribution due to volume and lift, required for sonic boom analysis, were computed by the use of methods described in references 11 and 15, respectively. These methods were modified, prior to their use for the AST-100 (ref. 2), to include angle of attack effects and were so used for the AST-105-1. These equivalent areas and the procedures of references 30 and 31 were employed to define near-field pressure signatures at three fuselage lengths below the aircraft. By the method of reference 32, these near-field pressure signatures were extrapolated to ground level. This method permits the inclusion of variations in atmospheric properties and flight conditions such as acceleration and flight path angle. Since these variations were input, the results include the effects thereof. The reflection factor used in these analyses was 1.9.

Sonic boom signatures were generated and plotted for a series of Mach numbers from transonic climb through supersonic cruise. From these waveform plots the maximum overpressure, $\Delta p_{max}$, was obtained and plotted, as a function of Mach number, in figure 54. It can be seen that at low supersonic speed $\Delta p_{max}$ is relatively high. Based on previous analysis and the trend of the overpressure - Mach number variation, a caustic (super boom) would probably occur on the ground at a Mach number of about 1.10. This is attributed to the

shock focusing effect of acceleration at low flight altitudes (see ref. 33). This super boom would occur, for the 100 percent passenger load factor case during transonic climb, at a distance of about 163 km (88 n.mi.) from brake release and hence take place well offshore of any land mass.

## MISSION ANALYSIS

The Supersonic Cruise Research (SCR) vehicle integration study reported herein is essentially an updating of prior work in order to incorporate, in a conceptual design, technology improvements in aerodynamics, propulsion, structures, and computational techniques. The design objective was to optimize a supersonic transport type aircraft for minimum size to achieve the mission goal by selecting the proper combination of aerodynamic, airframe, and propulsion systems. Accordingly, mission analysis was performed to determine performance characteristics for assessment of the capability of a particular configuration in relation to design mission goals.

### Requirements

Design.-

Payload - 273 passengers and baggage, i.e., 249.4 kN (56057 lbf)
Range - 8334 km (4500 n.mi.)
Speed - cruise at Mach = 2.62 at standard day +8°C temperature

Operational.-

Balanced takeoff field length not to exceed 3810 m (12500 ft) (performed at standard day +10°C temperature)

Approach speed - limited to 81.3 m/sec (158 kts)

Fuel.- (in addition to basic mission requirements)

Provision for (1) headwinds and off-nominal operations equal to five percent trip fuel

(2) thirty minutes in holding pattern at 3048 m (10000 ft)

(3) one missed approach and "go-around"

(4) 463 km (250 n.mi.) to alternate airport to be flown at best altitude and Mach number (subsonic)

The foregoing proposed fuel reserve allowances for supersonic fleet air carrier operations were taken from the recommendations of reference 34. They are based on the requirements contained in Federal Air Regulations, Part 121, (FAR 121), Sections 121.645 and 121.647 modified to include recommendations

from the Air Transport Association (ATA). Requirements given here establish the mission profile on which the performance evaluation is based.

## Propulsion Sizing Constraints

During the engine and aircraft sizing studies, thrust-to-weight ratios ranging from 0.20 to 0.40 were evaluated. With the exception of noise criteria, the principal factors effecting power plant size are as follows:

- Takeoff field length
- Safety regulations applicable to takeoff which included balanced field length and maintaining a given minimum rate of climb with one engine inoperative
- Adequate thrust to achieve optimum cruise altitude before reaching climb ceiling
- Adequate power for acceleration, particularly through high drag transonic region, to attain desired cruise speed
- Cruise efficiency (low fuel consumption)
- Adequate engine performance to provide for operation at higher than normal ambient temperature, power extraction to operate accessories, and service airbleed
- Safety regulation, applicable to the approach condition, which requires capability of "pulling up" and "going around" with one engine inoperative

## Method of Analysis

A NASA-Langley developed computer program, described in reference 5, was used for the sizing, configuration selection, and determination of mission performance characteristics. Baseline aerodynamic, propulsion, and weight data are required as inputs to the program.

Aerodynamic inputs required are: trimmed takeoff lift and drag coefficients, in and out of ground effect, as a function of angle of attack and flap deflection; high speed lift-drag polars; and zero-lift drag coefficients, as a function of Mach number.

Propulsion input data, provided by Pratt and Whitney Aircraft, consisted of engine characteristics such as gross thrust, fuel flow and ram drag for maximum climb, maximum cruise and part-power cruise conditions at various altitudes and Mach numbers.

Weight data required consisted of semidetailed (group weight level) weights for structural components, propulsion systems, systems and equipment, operating

systems, payload (passengers and baggage) and fuel. Weights were used to determine proportionality constants which were then used in scaling parameters during the sizing synthesis.

Through reiterative operations, an array of candidate aircraft were synthesized by varying input parameters such as thrust-to-weight ratio, wing loading, and design gross weight. Data generated for this array were plotted to establish the "thumbprint" sizing plot shown in figure 55. Since the study objective was to determine the size of the aircraft required to fly a given payload at fixed range, within criteria constraints, the data are displayed in the form of constant takeoff gross weight contours as a function of thrust-to-weight ratio and wing loading. From this "thumbprint" plot, a candidate aircraft having the best potential for achieving design mission goals was identified in terms of the essential sizing parameters. Principal design parameters of the selected configuration are:

- Takeoff (or design gross) weight - 3051.5 kN (686000 lbf)
- Installed thrust-to-weight ratio - .254 (sea level standard day +8$^{o}$C)
- Wing loading - 3926 Pa (82 lb/ft$^{2}$)

This configuration was then the subject of a more detailed analysis to determine pertinent performance characteristics in evaluating compliance with mission goals. The conceptual aircraft was "flown," via the computer program, (ref. 5) in accordance with selected mission profiles. The Mach number-altitude climb/descent and mission profiles for the study aircraft are shown in figures 56 and 57, respectively, For each segment of the profile, the program determined enroute details such as thrust and fuel required, altitude, speed, and end point time of the segments. The profile used in this study is composed of the following segments:

- Taxi-out - estimated fuel for ten minutes warm-up and taxi-out
- Takeoff - approximately one minute at full takeoff thrust with credit for distance - takeoff with 20 degree flaps, angle of attack at 8.5 degrees, at standard day +10$^{o}$C temperature, takeoff field length limited to 3810 m (12500 ft)
- Climb and accelerate - climb and accelerate according to schedule shown in figure 56, 20 degree flaps, at standard day +8$^{o}$C temperature with speed restricted to 128.7 m/sec (250 kts) below 3048 m (10,000 ft) altitude - above this altitude program determines optimum climb schedule and cruise altitude for maximum range unless thrust available is inadequate to achieve that altitude and a climb ceiling is therefore reached
- Cruise - cruise begins at either optimum altitude or climb ceiling. The program selects the optimum cruise altitude by determining the altitude at which the Breguet range factor, V (L/D) SFC, is a maximum

- Descent - Descent occurs in accordance with the descent schedule of figure 56. Deceleration, range, fuel, and time are computed. Fuel estimate is based on idle power fuel flow

- Taxi-in - fuel is estimated based on five minute taxi-in time at essentially idle power - this fuel taken out of reserves at destination

Results of the mission performance evaluation are summarized in table XVI. It should be noted that these results are valid for a standard day +8°C temperature. Since the trip range of 8234 km (4446 n.mi.), shown in table XVI, is 98.8 percent of the range objective, it is apparent that sizing is quite close to optimum. This "shortfall" could be made up by an increase of about 17.29 kN (3890 lbf) in fuel accompanied by an increase of 4.3 kN (973 lbf) in engine and structural weights. Cruise L/D, an indicator of aerodynamic efficiency, is 9.09 (averaged). Start of cruise L/D is about four percent higher for the AST-105-1 than for the 292 passenger AST-100.

## Off-Design Operation

Since it is quite likely that the aircraft may, on occasion, be required to operate subsonically and (or) at less than 100 percent passenger load factor, additional mission analyses were performed for several cruise speeds and at a sufficient number of reduced payloads to generate the plot of figure 58. From this figure it can be seen, as would be expected, that operating off-design from supersonic cruise results in degraded performance. However, if subsonic cruise were to be necessary with the AST-105-1, cruise at M = 0.90 would provide better payload-range characteristics than cruise at M = 0.95.

The relationship between length of subsonic flight segment and total range for several passenger load factors was determined through further mission analysis. Results for two of the passenger load factors (60 and 100 percent) used in the analysis are shown in figure 59.

To establish the impact of either technology improvements or, in the case of over-optimism, deficiencies, a series of off-design evaluations were performed. Parameters considered as variables are changes in structural weight ($\Delta$STW), aerodynamic drag ($\Delta C_D$), and specific fuel consumption ($\Delta$SFC). Range sensitivity to these parameters is presented in figure 60.

## ECONOMICS

For the airline, as potential purchaser of transport aircraft, a significant item of consideration is profitability in terms of expected return on investment (ROI) in equipment. Therefore, ROI determined with as much realism as possible, is an essential element in early assessment of the economic viability of a conceptual design. Hence, a value for ROI was established in relation to fare-range points for the AST-105-1.

A NASA-Langley unpublished computer program was used for the economic analyses reported here. It consists of a direct operating cost (DOC) module

based on the Air Transport Association model (ref. 35), an indirect operating cost (IOC) module based on a Lockheed-California Company model (ref. 36) and a ROI module. The first two modules provide part of the input required by the latter.

Basic inputs to the DOC and IOC modules are presented in table XVII. Monetary inputs and outputs are in terms of 1976 dollars. Analyses were performed for both 60 and 100 percent passenger load factors at subsonic (M = 0.90) and supersonic cruise (M = 2.62) for various ranges. The effect of these parameters on DOC can be seen in figure 61.

The value of ROI was not calculated per se but rather was initially assumed and subsequently established. In brief, the procedure was as follows: cash flow in (sum of depreciation and profit after taxes and interest) was determined for each year of aircraft life and an interactive, repetitive calculation was performed which successively selected larger values of revenue to determine the actual revenue required to balance discounted cash flow in against cash flow out (initial cash investment). The discount rate or "internal" ROI was fixed, in this case at 15 percent, with fares and revenues necessary for cash flow in to balance initial cash investment being computed.

Results, in terms of ticket price variation with range, for an ROI of 15 percent are presented in figure 62 for the aforementioned passenger load factors and cruise speeds. From this plot of ticket price, it is apparent that operation of the AST-105-1 in the subsonic cruise mode would impose a significant burden on the fare-paying passenger. Hence, subsonic operation would not be economically viable from the traveler's viewpoint.

## CONCLUDING REMARKS

A new Advanced Supersonic Technology (AST) configuration designated AST-105-1 has been defined by application of: an expanded data base developed in response to previous aerodynamic concerns such as low-speed trim and longitudinal, lateral-directional stability and control; a recently developed aircraft sizing and performance computer program; a new noise prediction program; and, a new engine concept by Pratt and Whitney Aircraft, which offers prospect of noise reduction by the technique of coannular nozzle design. It should be noted that the AST-105-1 has a transpacific design range objective with 273 passengers whereas previous NASA-Langley AST configurations had a transatlantic range objective with 292 passengers; both at a hot day cruise Mach number of 2.62.

Lift-to-drag ratio, L/D, at the start of cruise is approximately four percent higher for the AST-105-1 than for the AST-100. This corresponds to an increment in L/D of 0.32.

Trimmable center-of-gravity range is from 42.55 to 60.10 percent of the reference mean aerodynamic chord, or a delta shift of 4.7 m (15.5 ft). Due to the inherently high positive dihedral effect of arrow-wing configurations, especially in high-lift approach, 75 percent of the available lateral control

is insufficient for 15.4 m/sec (30 kt) crosswind operation by the AST-105-1; the limiting crosswind being 11.6 m/sec (22.5 kt). Crosswind landing gear or a significant reduction (approximately 25 percent) in positive dihedral would be required to meet the criteria. Calculated low-speed wing shape for arrow-wing AST concepts, although not yet wind tunnel tested in high-lift, indicates significant geometric anhedral which would reduce the extent of the problem but necessitate a longer landing gear. If roll control power is increased to meet lateral trim requirements there will also be an attendant improvement in lateral response as gauged by Pilot Rating. The limited data available on forebody strakes indicate a potentially significant contribution to lateral-directional stability. Hence, further testing of such devices on AST type configurations is recommended.

Mission or trip range for the AST-105-1, computed for a standard $+8^{o}$C day, is 100 km (54 n.mi.) less than the design goal of 8334 km (4500 n.mi.). This is 98.8 percent of the design objective, which indicates that the design point (thrust-to-weight and wing loading) defined by the Langley Aircraft Sizing and Performance Program is quite close to optimum. This "shortfall" in range could be covered by an increase of about 17.29 kN (3890 lbf) of fuel with an associated increase of 4.3 kN (973 lbf) in inert weight. Adequate volume is available for this amount of fuel.

Centerline and maximum sideline noise (jet only) was calculated for both conventional (without power cutback) takeoff procedure and normal power takeoff with accelerating climb followed by cutback. The latter takeoff procedure results in a factor of two reduction in area covered by the 115 EPNdB noise contour. Initial noise results from advanced programmed throttle takeoff and approach operating procedures, not yet optimized, indicate that such can be an important additional method of noise alleviation.

The AST-105-1 would, during transonic climb, generate a caustic or super boom but it would occur far offshore of any inhabited area at about 163 km (88 n.mi.) from brake release for the 100 per cent passenger load factor condition.

Off-design operation of the AST-105-1 in the subsonic cruise mode at either 100 or 60 percent passenger load factor would not be monetarily attractive to the fare paying passenger.

## REFERENCES


1. Advanced Supersonic Technology Concept Study, Reference Characteristics. NASA CR-132374, 1973.

2. Baber, Hal T., Jr.; and Swanson, E. E.: Advanced Supersonic Technology Concept AST-100 Characteristics Developed in a Baseline - Update Study. NASA TM X-72815, 1976.

3. Smith, Paul M.: Low-Speed Aerodynamic Characteristics from Wind-Tunnel Tests of a Large-Scale Advanced Arrow-Wing Supersonic-Cruise Transport Concept. NASA CR-145280, 1978.

4. Coe, Paul L., Jr.; Smith, Paul M.; and Parlett, Lysle P.: Low-Speed Wind Tunnel Investigation of an Advanced Supersonic Cruise Arrow-Wing Configuration. NASA TM-74043, 1977.

5. Fetterman, David E., Jr.: Preliminary Sizing and Performance Evaluation of Supersonic Cruise Aircraft, NASA TM X-73936, 1976.

6. Raney, John P.: Noise Prediction Technology for CTOL Aircraft. NASA TM-78700, 1978.

7. Mechtly, E. A.: The International System of Units - Physical Constants and Conversion Factors (Second Revision), NASA SP-7012, 1973.

8. Advanced Supersonic Configurations Studies Using Multicycle Engines for Civil Aircraft. NASA CR-132723, 1975.

9. Airplane Turbulent Skin-Friction Drag. NASA Program Number D1266. (See Ref. 12)

10. Grantham, William D.; Nguyen, Luat T.; Neubauer, Milton, J., Jr.; and Smith, Paul M.: Simulator Study of the Low-Speed Handling Qualities of a Supersonic Cruise Arrow-Wing Transport Configuration During Approach and Landing. NASA CP-001, Part 1, 1976.

11. Harris, Roy V., Jr.: An Analysis and Correlation of Aircraft Wave Drag. NASA TM X-947, 1964.

12. Sommer, Simon C.; and Short, Barbara, J.: Free Flight Measurements of Turbulent Boundary Layer Skin Friction in the Presence of Severe Aerodynamic Heating at Mach Numbers from 2.8 to 7.0. NACA TN 3391, 1955.

13. Hoerner, S. F.: Fluid Dynamic Drag. 1965. (Library of Congress Catalogue Card No. 64-19666)

14. Miranda, Luis; Elliot, R. D.; and Baker, W. M.: A Generalized Vortex Lattice Method for Subsonic and Supersonic Flow Applications. NASA CR-2865, 1977.

15. Carlson, Harry W.; and Miller, David S.: Numerical Methods for the Design and Analysis of Wings at Supersonic Speeds. NASA TN D-7713, 1974.

16. Mach 2.7 Fixed Wind SST Model 969-336C (SCAT 15F). The Boeing Company, Document No. D6A-11666-1, 1969.

17. Wrenn, G. A.; McCullers, L. A.; and Newsom, J. R.: Structural and Aeroelastic Studies of a Supersonic Arrow Wing Configuration. NASA CR-145325, 1977.

18. Studies of the Impact of Advanced Technologies Applied to Supersonic Transport Aircraft. Douglas Aircraft Company, MDC J-4394, 1973.

19. Lockwood, Vernard E.: Effect of Leading-Edge Contour and Vertical-Tail Configuration on the Low-Speed Stability Characteristics of a Supersonic Transport Model Having a Highly Swept Arrow-Wing, NASA TM-78683, 1978.

20. Advanced Supersonic Technology, Liquid Hydrogen Concepts Study - Volume II. NASA CR-132616, 1976.

21. Flying Qualities of Piloted Airplanes. Military Specification MIL-F-8785 B (ASG), 1969.

22. Shomber, H. A.; and Gertsen, W. M.: Longitudinal Handling Qualities Criteria: An Evaluation. Journal of Aircraft, Vol. 4, No. 4, 1967.

23. Sudderth, Robert W.; Bohn, Jeff G.; Caniff, Martin A.; and Bennett, Gregory R.: Development of Longitudinal Handling Qualities Criteria for Large Advanced Supersonic Aircraft. NASA CR-137635, 1975.

24. Bisgood, P. L: A Review of Recent Research on Handling Qualities, and Its Application to the Handling Problems of Large Aircraft. Ministry of Aviation, R&M No. 3458, 1964.

25. Grantham, William D.; Nguyen, Luat T.; Deal, Perry L.; Neubauer, Milton, J., Jr.; Smith, Paul M.; and Gregory, Frederick D.: Ground-Based and In-Flight Simulator Studies of Low-Speed Handling Characteristics of Two Supersonic Cruise Transport Concepts. NASA TP-1240, July 1978.

26. Aerospace Recommended Practice - Design Objectives for Flying Qualities for Civil Transport Aircraft. ARP 842B, Society of Automotive Engineers, 1964, (revised 1970).

27. Hines, R. W.: Advanced Supersonic Transport Propulsion Requirements. Pratt & Whitney Aircraft, AIAA/SAE 13th Propulsion Conference, Orlando, Florida, July 11-13, 1977.

28. Koncek, J. L.; and Syberg, J.: Transonic and Supersonic Tests of a Mach 2.65 Mixed Compression Axisymmetric Intake. NASA CR-1977, 1972.

29. DOT/FAA Noise Standards: Aircraft Type and Airworthiness Certification, FAR Part 36, June 1974.

30. Carlson, Harry W.: Correlation of Sonic Boom Theory with Wind Tunnel and Flight Measurements. NASA TR R-213, 1964.

31. Middleton, Wilbur D.; and Carlson, Harry W.: A Numerical Method for Calculating Near-Field Sonic-Boom Pressure Signatures. NASA TN D-3982, 1965.

32. Thomas, Charles L.: Extrapolation of Sonic Boom Pressure Signatures by the Wave Form Parameter Method. NASA TN D-6832, 1972.

33. Haglund, George T.; and Kane, Edward J.: Effect of SST Operational Maneuvers on Sonic Boom. AIAA Paper No. 72-196, 1972.

34. An Airline's View of Reserve Fuel Requirements for the Supersonic Transport. Lockheed-California Company and Trans World Airlines, Inc., LR 26133, 1973.

35. Standard Method of Estimating Comparative Direct Operating Costs of Turbine Powered Transport Airplanes. Air Transport Association of America, 1967.

36. Indirect Operating Expense Coefficients, Years 1963 through 1977. Lockheed-California Company, COA/1277, 1978.

TABLE I.- AST-105-1 GEOMETRIC CHARACTERISTICS

| GEOMETRY | | WING | HORIZONTAL | VERTICAL | WING FIN |
|---|---|---|---|---|---|
| AREA(GROSS), S | $m^2$ ($ft^2$) | 857.31 (9228) | 83.15 (895) | 33.26 (358) | 18.21 (196) |
| MAC (GROSS), $\bar{c}$ | m (ft) | 31.25 (102.53) | 8.98 (29.46) | 8.95 (29.37) | 7.21 (23.64) |
| AREA (REF), $S_{REF}$ | $m^2$ ($ft^2$) | 777.23 (8366) | ——— | ——— | ——— |
| MAC (REF), $\bar{c}_{REF}$ | m (ft) | 26.87 (88.16) | ——— | ——— | ——— |
| AREA (EXPOSED), $S_{EXP}$ | $m^2$ $ft^2$ | ——— | 57.60 (620) | 33.26 (358) | 18.21 (196) |
| SPAN, b | m (ft) | 38.47 (126.22) | 10.55 (34.60) | 4.19 (13.74) | 3.00 (9.85) |
| ASPECT RATIO(GROSS) | | 1.721 | 1.338 | .527 | .495 |
| ASPECT RATIO (REF) | | 1.904 | ——— | ——— | ——— |
| SWEEP, $\Lambda_{LE}$ | DEG | 74 70.84 60 | 55 | 68.2 | 73.42 |
| ROOT CHORD | m (ft) | 51.12 (167.71) | 12.98 (42.57) | 12.84 (42.14) | 10.67 (35.00) |
| TIP CHORD | m (ft) | 4.92 (16.16) | 2.79 (9.15) | 3.04 (9.99) | 1.45 (4.76) |
| ROOT t/c | % | ——— | 3.000 | 2.996 | 2.996 |
| TIP t/c | % | ——— | 3.000 | 2.996 | 2.996 |
| TAPER RATIO, $\lambda$ | | ——— | .215 | .237 | .136 |
| DIHEDRAL | DEG | ——— | -15 | ——— | ——— |
| VOL. COEFF. (GROSS), $\bar{V}$ ⊛ | | ——— | .113 | .041 | .012(EACH) |
| VOL. COEFF. (REF), $\bar{V}$ ✳✳ | | ——— | .146 | .046 | .014(EACH) |

⊛ BASED ON GROSS WING CHARACTERISTICS

✳✳ BASED ON REFERENCE WING CHARACTERISTICS

SEE Fig. 4 FOR TAIL AND WING FIN "ARMS" (WING .25C TO SURFACE .25C)

TABLE II.- LOW SPEED TRIMMED LIFT AND DRAG COEFFICIENTS

$L_{1,2}$= 30°, $L_6$= K45°; $t_3 = t_4$ = 5°; CG = .601$\bar{c}$, OGE, LANDING GEAR RETRACTED

$t_1 = t_2 = 0°$

| | | | | | | | | | | | | | |
|---|---|---|---|---|---|---|---|---|---|---|---|---|---|
| α, deg | -3.73 | -2.50 | -0.70 | 0.50 | 1.75 | 2.95 | 4.20 | 5.40 | 6.65 | 9.10 | 14.10 | 17.30 | 21.75 |
| $C_L$ | 0 | .05 | .123 | .173 | .223 | .273 | .323 | .373 | .423 | .523 | .723 | .850 | 1.023 |
| $C_D$ | .0164 | .0156 | .0151 | .0163 | .0190 | .0236 | .0305 | .0397 | .0510 | .0811 | .1769 | .2728 | .4344 |

$t_1 = t_2 = 10°$

| | | | | | | | | | | | | | |
|---|---|---|---|---|---|---|---|---|---|---|---|---|---|
| α, deg | -4.93 | -3.63 | -1.70 | -0.27 | 1.00 | 2.25 | 3.53 | 4.75 | 6.05 | 8.47 | 13.50 | 16.47 | 21.27 |
| $C_L$ | 0 | .05 | .1353 | .1853 | .2353 | .2853 | .3353 | .3853 | .4353 | .5353 | .7353 | .850 | 1.0353 |
| $C_D$ | .0204 | .0187 | .0177 | .0188 | .0213 | .0258 | .0324 | .0411 | .0523 | .0821 | .1773 | .2631 | .4361 |

$t_1 = t_2 = 20°$

| | | | | | | | | | | | | | |
|---|---|---|---|---|---|---|---|---|---|---|---|---|---|
| α, deg | -6.00 | -4.80 | -3.50 | -2.25 | -1.00 | 0.25 | 1.50 | 2.75 | 4.00 | 5.25 | 7.75 | 12.87 | 15.47 | 20.83 |
| $C_L$ | 0 | .05 | .10 | .15 | .20 | .25 | .30 | .35 | .40 | .45 | .55 | .75 | .85 | 1.05 |
| $C_D$ | .0294 | .0266 | .0248 | .0241 | .0248 | .0268 | .0305 | .0363 | .0441 | .0543 | .0825 | .1734 | .2475 | .4385 |

$t_1 = t_2 = 30°$

| | | | | | | | | | | | | | |
|---|---|---|---|---|---|---|---|---|---|---|---|---|---|
| α, deg | -6.90 | -5.63 | -4.40 | -2.75 | -1.47 | -0.25 | 1.00 | 2.25 | 3.55 | 4.80 | 7.35 | 12.50 | 14.75 | 20.60 |
| $C_L$ | 0 | .05 | .10 | .1666 | .2166 | .2666 | .3166 | .3666 | .4166 | .4666 | .5666 | .7666 | .850 | 1.0666 |
| $C_D$ | .0418 | .0381 | .0353 | .0335 | .0340 | .0359 | .0399 | .0462 | .0552 | .0661 | .0954 | .1910 | .2523 | .4709 |

TABLE III.- HIGH SPEED DRAG POLAR DATA

MACH NUMBER = .50
ITAIL = 4.0 DEG

CDFRIC = .006336
CDROUGH = .000285
CDPO = .001922

| CL | CDI TAIL | CD TOTAL | L/D |
|---|---|---|---|
| 0.00 | .000084 | .010556 | 0.000 |
| .01 | .000096 | .010064 | .994 |
| .02 | .000103 | .009644 | 2.074 |
| .03 | .000106 | .009296 | 3.227 |
| .04 | .000105 | .009019 | 4.435 |
| .05 | .000101 | .008816 | 5.672 |
| .06 | .000095 | .008686 | 6.907 |
| .07 | .000087 | .008631 | 8.110 |
| .08 | .000079 | .008651 | 9.248 |
| .09 | .000069 | .008746 | 10.290 |
| .10 | .000058 | .008915 | 11.217 |
| .11 | .000043 | .009156 | 12.014 |
| .12 | .000023 | .009470 | 12.672 |
| .13 | -.000001 | .009854 | 13.192 |
| .14 | -.000028 | .010312 | 13.577 |
| .16 | -.000087 | .011450 | 13.974 |
| .18 | -.000144 | .012894 | 13.961 |
| .20 | -.000204 | .014639 | 13.662 |
| .22 | -.000276 | .016677 | 13.192 |
| .24 | -.000360 | .019006 | 12.628 |
| .28 | -.000553 | .024552 | 11.404 |
| .32 | -.000757 | .031303 | 10.223 |
| .36 | -.000998 | .039233 | 9.176 |
| .40 | -.001300 | .048318 | 8.278 |
| .45 | -.001666 | .061398 | 7.329 |
| .50 | -.001800 | .076609 | 6.527 |

MACH NUMBER = .60
ITAIL = 4.0 DEG

CDFRIC = .006188
CDROUGH = .000278
CDPO = .001922

| CL | CDI TAIL | CD TOTAL | L/D |
|---|---|---|---|
| 0.00 | .000099 | .010537 | 0.000 |
| .01 | .000109 | .010025 | .998 |
| .02 | .000114 | .009584 | 2.087 |
| .03 | .000115 | .009215 | 3.256 |
| .04 | .000112 | .008920 | 4.484 |
| .05 | .000106 | .008699 | 5.748 |
| .06 | .000099 | .008552 | 7.016 |
| .07 | .000090 | .008482 | 8.253 |
| .08 | .000081 | .008488 | 9.425 |
| .09 | .000073 | .008571 | 10.500 |
| .10 | .000063 | .008730 | 11.454 |
| .11 | .000050 | .008963 | 12.273 |
| .12 | .000033 | .009268 | 12.947 |
| .13 | .000010 | .009645 | 13.479 |
| .14 | -.000018 | .010093 | 13.871 |
| .16 | -.000082 | .011212 | 14.270 |
| .18 | -.000146 | .012638 | 14.242 |
| .20 | -.000210 | .014372 | 13.916 |
| .22 | -.000279 | .016409 | 13.407 |
| .24 | -.000354 | .018747 | 12.802 |
| .28 | -.000521 | .024328 | 11.509 |
| .32 | -.000713 | .031114 | 10.285 |
| .36 | -.000958 | .039077 | 9.213 |
| .40 | -.001268 | .048205 | 8.298 |
| .45 | -.001654 | .061346 | 7.335 |
| .50 | -.001810 | .076639 | 6.524 |

TABLE III.- CONTINUED

MACH NUMBER = .80
ITAIL = 4.0 DEG

CDFRIC = .005941
CDROUGH = .000267
CDPD = .001957

| CL | CDI TAIL | CD TOTAL | L/D |
|---|---|---|---|
| 0.00 | .000101 | .010689 | 0.000 |
| .01 | .000111 | .010114 | .989 |
| .02 | .000117 | .009616 | 2.080 |
| .03 | .000118 | .009194 | 3.263 |
| .04 | .000117 | .008850 | 4.520 |
| .05 | .000113 | .008583 | 5.825 |
| .06 | .000106 | .008395 | 7.147 |
| .07 | .000098 | .008286 | 8.448 |
| .08 | .000088 | .008255 | 9.691 |
| .09 | .000077 | .008305 | 10.837 |
| .10 | .000065 | .008433 | 11.858 |
| .11 | .000050 | .008639 | 12.733 |
| .12 | .000032 | .008923 | 13.448 |
| .13 | .000011 | .009284 | 14.002 |
| .14 | -.000013 | .009724 | 14.398 |
| .16 | -.000064 | .010840 | 14.761 |
| .18 | -.000121 | .012273 | 14.666 |
| .20 | -.000181 | .014025 | 14.260 |
| .22 | -.000249 | .016092 | 13.671 |
| .24 | -.000323 | .018474 | 12.991 |
| .28 | -.000486 | .024192 | 11.574 |
| .32 | -.000659 | .031188 | 10.260 |
| .36 | -.000852 | .039455 | 9.124 |
| .40 | -.001095 | .048960 | 8.170 |
| .45 | -.001463 | .062590 | 7.190 |
| .50 | -.001697 | .078368 | 6.380 |

MACH NUMBER = .95
ITAIL = 4.0 DEG

CDFRIC = .005891
CDROUGH = .000395
CDPD = .002886

| CL | CDI TAIL | CD TOTAL | L/D |
|---|---|---|---|
| 0.00 | .000108 | .013088 | 0.000 |
| .01 | .000116 | .012303 | .813 |
| .02 | .000120 | .011607 | 1.723 |
| .03 | .000122 | .011002 | 2.727 |
| .04 | .000121 | .010486 | 3.815 |
| .05 | .000118 | .010060 | 4.970 |
| .06 | .000113 | .009724 | 6.170 |
| .07 | .000106 | .009479 | 7.385 |
| .08 | .000097 | .009324 | 8.580 |
| .09 | .000087 | .009259 | 9.720 |
| .10 | .000074 | .009285 | 10.770 |
| .11 | .000059 | .009400 | 11.702 |
| .12 | .000042 | .009606 | 12.493 |
| .13 | .000023 | .009902 | 13.129 |
| .14 | .000003 | .010290 | 13.606 |
| .16 | -.000036 | .011342 | 14.107 |
| .18 | -.000077 | .012761 | 14.106 |
| .20 | -.000128 | .014540 | 13.755 |
| .22 | -.000190 | .016676 | 13.192 |
| .24 | -.000259 | .019175 | 12.516 |
| .28 | -.000404 | .025272 | 11.080 |
| .32 | -.000557 | .032838 | 9.745 |
| .36 | -.000719 | .041870 | 8.598 |
| .40 | -.000920 | .052339 | 7.642 |
| .45 | -.001243 | .067430 | 6.674 |
| .50 | -.001556 | .084838 | 5.894 |

TABLE III.- CONTINUED

MACH NUMBER = 1.05
ITAIL = 4.0 DEG

CDWAVE = .002570
CDFRIC = .005654
CDROUGH = .000492
CDPD = .001492

| CL | CDI TAIL | CD TOTAL | L/D |
|---|---|---|---|
| 0.00 | .000359 | .015266 | 0.000 |
| .01 | .000303 | .014262 | .701 |
| .02 | .000246 | .013364 | 1.497 |
| .03 | .000187 | .012570 | 2.387 |
| .04 | .000126 | .011881 | 3.367 |
| .05 | .000063 | .011296 | 4.426 |
| .06 | -.000002 | .010816 | 5.547 |
| .07 | -.000070 | .010441 | 6.704 |
| .08 | -.000139 | .010171 | 7.865 |
| .09 | -.000210 | .010006 | 8.995 |
| .10 | -.000283 | .009945 | 10.055 |
| .11 | -.000358 | .009989 | 11.012 |
| .12 | -.000435 | .010138 | 11.836 |
| .13 | -.000515 | .010392 | 12.510 |
| .14 | -.000596 | .010750 | 13.023 |
| .16 | -.000764 | .011781 | 13.581 |
| .18 | -.000940 | .013231 | 13.604 |
| .20 | -.001125 | .015101 | 13.244 |
| .22 | -.001317 | .017389 | 12.652 |
| .24 | -.001517 | .020096 | 11.943 |
| .28 | -.001942 | .026768 | 10.460 |
| .32 | -.002399 | .035115 | 9.113 |
| .36 | -.002887 | .045139 | 7.975 |
| .40 | -.003408 | .056840 | 7.037 |
| .45 | -.004104 | .073822 | 6.096 |
| .50 | -.004850 | .093423 | 5.352 |

MACH NUMBER = 1.10
ITAIL = 4.0 DEG

CDWAVE = .002599
CDFRIC = .005594
CDROUGH = .000559
CDPD = .002228

| CL | CDI TAIL | CD TOTAL | L/D |
|---|---|---|---|
| 0.00 | .000296 | .015900 | 0.000 |
| .01 | .000262 | .014908 | .671 |
| .02 | .000224 | .014023 | 1.426 |
| .03 | .000182 | .013245 | 2.265 |
| .04 | .000137 | .012574 | 3.181 |
| .05 | .000087 | .012010 | 4.163 |
| .06 | .000032 | .011554 | 5.193 |
| .07 | -.000026 | .011204 | 6.248 |
| .08 | -.000088 | .010962 | 7.298 |
| .09 | -.000154 | .010827 | 8.313 |
| .10 | -.000224 | .010799 | 9.260 |
| .11 | -.000298 | .010878 | 10.112 |
| .12 | -.000377 | .011064 | 10.846 |
| .13 | -.000459 | .011358 | 11.446 |
| .14 | -.000546 | .011758 | 11.906 |
| .16 | -.000731 | .012881 | 12.421 |
| .18 | -.000932 | .014432 | 12.472 |
| .20 | -.001149 | .016412 | 12.186 |
| .22 | -.001383 | .018820 | 11.690 |
| .24 | -.001632 | .021657 | 11.082 |
| .28 | -.002180 | .028616 | 9.785 |
| .32 | -.002793 | .037289 | 8.582 |
| .36 | -.003471 | .047677 | 7.551 |
| .40 | -.004213 | .059779 | 6.691 |
| .45 | -.005232 | .077316 | 5.820 |
| .50 | -.006352 | .097533 | 5.126 |

TABLE III.- CONTINUED

MACH NUMBER = 1.20
ITAIL = 4.0 DEG

CDWAVE = .002721
CDFRIC = .005482
CDROUGH = .000614
CDPO = .002561

| CL | CDI TAIL | CD TOTAL | L/D |
|---|---|---|---|
| 0.00 | .000253 | .015831 | 0.000 |
| .01 | .000240 | .014895 | .671 |
| .02 | .000221 | .014067 | 1.422 |
| .03 | .000195 | .013346 | 2.248 |
| .04 | .000162 | .012733 | 3.141 |
| .05 | .000121 | .012227 | 4.089 |
| .06 | .000074 | .011829 | 5.072 |
| .07 | .000020 | .011538 | 6.067 |
| .08 | -.000042 | .011355 | 7.046 |
| .09 | -.000110 | .011279 | 7.980 |
| .10 | -.000185 | .011310 | 8.842 |
| .11 | -.000268 | .011449 | 9.608 |
| .12 | -.000357 | .011695 | 10.260 |
| .13 | -.000454 | .012049 | 10.789 |
| .14 | -.000557 | .012511 | 11.191 |
| .16 | -.000785 | .013755 | 11.632 |
| .18 | -.001041 | .015430 | 11.666 |
| .20 | -.001325 | .017534 | 11.406 |
| .22 | -.001637 | .020069 | 10.962 |
| .24 | -.001977 | .023033 | 10.420 |
| .28 | -.002742 | .030250 | 9.256 |
| .32 | -.003619 | .039186 | 8.166 |
| .36 | -.004608 | .049842 | 7.223 |
| .40 | -.005709 | .062216 | 6.429 |
| .45 | -.007244 | .080102 | 5.618 |
| .50 | -.008954 | .100674 | 4.967 |

MACH NUMBER = 1.30
ITAIL = 4.0 DEG

CDWAVE = .002911
CDFRIC = .005373
CDROUGH = .000586
CDPO = .002521

| CL | CDI TAIL | CD TOTAL | L/D |
|---|---|---|---|
| 0.00 | .000283 | .015368 | 0.000 |
| .01 | .000269 | .014486 | .690 |
| .02 | .000247 | .013713 | 1.458 |
| .03 | .000219 | .013049 | 2.299 |
| .04 | .000183 | .012494 | 3.202 |
| .05 | .000140 | .012047 | 4.150 |
| .06 | .000090 | .011709 | 5.124 |
| .07 | .000033 | .011480 | 6.098 |
| .08 | -.000031 | .011360 | 7.042 |
| .09 | -.000103 | .011348 | 7.931 |
| .10 | -.000182 | .011446 | 8.737 |
| .11 | -.000268 | .011652 | 9.441 |
| .12 | -.000361 | .011967 | 10.028 |
| .13 | -.000461 | .012391 | 10.492 |
| .14 | -.000568 | .012923 | 10.833 |
| .16 | -.000805 | .014315 | 11.177 |
| .18 | -.001070 | .016142 | 11.151 |
| .20 | -.001364 | .018404 | 10.867 |
| .22 | -.001686 | .021102 | 10.426 |
| .24 | -.002037 | .024235 | 9.903 |
| .28 | -.002826 | .031806 | 8.803 |
| .32 | -.003729 | .041119 | 7.782 |
| .36 | -.004747 | .052172 | 6.900 |
| .40 | -.005880 | .064967 | 6.157 |
| .45 | -.007458 | .083408 | 5.395 |
| .50 | -.009215 | .104570 | 4.781 |

TABLE III.- CONTINUED

MACH NUMBER = 1.40
ITAIL = 5.0 DEG

CDWAVE = .002863
CDFRIC = .005276
CDROUGH = .000549
CDPO = .002356

| CL | CDI TAIL | CD TOTAL | L/D |
|---|---|---|---|
| 0.00 | .000303 | .014624 | 0.000 |
| .01 | .000304 | .013807 | .724 |
| .02 | .000298 | .013100 | 1.527 |
| .03 | .000286 | .012504 | 2.399 |
| .04 | .000267 | .012019 | 3.328 |
| .05 | .000241 | .011645 | 4.294 |
| .06 | .000209 | .011381 | 5.272 |
| .07 | .000170 | .011227 | 6.235 |
| .08 | .000125 | .011185 | 7.152 |
| .09 | .000073 | .011253 | 7.998 |
| .10 | .000015 | .011432 | 8.747 |
| .11 | -.000050 | .011721 | 9.385 |
| .12 | -.000122 | .012121 | 9.900 |
| .13 | -.000200 | .012632 | 10.291 |
| .14 | -.000285 | .013254 | 10.563 |
| .16 | -.000474 | .014829 | 10.790 |
| .18 | -.000689 | .016846 | 10.685 |
| .20 | -.000931 | .019306 | 10.359 |
| .22 | -.001199 | .022209 | 9.906 |
| .24 | -.001493 | .025555 | 9.392 |
| .28 | -.002161 | .033574 | 8.340 |
| .32 | -.002933 | .043364 | 7.379 |
| .36 | -.003811 | .054924 | 6.555 |
| .40 | -.004794 | .068255 | 5.860 |
| .45 | -.006170 | .087409 | 5.148 |
| .50 | -.007710 | .109329 | 4.573 |

MACH NUMBER = 1.60
ITAIL = 5.0 DEG

CDWAVE = .002605
CDFRIC = .005098
CDROUGH = .000474
CDPO = .002012

| CL | CDI TAIL | CD TOTAL | L/D |
|---|---|---|---|
| 0.00 | .000097 | .012746 | 0.000 |
| .01 | .000101 | .012045 | .830 |
| .02 | .000102 | .011458 | 1.746 |
| .03 | .000098 | .010986 | 2.731 |
| .04 | .000090 | .010629 | 3.763 |
| .05 | .000077 | .010387 | 4.814 |
| .06 | .000060 | .010259 | 5.848 |
| .07 | .000038 | .010247 | 6.831 |
| .08 | .000012 | .010349 | 7.730 |
| .09 | -.000018 | .010567 | 8.517 |
| .10 | -.000053 | .010899 | 9.175 |
| .11 | -.000092 | .011346 | 9.695 |
| .12 | -.000135 | .011908 | 10.077 |
| .13 | -.000183 | .012585 | 10.330 |
| .14 | -.000235 | .013376 | 10.466 |
| .16 | -.000352 | .015304 | 10.454 |
| .18 | -.000487 | .017692 | 10.174 |
| .20 | -.000640 | .020539 | 9.738 |
| .22 | -.000810 | .023845 | 9.226 |
| .24 | -.000997 | .027611 | 8.692 |
| .28 | -.001425 | .036521 | 7.667 |
| .32 | -.001922 | .047269 | 6.770 |
| .36 | -.002490 | .059856 | 6.014 |
| .40 | -.003128 | .074280 | 5.385 |
| .45 | -.004023 | .094894 | 4.742 |
| .50 | -.005028 | .118380 | 4.224 |

TABLE III.- CONTINUED

MACH NUMBER = 1.80
ITAIL = 5.0 DEG

CDWAVE = .002438
CDFRIC = .004924
CDROUGH = .000414
CDPO = .001661

| CL | CDI TAIL | CD TOTAL | L/D |
|---|---|---|---|
| 0.00 | .000133 | .011407 | 0.000 |
| .01 | .000136 | .010803 | .926 |
| .02 | .000133 | .010315 | 1.939 |
| .03 | .000126 | .009943 | 3.017 |
| .04 | .000115 | .009689 | 4.129 |
| .05 | .000098 | .009551 | 5.235 |
| .06 | .000077 | .009529 | 6.296 |
| .07 | .000051 | .009625 | 7.273 |
| .08 | .000021 | .009837 | 8.132 |
| .09 | -.000014 | .010166 | 8.853 |
| .10 | -.000055 | .010612 | 9.423 |
| .11 | -.000099 | .011174 | 9.844 |
| .12 | -.000149 | .011854 | 10.123 |
| .13 | -.000203 | .012650 | 10.277 |
| .14 | -.000262 | .013562 | 10.323 |
| .16 | -.000394 | .015738 | 10.167 |
| .18 | -.000546 | .018380 | 9.793 |
| .20 | -.000716 | .021489 | 9.307 |
| .22 | -.000905 | .025065 | 8.777 |
| .24 | -.001113 | .029108 | 8.245 |
| .28 | -.001586 | .038595 | 7.255 |
| .32 | -.002135 | .049950 | 6.406 |
| .36 | -.002760 | .063172 | 5.699 |
| .40 | -.003460 | .078262 | 5.111 |
| .45 | -.004442 | .099750 | 4.511 |
| .50 | -.005543 | .124157 | 4.027 |

MACH NUMBER = 2.00
ITAIL = 4.0 DEG

CDWAVE = .002246
CDFRIC = .004753
CDROUGH = .000356
CDPO = .001326

| CL | CDI TAIL | CD TOTAL | L/D |
|---|---|---|---|
| 0.00 | .000033 | .010111 | 0.000 |
| .01 | .000042 | .009592 | 1.043 |
| .02 | .000045 | .009192 | 2.176 |
| .03 | .000043 | .008912 | 3.366 |
| .04 | .000036 | .008751 | 4.571 |
| .05 | .000024 | .008710 | 5.741 |
| .06 | .000007 | .008788 | 6.827 |
| .07 | -.000015 | .008986 | 7.790 |
| .08 | -.000042 | .009303 | 8.599 |
| .09 | -.000075 | .009740 | 9.241 |
| .10 | -.000113 | .010296 | 9.713 |
| .11 | -.000155 | .010971 | 10.026 |
| .12 | -.000203 | .011766 | 10.198 |
| .13 | -.000256 | .012681 | 10.252 |
| .14 | -.000315 | .013715 | 10.208 |
| .16 | -.000446 | .016142 | 9.912 |
| .18 | -.000598 | .019046 | 9.451 |
| .20 | -.000771 | .022428 | 8.917 |
| .22 | -.000964 | .026288 | 8.369 |
| .24 | -.001178 | .030626 | 7.836 |
| .28 | -.001667 | .040736 | 6.874 |
| .32 | -.002237 | .052757 | 6.066 |
| .36 | -.002890 | .066690 | 5.398 |
| .40 | -.003625 | .082534 | 4.846 |
| .45 | -.004659 | .105028 | 4.285 |
| .50 | -.005820 | .130508 | 3.831 |

TABLE III.- CONTINUED

MACH NUMBER = 2.20
ITAIL = 5.0 DEG

CDWAVE = .002104
CDFRIC = .004593
CDROUGH = .000317
CDPO = .000977

| CL | CDI TAIL | CD TOTAL | L/D |
|---|---|---|---|
| 0.00 | .000195 | .009323 | 0.000 |
| .01 | .000202 | .008850 | 1.130 |
| .02 | .000204 | .008502 | 2.352 |
| .03 | .000200 | .008280 | 3.623 |
| .04 | .000191 | .008184 | 4.888 |
| .05 | .000176 | .008212 | 6.088 |
| .06 | .000157 | .008367 | 7.171 |
| .07 | .000132 | .008647 | 8.096 |
| .08 | .000102 | .009052 | 8.838 |
| .09 | .000067 | .009583 | 9.392 |
| .10 | .000026 | .010239 | 9.767 |
| .11 | -.000019 | .011021 | 9.981 |
| .12 | -.000070 | .011928 | 10.060 |
| .13 | -.000127 | .012961 | 10.030 |
| .14 | -.000188 | .014119 | 9.916 |
| .16 | -.000327 | .016812 | 9.517 |
| .18 | -.000486 | .020007 | 8.997 |
| .20 | -.000667 | .023704 | 8.438 |
| .22 | -.000869 | .027902 | 7.885 |
| .24 | -.001091 | .032603 | 7.361 |
| .28 | -.001599 | .043511 | 6.435 |
| .32 | -.002191 | .056426 | 5.671 |
| .36 | -.002867 | .071349 | 5.046 |
| .40 | -.003626 | .088280 | 4.531 |
| .45 | -.004694 | .112267 | 4.008 |
| .50 | -.005892 | .139391 | 3.587 |

MACH NUMBER = 2.40
ITAIL = 5.0 DEG

CDWAVE = .002035
CDFRIC = .004443
CDROUGH = .000284
CDPO = .000903

| CL | CDI TAIL | CD TOTAL | L/D |
|---|---|---|---|
| 0.00 | .000171 | .008889 | 0.000 |
| .01 | .000180 | .008422 | 1.187 |
| .02 | .000183 | .008092 | 2.472 |
| .03 | .000180 | .007897 | 3.799 |
| .04 | .000172 | .007839 | 5.103 |
| .05 | .000158 | .007916 | 6.316 |
| .06 | .000138 | .008130 | 7.380 |
| .07 | .000112 | .008480 | 8.255 |
| .08 | .000080 | .008966 | 8.922 |
| .09 | .000042 | .009589 | 9.386 |
| .10 | -.000001 | .010347 | 9.664 |
| .11 | -.000051 | .011242 | 9.785 |
| .12 | -.000106 | .012273 | 9.778 |
| .13 | -.000167 | .013440 | 9.673 |
| .14 | -.000234 | .014743 | 9.496 |
| .16 | -.000385 | .017758 | 9.010 |
| .18 | -.000560 | .021318 | 8.444 |
| .20 | -.000758 | .025422 | 7.867 |
| .22 | -.000979 | .030071 | 7.316 |
| .24 | -.001224 | .035264 | 6.806 |
| .28 | -.001784 | .047285 | 5.922 |
| .32 | -.002437 | .061485 | 5.205 |
| .36 | -.003184 | .077863 | 4.623 |
| .40 | -.004024 | .096420 | 4.148 |
| .45 | -.005206 | .122681 | 3.668 |
| .50 | -.006534 | .152345 | 3.282 |

TABLE III.- CONCLUDED

MACH NUMBER = 2.62
ITAIL = 4.0 DEG

CDWAVE = .002068
CDFRIC = .004292
CDROUGH = .000258
CDPD = .001025

| CL | CDI TAIL | CD TOTAL | L/D |
|---|---|---|---|
| 0.00 | .000076 | .008826 | 0.000 |
| .01 | .000086 | .008321 | 1.202 |
| .02 | .000090 | .007970 | 2.509 |
| .03 | .000088 | .007773 | 3.859 |
| .04 | .000080 | .007730 | 5.175 |
| .05 | .000067 | .007840 | 6.378 |
| .06 | .000047 | .008104 | 7.404 |
| .07 | .000021 | .008522 | 8.214 |
| .08 | -.000010 | .009094 | 8.797 |
| .09 | -.000048 | .009819 | 9.166 |
| .10 | -.000091 | .010699 | 9.347 |
| .11 | -.000140 | .011732 | 9.376 |
| .12 | -.000196 | .012919 | 9.289 |
| .13 | -.000257 | .014259 | 9.117 |
| .14 | -.000324 | .015754 | 8.887 |
| .16 | -.000476 | .019204 | 8.331 |
| .18 | -.000652 | .023270 | 7.735 |
| .20 | -.000852 | .027951 | 7.155 |
| .22 | -.001075 | .033247 | 6.617 |
| .24 | -.001322 | .039159 | 6.129 |
| .28 | -.001887 | .052827 | 5.300 |
| .32 | -.002547 | .068956 | 4.641 |
| .36 | -.003303 | .087547 | 4.112 |
| .40 | -.004153 | .108598 | 3.683 |
| .45 | -.005349 | .138372 | 3.252 |
| .50 | -.006693 | .171992 | 2.907 |

TABLE IV.- LOW SPEED FORCE AND MOMENT COEFFICIENTS AND FORCE DERIVATIVES

| $\alpha$, deg | $C_{X_{(\delta_f = 0)}}$ | $C_{Z_{(\delta_f = 0)}}$ | $C_{X_{\delta_f}}$, $deg^{-1}$ | $C_{Z_{\delta_f}}$, $deg^{-1}$ | $C_{X_{LG}}$ | $C_{Z_{LG}}$ | $C_{m_{LG}}$ |
|---|---|---|---|---|---|---|---|
| | | | $\delta_f = 0°$ | | | | |
| -8 | .01429 | .19892 | -.00032 | -.00579 | -.01023 | .00144 | -.0015 |
| -4 | -.01600 | .03921 | -.00026 | -.00567 | -.00959 | .00067 | -.0015 |
| 0 | -.01420 | -.11900 | -.00020 | -.00554 | -.00902 | 0 | -.0014 |
| 4 | -.00596 | -.27609 | -.00017 | -.00546 | -.00849 | -.00059 | -.0014 |
| 8 | .00128 | -.43304 | -.00015 | -.00539 | -.00805 | -.00113 | -.0013 |
| 12 | .00510 | -.59494 | -.00013 | -.00535 | -.00764 | -.00162 | -.0013 |
| 16 | -.00441 | -.76172 | -.00012 | -.00533 | -.00728 | -.00209 | -.0012 |
| 20 | -.03002 | -.95166 | -.00010 | -.00533 | -.00694 | -.00253 | -.0012 |
| 24 | -.04580 | -1.14148 | -.00010 | -.00536 | -.00663 | -.00295 | -.0012 |
| | | | $\delta_f = 10°$ | | | | |
| -8 | -.02054 | .14124 | -.00022 | -.00616 | -.01001 | .00141 | -.0015 |
| -4 | -.02195 | -.00849 | -.00010 | -.00606 | -.00941 | .00066 | -.0014 |
| 0 | -.01930 | -.17200 | .00002 | -.00593 | -.00887 | 0 | -.0014 |
| 4 | -.01089 | -.32455 | .00012 | -.00586 | -.00839 | -.00059 | -.0014 |
| 8 | -.00420 | -.48026 | .00022 | -.00576 | -.00797 | -.00112 | -.0013 |
| 12 | .00012 | -.64507 | .00029 | -.00570 | -.00759 | -.00161 | -.0013 |
| 16 | -.00803 | -.81478 | .00038 | -.00566 | -.00724 | -.00208 | -.0012 |
| 20 | -.02643 | -.99079 | .00042 | -.00564 | -.00692 | -.00252 | -.0012 |
| 24 | -.05038 | -1.17836 | .00049 | -.00560 | -.00661 | -.00294 | -.0012 |

TABLE IV.- CONCLUDED

| $\alpha$, deg | $C_{x_{(\delta_f = 0)}}$ | $C_{z_{(\delta_f = 0)}}$ | $C_{x_{\delta_f}}$, $deg^{-1}$ | $C_{z_{\delta_f}}$, $deg^{-1}$ | $C_{x_{LG}}$ | $C_{z_{LG}}$ | $C_{m_{LG}}$ |
|---|---|---|---|---|---|---|---|
| | | | $\delta_f = 20°$ | | | | |
| -8 | -.02653 | .08855 | -.00017 | -.00666 | -.00979 | .00138 | -.0015 |
| -4 | -.03068 | -.06602 | 0 | -.00651 | -.00924 | .00065 | -.0014 |
| 0 | -.02670 | -.22700 | .00015 | -.00640 | -.00874 | 0 | -.0014 |
| 4 | -.01687 | -.38512 | .00030 | -.00627 | -.00829 | -.00058 | -.0013 |
| 8 | -.00632 | -.54417 | .00041 | -.00617 | -.00789 | -.00111 | -.0013 |
| 12 | -.00171 | -.69658 | .00052 | -.00606 | -.00754 | -.00160 | -.0012 |
| 16 | -.00941 | -.86511 | .00063 | -.00599 | -.00720 | -.00206 | -.0012 |
| 20 | -.02995 | -1.04102 | .00073 | -.00590 | -.00689 | -.00251 | -.0012 |
| 24 | -.04811 | -1.22771 | .00082 | -.00586 | -.00660 | -.00294 | -.0012 |
| | | | $\delta_f = 30°$ | | | | |
| -8 | -.04168 | .04827 | .00024 | -.00642 | -.00966 | .00136 | -.0015 |
| -4 | -.04302 | -.10927 | .00021 | -.00622 | -.00912 | .00064 | -.0014 |
| 0 | -.03670 | -.26900 | .00015 | -.00610 | -.00863 | 0 | -.0014 |
| 4 | -.02757 | -.42997 | .00007 | -.00602 | -.00821 | -.00057 | -.0013 |
| 8 | -.02001 | -.58548 | .00007 | -.00601 | -.00783 | -.00110 | -.0013 |
| 12 | -.01114 | -.73641 | .00006 | -.00604 | -.00748 | -.00159 | -.0012 |
| 16 | -.03348 | -.90738 | .00014 | -.00617 | -.00716 | -.00205 | -.0012 |
| 20 | -.05735 | -1.08505 | .00038 | -.00627 | -.00687 | -.00250 | -.0012 |
| 24 | -.08560 | -1.27724 | .00084 | -.00640 | -.00660 | -.00294 | -.0012 |

TABLE V.- LOW SPEED PITCHING MOMENT COEFFICIENT, $C_m$

| $\alpha$, deg \ $\delta_t$, deg | -20 | -15 | -10 | -5 | 0 | 5 | 10 | 15 | 20 |
|---|---|---|---|---|---|---|---|---|---|
| | | | | | $\delta_f = 0°$ | | | | |
| -8 | .1320 | .1107 | .0841 | .0525 | .0212 | -.0047 | -.0298 | -.0643 | -.0795 |
| -4 | .1372 | .1182 | .0916 | .0610 | .0295 | .0034 | -.0212 | -.0470 | -.0720 |
| 0 | .1421 | .1222 | .0969 | .0675 | .0367 | .0100 | -.0141 | -.0397 | -.0645 |
| 4 | .1454 | .1257 | .1013 | .0727 | .0420 | .0162 | -.0079 | -.0327 | -.0580 |
| 8 | .1482 | .1278 | .1032 | .0770 | .0480 | .0232 | -.0019 | -.0273 | -.0530 |
| 12 | .1507 | .1292 | .1054 | .0797 | .0530 | .0272 | .0021 | -.0220 | -.0483 |
| 16 | .1543 | .1320 | .1094 | .0850 | .0603 | .0333 | .0082 | -.0187 | -.0460 |
| 20 | .1617 | .1390 | .1161 | .0942 | .0720 | .0422 | .0146 | -.0130 | -.0410 |
| 24 | .1727 | .1493 | .1270 | .1072 | .0871 | .0582 | .0304 | .0020 | -.0285 |
| | | | | | $\delta_f = 10°$ | | | | |
| -8 | .1229 | .1077 | .0814 | .0490 | .0132 | -.0152 | -.0410 | -.0620 | -.0836 |
| -4 | .1345 | .1186 | .0922 | .0590 | .0210 | -.0027 | -.0265 | -.0495 | -.0714 |
| 0 | .1429 | .1260 | .0987 | .0653 | .0280 | .0062 | -.0159 | -.0387 | -.0615 |
| 4 | .1489 | .1300 | .1026 | .0712 | .0362 | .0132 | -.0092 | -.0320 | -.0549 |
| 8 | .1512 | .1302 | .1033 | .0723 | .0392 | .0153 | -.0086 | -.0310 | -.0526 |
| 12 | .1618 | .1370 | .1093 | .0770 | .0432 | .0178 | -.0060 | -.0278 | -.0500 |
| 16 | .1678 | .1412 | .1131 | .0828 | .0521 | .0255 | .0013 | -.0260 | -.0450 |
| 20 | .1685 | .1443 | .1185 | .0914 | .0636 | .0361 | .0114 | -.0215 | -.0355 |
| 24 | .1694 | .1466 | .1234 | .1014 | .0794 | .0533 | .0284 | -.0140 | -.0233 |

TABLE V.- CONCLUDED

| $\alpha$, deg \ $\delta_t$, deg | -20 | -15 | -10 | -5 | 0 | 5 | 10 | 15 | 20 |
|---|---|---|---|---|---|---|---|---|---|
| | | | | | $\delta_f = 20°$ | | | | |
| -8 | .1088 | .0978 | .0742 | .0422 | .0049 | -.0267 | -.0552 | -.0833 | -.1123 |
| -4 | .1170 | .1050 | .0808 | .0485 | .0116 | -.0178 | -.0458 | -.0757 | -.1043 |
| 0 | .1227 | .1092 | .0844 | .0523 | .0162 | -.0128 | -.0405 | -.0681 | -.0973 |
| 4 | .1258 | .1107 | .0860 | .0545 | .0193 | -.0088 | -.0356 | -.0630 | -.0910 |
| 8 | .1301 | .1143 | .0896 | .0590 | .0241 | -.0047 | -.0314 | -.0585 | -.0867 |
| 12 | .1376 | .1183 | .0926 | .0627 | .0300 | .0014 | -.0257 | -.0543 | -.0822 |
| 16 | .1450 | .1218 | .0958 | .0677 | .0378 | .0087 | -.0189 | -.0490 | -.0760 |
| 20 | .1466 | .1238 | .0992 | .0730 | .0464 | .0147 | -.0135 | -.0420 | -.0665 |
| 24 | .1451 | .1273 | .1064 | .0836 | .0587 | .0260 | -.0028 | -.0325 | -.0543 |
| | | | | | $\delta_f = 30°$ | | | | |
| -8 | .1007 | .0856 | .0606 | .0293 | -.0062 | -.0358 | -.0630 | -.0863 | -.1120 |
| -4 | .1109 | .0975 | .0728 | .0403 | .0033 | -.0255 | -.0517 | -.0780 | -.1055 |
| 0 | .1162 | .0986 | .0724 | .0420 | .0079 | -.0195 | -.0449 | -.0723 | -.0990 |
| 4 | .1225 | .1022 | .0758 | .0447 | .0115 | -.0157 | -.0412 | -.0673 | -.0937 |
| 8 | .1299 | .1087 | .0816 | .0498 | .0159 | -.0108 | -.0363 | -.0627 | -.0887 |
| 12 | .1364 | .1157 | .0879 | .0572 | .0232 | -.0043 | -.0310 | -.0573 | -.0845 |
| 16 | .1421 | .1215 | .0952 | .0653 | .0330 | .0045 | -.0215 | -.0507 | -.0793 |
| 20 | .1472 | .1270 | .1022 | .0744 | .0445 | .0130 | -.0142 | .0430 | -.0720 |
| 24 | .1469 | .1301 | .1075 | .0827 | .0551 | .0200 | -.0040 | -.0322 | -.0620 |

TABLE VI.- LOW SPEED LATERAL-DIRECTIONAL STABILITY AND CONTROL DERIVATIVES

| $\alpha$, deg / $deg^{-1}$ | $C_{y_{\delta_a}}$ | $C_{y_{fl_o}}$ | $C_{y_{fl_i}}$ | $C_{l_{\delta_a}}$ | $C_{l_{fl_o}}$ | $C_{l_{fl_i}}$ | $C_{m_{\delta_a}}$ | $C_{n_{fl_o}}$ | $C_{n_{fl_i}}$ |
|---|---|---|---|---|---|---|---|---|---|
| | | | | $\delta_f = 0°$ | | | | | |
| -8 | -.000353 | -.000090 | -.000010 | .000474 | .000365 | .000498 | .000094 | -.000011 | .000081 |
| -4 | -.000380 | -.000080 | -.000160 | .000471 | .000354 | .000496 | .000094 | .000050 | .000081 |
| 0 | -.000400 | -.000070 | -.000265 | .000465 | .000331 | .000492 | .000093 | .000100 | .000080 |
| 4 | -.000411 | -.000061 | -.000328 | .000451 | .000294 | .000484 | .000090 | .000130 | .000076 |
| 8 | -.000410 | -.000054 | -.000349 | .000430 | .000245 | .000470 | .000086 | .000140 | .000070 |
| 12 | -.000390 | -.000047 | -.000340 | .000401 | .000192 | .000453 | .000080 | .000119 | .000060 |
| 16 | -.000350 | -.000042 | -.000304 | .000364 | .000144 | .000429 | .000082 | .000070 | .000060 |
| 20 | -.000292 | -.000040 | -.000251 | .000325 | .000104 | .000410 | .000101 | .000019 | .000079 |
| 24 | -.000209 | -.000040 | -.000184 | .000285 | .000079 | .000395 | .000133 | -.000026 | .000109 |
| | | | | $\delta_f = 10°$ | | | | | |
| -8 | -.000362 | -.000086 | -.000059 | .000474 | .000364 | .000498 | .000094 | .000008 | .000081 |
| -4 | -.000386 | -.000076 | -.000194 | .000470 | .000349 | .000496 | .000094 | .000066 | .000081 |
| 0 | -.000404 | -.000069 | -.000286 | .000461 | .000322 | .000490 | .000091 | .000110 | .000079 |
| 4 | -.000412 | -.000059 | -.000337 | .000446 | .000283 | .000480 | .000090 | .000135 | .000075 |
| 8 | -.000406 | -.000052 | -.000350 | .000424 | .000233 | .000466 | .000085 | .000138 | .000068 |
| 12 | -.000383 | -.000046 | -.000334 | .000394 | .000182 | .000448 | .000080 | .000110 | .000059 |
| 16 | -.000341 | -.000041 | -.000297 | .000358 | .000136 | .000426 | .000084 | .000063 | .000063 |
| 20 | -.000279 | -.000040 | -.000240 | .000319 | .000099 | .000408 | .000105 | .000011 | .000083 |
| 24 | -.000194 | -.000039 | -.000173 | .000279 | .000076 | .000393 | .000139 | -.000033 | .000114 |

TABLE VI.- CONTINUED

| $\alpha$, deg / $deg^{-1}$ | $C_{y_{\delta_a}}$ | $C_{y_{fl_o}}$ | $C_{y_{fl_i}}$ | $C_{l_{\delta_a}}$ | $C_{l_{fl_o}}$ | $C_{l_{fl_i}}$ | $C_{m_{\delta_a}}$ | $C_{n_{fl_o}}$ | $C_{n_{fl_i}}$ |
|---|---|---|---|---|---|---|---|---|---|
| | | | | $\delta_f = 20°$ | | | | | |
| -8 | -.000370 | -.000084 | -.000104 | .000474 | .000360 | .000497 | .000094 | .000026 | .000081 |
| -4 | -.000392 | -.000074 | -.000224 | .000469 | .000343 | .000494 | .000093 | .000079 | .000081 |
| 0 | -.000407 | -.000066 | -.000303 | .000459 | .000313 | .000488 | .000091 | .000117 | .000079 |
| 4 | -.000412 | -.000057 | -.000343 | .000440 | .000271 | .000478 | .000089 | .000138 | .000074 |
| 8 | -.000402 | -.000050 | -.000349 | .000417 | .000220 | .000462 | .000084 | .000134 | .000065 |
| 12 | -.000376 | -.000045 | -.000327 | .000386 | .000171 | .000442 | .000080 | .000101 | .000058 |
| 16 | -.000331 | -.000041 | -.000286 | .000350 | .000128 | .000422 | .000087 | .000051 | .000066 |
| 20 | -.000266 | -.000039 | -.000228 | .000361 | .000094 | .000404 | .000110 | .000002 | .000088 |
| 24 | -.000186 | -.000039 | -.000161 | .000282 | .000073 | .000391 | .000144 | -.000039 | .000120 |
| | | | | $\delta_f = 30°$ | | | | | |
| -8 | -.000374 | -.000081 | -.000132 | .000473 | .000358 | .000497 | .000094 | .000039 | .000081 |
| -4 | -.000396 | -.000072 | -.000245 | .000466 | .000338 | .000494 | .000093 | .000090 | .000080 |
| 0 | -.000409 | -.000064 | -.000316 | .000456 | .000305 | .000486 | .000091 | .000124 | .000078 |
| 4 | -.000412 | -.000056 | -.000346 | .000436 | .000259 | .000474 | .000088 | .000139 | .000071 |
| 8 | -.000398 | -.000049 | -.000346 | .000411 | .000210 | .000459 | .000083 | .000130 | .000064 |
| 12 | -.000367 | -.000045 | -.000320 | .000378 | .000160 | .000437 | .000080 | .000090 | .000058 |
| 16 | -.000318 | -.000041 | -.000276 | .000341 | .000120 | .000418 | .000091 | .000040 | .000070 |
| 20 | -.000252 | -.000039 | -.000217 | .000304 | .000089 | .000402 | .000116 | -.000006 | .000093 |
| 24 | -.000163 | -.000039 | -.000152 | .000266 | .000071 | .000390 | .000149 | -.000044 | .000124 |

TABLE VI.- CONTINUED

| $\alpha$, deg \ deg$^{-1}$ | $C_{y_{\delta_r}}$ | $C_{l_{\delta_r}}$ | $C_{n_{\delta_r}}$ | $C_{y_{\delta_r}}$ | $C_{l_{\delta_r}}$ | $C_{n_{\delta_r}}$ | $C_{y_{\delta_r}}$ | $C_{l_{\delta_r}}$ | $C_{n_{\delta_r}}$ |
|---|---|---|---|---|---|---|---|---|---|
| | $\delta_f = 0°$ | | | | $\delta_f = 10°$ | | | $\delta_f = 20°$ | |
| -8 | .00232 | .00030 | -.00102 | .00209 | .00026 | -.00114 | .00197 | .00023 | -.00126 |
| -4 | .00178 | .00020 | -.00137 | .00167 | .00019 | -.00144 | .00157 | .00018 | -.00150 |
| 0 | .00144 | .00016 | -.00157 | .00138 | .00015 | -.00161 | .00134 | .00015 | -.00163 |
| 4 | .00127 | .00016 | -.00165 | .00125 | .00016 | -.00166 | .00124 | .00017 | -.00165 |
| 8 | .00125 | .00019 | -.00163 | .00126 | .00021 | -.00161 | .00128 | .00022 | -.00159 |
| 12 | .00135 | .00026 | -.00152 | .00138 | .00028 | -.00149 | .00143 | .00030 | -.00146 |
| 16 | .00158 | .00036 | -.00133 | .00162 | .00037 | -.00130 | .00169 | .00040 | -.00125 |
| 20 | .00191 | .00047 | -.00108 | .00198 | .00049 | -.00103 | .00207 | .00051 | -.00098 |
| 24 | .00235 | .00058 | -.00078 | .00243 | .00061 | -.00073 | .00252 | .00063 | -.00067 |

| | $\delta_f = 30°$ | | |
|---|---|---|---|
| -8 | .00181 | .00021 | -.00135 |
| -4 | .00149 | .00016 | -.00154 |
| 0 | .00131 | .00016 | -.00163 |
| 4 | .00125 | .00019 | -.00164 |
| 8 | .00130 | .00024 | -.00156 |
| 12 | .00147 | .00032 | -.00141 |
| 6 | .00176 | .00041 | -.00122 |
| 20 | .00213 | .00052 | -.00093 |
| 24 | .00258 | .00064 | -.00062 |

TABLE VI.- CONCLUDED

| $\alpha$, deg \ deg$^{-1}$ | $C_{y_\beta}$ | $C_{l_\beta}$ | $C_{n_\beta}$ | $C_{y_\beta}$ | $C_{l_\beta}$ | $C_{n_\beta}$ | $C_{y_\beta}$ | $C_{l_\beta}$ | $C_{n_\beta}$ |
|---|---|---|---|---|---|---|---|---|---|
| | | $\delta_f = 0°$ | | | $\delta_f = 10°$ | | | $\delta_f = 20°$ | |
| -8 | -.00810 | .00151 | .00279 | -.00819 | .00039 | .00271 | -.00819 | .00023 | .00262 |
| -4 | -.00726 | .00039 | .00258 | -.00756 | -.00035 | .00260 | -.00756 | -.00052 | .00259 |
| 0 | -.00614 | -.00063 | .00269 | -.00624 | -.00088 | .00273 | -.00624 | -.00130 | .00282 |
| 4 | -.00481 | -.00144 | .00290 | -.00500 | -.00158 | .00296 | -.00500 | -.00200 | .00296 |
| 8 | -.00306 | -.00194 | .00298 | -.00316 | -.00199 | .00289 | -.00316 | -.00223 | .00289 |
| 12 | -.00065 | -.00295 | .00256 | -.00075 | -.00313 | .00239 | -.00075 | -.00327 | .00230 |
| 16 | .00285 | -.00458 | .00170 | .00268 | -.00480 | .00153 | .00268 | -.00483 | .00140 |
| 20 | .00899 | -.00604 | .00175 | .00815 | -.00604 | .00163 | .00875 | -.00598 | .00162 |
| 24 | .02373 | -.00719 | .00500 | .02283 | -.00704 | .00500 | .002283 | -.00684 | .00900 |

| | | $\delta_f = 30°$ | |
|---|---|---|---|
| -8 | -.00810 | .00094 | .00253 |
| -4 | -.00726 | -.00036 | .00271 |
| 0 | -.00614 | -.00155 | .00294 |
| 4 | -.00481 | -.00232 | .00299 |
| 8 | -.00306 | -.00252 | .00294 |
| 12 | -.00065 | -.00328 | .00231 |
| 16 | .00285 | -.00469 | .00134 |
| 20 | .00899 | -.00585 | .00168 |
| 24 | .02263 | -.00662 | .00500 |

TABLE VII.- DIMENSIONAL AND MASS CHARACTERISTICS (LANDING CONDITION)

| | |
|---|---|
| Reference wing area, $m^2$ ($ft^2$) | 777.23 (8 366) |
| Wing span, m (ft) | 38.47 (126.22) |
| Wing leading-edge sweep, deg (see fig. ) | 74.00/70.84/60.00 |
| Reference mean aerodynamic chord, m (ft) | 38.47 (126.215) |
| Center-of-gravity location, percent $\bar{c}$ | 60.10 |
| Static margin, percent | -3.7 |
| Take-off weight, MN (lbf) | 3.051 (686 000) |
| $I_X$, kg-$m^2$ (slug-$ft^2$) | 10 222 900 (7 540 000) |
| $I_Y$, kg-$m^2$ (slug-$ft^2$) | 74 448 240 (54 910 000) |
| $I_Z$, kg-$m^2$ (slug-$ft^2$) | 82 339 130 (60 730 000) |
| $I_{XZ}$, kg-$m^2$ (slug-$ft^2$) | -2 087 970 (-1 540 000) |
| Landing weight, MN (lbf) | 1.743 (392 250) |
| $I_X$, kg-$m^2$ (slug-$ft^2$) | 5 667 340 (4 180 000) |
| $I_Y$, kg-$m^2$ (slug-$ft^2$) | 68 740 230 (50 700 000) |
| $I_Z$, kg-$m^2$ (slug-$ft^2$) | 72 333 160 (53 335 000) |
| $I_{XZ}$, kg-$m^2$ (slug-$ft^2$) | -1 586 310 (-1 170 000) |
| Maximum control surface deflections: | |
| $\delta_t$, deg | ±20 |
| $\delta_f$, deg | 0 to 20 |
| $\delta_a$, deg | ±35 |
| $\delta_{afo}$, deg | ±30 |
| $\delta_{afi}$, deg | ±10 |
| $\delta_r$, deg | ±25 |
| Maximum control surface deflection rates: | |
| $\dot{\delta}_t$, deg/sec | ±50 |
| $\dot{\delta}_f$, deg/sec | ±10 |
| $\dot{\delta}_a$, deg/sec | ±70 |
| $\dot{\delta}_{afo}$, deg/sec | ±40 |
| $\dot{\delta}_{afi}$, deg/sec | ±40 |
| $\dot{\delta}_r$, deg/sec | ±50 |

TABLE VIII.- LOW SPEED DYNAMIC STABILITY DERIVATIVES

| $\alpha$, deg \ rad$^{-1}$ | $C_{m_q}$ | $C_{m_{\dot{\alpha}}}$ | $C_{y_p}$ | $C_{l_p}$ | $C_{m_p}$ | $C_{y_r}$ | $C_{l_r}$ | $C_{m_r}$ |
|---|---|---|---|---|---|---|---|---|
| | | | $\delta_f = 0°$ | | | | | |
| -8 | -1.2997 | -.1957 | -.5085 | -.1782 | -.1001 | .5946 | -.0551 | -.4705 |
| -4 | -1.2967 | -.1902 | -.1301 | -.1471 | -.1101 | .4785 | -.0050 | -.4955 |
| 0 | -1.2932 | -.1822 | .3153 | -.1301 | -.1151 | .4304 | .0501 | -.4975 |
| 4 | -1.2907 | -.1709 | .5826 | -.1221 | -.1071 | .4204 | .1131 | -.4825 |
| 8 | -1.2862 | -.1558 | .9339 | -.1261 | -.0831 | .4555 | .1802 | -.4404 |
| 12 | -1.2812 | -.1300 | 1.2883 | -.1471 | -.0330 | .5235 | .2533 | -.3734 |
| 16 | -1.2712 | -.0873 | 1.6346 | -.1902 | .0571 | .6256 | .3403 | -.2703 |
| 20 | -1.2702 | -.0143 | 1.8939 | -.2462 | .1902 | .7638 | .4505 | -.1031 |
| 24 | -1.2832 | .1136 | 2.0120 | -.4074 | .3764 | .9459 | .5836 | .1502 |
| | | | $\delta_f = 10°$ | | | | | |
| -8 | -1.2992 | -.1942 | -.3934 | -.1752 | -.1031 | .5536 | -.0420 | -.4805 |
| -4 | -1.2962 | -.1877 | -.0390 | -.1421 | -.1151 | .4585 | .0100 | -.4985 |
| 0 | -1.2932 | -.1792 | .3303 | -.1301 | -.1181 | .4224 | .0651 | -.4955 |
| 4 | -1.2892 | -.1677 | .6707 | -.1221 | -.1051 | .4254 | .1261 | -.4735 |
| 8 | -1.2832 | -.1511 | 1.0140 | -.1331 | -.0751 | .4655 | .1952 | -.4264 |
| 12 | -1.2772 | -.1216 | 1.3564 | -.1562 | -.0200 | .5415 | .2673 | -.3564 |
| 16 | -1.2747 | -.0762 | 1.6817 | -.1982 | .0751 | .6456 | .3554 | -.2472 |
| 20 | -1.2767 | .0059 | 1.9219 | -.2653 | .2162 | .7878 | .4675 | -.0671 |
| 24 | -1.2887 | .1451 | 2.0190 | -.4404 | .4174 | .9870 | .6106 | .2102 |

TABLE VIII.- CONCLUDED

| $\alpha$, deg \ $rad^{-1}$ | $C_{m_q}$ | $C_{m_{\dot{\alpha}}}$ | $C_{y_p}$ | $C_{l_p}$ | $C_{m_p}$ | $C_{y_r}$ | $C_{l_r}$ | $C_{m_r}$ |
|---|---|---|---|---|---|---|---|---|
| | | | $\delta_f = 20°$ | | | | | |
| -8 | -1.2977 | -.1922 | -.2883 | -.1582 | -.1051 | .5175 | -.0250 | -.4865 |
| -4 | -1.2962 | -.1862 | .0621 | -.1381 | -.1881 | .4434 | .0230 | -.5005 |
| 0 | -1.2922 | -.1767 | .4054 | -.1201 | -.1151 | .4204 | .0801 | -.4925 |
| 4 | -1.2877 | -.1632 | .7538 | -.1221 | -.1001 | .4334 | .1431 | -.4635 |
| 8 | -1.2832 | -.1439 | 1.0961 | -.1371 | -.0651 | .4825 | .2132 | -.4134 |
| 12 | -1.2777 | -.1124 | 1.4384 | -.1632 | 0 | .5656 | .2883 | -.3353 |
| 16 | -1.2747 | -.0605 | 1.7357 | -.2152 | .1031 | .6727 | .3784 | -.2152 |
| 20 | -1.2772 | .0328 | 1.9550 | -.3103 | .2533 | .8258 | .4935 | -.0200 |
| 24 | -1.2907 | .1819 | 2.0220 | -.4905 | .4635 | 1.0260 | .6406 | .2773 |
| | | | $\delta_f = 30°$ | | | | | |
| -8 | -1.2972 | -.1917 | -.2078 | -.1491 | -.1066 | .4996 | -.0180 | -.4923 |
| -4 | -1.2957 | -.1838 | .1248 | -.1280 | -.1092 | .4279 | .0403 | -.4923 |
| 0 | -1.2921 | -.1745 | .4851 | -.1209 | -.1074 | .4306 | .0943 | -.4850 |
| 4 | -1.2876 | -.1621 | .8349 | -.1240 | -.0944 | .4470 | .1551 | -.4465 |
| 8 | -1.2831 | -.1396 | 1.1677 | -.1410 | -.0590 | .5003 | .2200 | -.4002 |
| 12 | -1.2762 | -.1043 | 1.5006 | -.1673 | .0245 | .5832 | .3002 | -.3172 |
| 16 | -1.2747 | -.0468 | 1.7870 | -.2243 | .1270 | .6952 | .4000 | -.1830 |
| 20 | -1.2791 | .0511 | 1.9710 | -.3261 | .2782 | .8500 | .5155 | .0159 |
| 24 | -1.2937 | .2083 | 2.0201 | -.5181 | .4961 | 1.0600 | .6616 | .3331 |

TABLE IX.- DYNAMIC STABILITY CHARACTERISTICS

(a) AST-105-1

(Approach speed = 158 knots)

| Parameters | Augmentation | | | | Satisfactory Criterion | Acceptable Criterion |
|---|---|---|---|---|---|---|
| | None | HSAS * | SCAS * | Modified SCAS * | | |
| **Short-period mode** | | | | | | |
| $\omega_{sp}$, rad/sec | .167 | .704 | 1.394 | 1.394 | See figure (33a) | See figure 33(a) |
| $P_{sp}$, sec | 44.88 | 12.63 | 24.63 | 24.63 | ---------- | ---------- |
| $\zeta_{sp}$ | .542 | .708 | .983 | .983 | 0.35 to 1.30 | 0.25 to 2.00 |
| $L\alpha/\omega_{sp}$ | 2.91 | .688 | .348 | .348 | See figure 33(b) | See figure 33(b) |
| $n/\alpha$, g units/rad | 4.02 | 4.02 | 4.02 | 4.02 | See figure 33(a) | See figure 33(a) |
| **Long-period (aperiodic) mode** | | | | | | |
| $t_2$, sec | 5.32 | $\infty$ | $\infty$ | $\infty$ | ---------- | >6 |
| **Long-period (periodic) mode** | | | | | | |
| $\omega_{ph}$, rad/sec | ---- | .089 | .087 | .087 | ---------- | ---------- |
| $P_{ph}$, sec | ---- | 84.98 | 89.64 | 89.74 | ---------- | ---------- |
| $\zeta_{ph}$ | ---- | .555 | .597 | .597 | $\geq$0.04 | $\geq$0 |
| **Roll mode** | | | | | | |
| $\tau_R$, sec | 1.536 | .282 | .321 | .117 | $\geq$1.4 | $\geq$3.0 |
| **Spiral mode** | | | | | | |
| $t_{1/2}$, sec | 32.46 | 50.26 | $\infty$ | $\infty$ | ---------- | ---------- |
| **Dutch roll mode** | | | | | | |
| $\omega_d$, rad/sec | .937 | .541 | 1.117 | .740 | $\geq$0.4 | $\geq$0.4 |
| $\zeta_d$ | .109 | .359 | .220 | .229 | $\geq$0.08 | $\geq$0.02 |
| $\zeta_d\omega_d$, rad/sec | .102 | .194 | .243 | .169 | $\geq$0.15 | $\geq$0.05 |
| $P_d$, sec | 6.75 | 12.43 | 5.77 | 8.62 | ---------- | ---------- |
| $\phi/\beta$ | 2.81 | 2.68 | .78 | .78 | ---------- | ---------- |
| **Roll-control parameters** | | | | | | |
| $\omega_\phi/\omega_d$ | .638 | 1.106 | 1.017 | 1.006 | 0.30 to 1.15 | 0.65 to 1.35 |
| $\zeta_\phi/\zeta_d$ | .190 | .636 | 1.202 | 1.004 | ---------- | ---------- |

* Autothrottle on.

TABLE IX.- CONCLUDED

(b) Baseline concept, ref. 25
(Approach speed = 153 knots)

| Parameters | Augmentation | | | | Satisfactory Criterion | Acceptable Criterion |
|---|---|---|---|---|---|---|
| | None | HSAS * | SCAS * | Modified SCAS * | | |
| **Short-period mode** | | | | | | |
| $\omega_{sp}$, rad/sec . . . | 0.171 | 0.751 | 1.534 | 1.534 | See figure 33(a) | See figure 33(a) |
| $P_{sp}$, sec . . . . . | 42.72 | 8.71 | 15.12 | 15.12 | ---------- | ---------- |
| $\zeta_{sp}$ . . . . . | 0.507 | 0.693 | 1.036 | 1.036 | 0.35 to 1.30 | 0.25 to 2.00 |
| $L\alpha/\omega_{sp}$ . . . . . | 2.32 | 0.529 | 0.259 | 0.259 | See figure 33(b) | See figure 33(b) |
| $n/\alpha$, g units/rad . | 3.19 | 3.19 | 3.19 | 3.19 | See figure 33(a) | See figure 33(a) |
| **Long-period (aperiodic) mode** | | | | | | |
| $t_2$, sec . . . . . | 4.79 | 43.86 | $\infty$ | $\infty$ | ---------- | >6 |
| **Long-period (periodic) mode** | | | | | | |
| $\omega_{ph}$, rad/sec . . . | ---- | 0.067 | 0.080 | 0.080 | ---------- | ---------- |
| $P_{ph}$, sec . . . . . | ---- | 125.2 | 98.9 | 98.9 | ---------- | ---------- |
| $\zeta_{ph}$ . . . . . | ---- | 0.649 | 0.609 | 0.609 | $\geq$0.04 | $\geq$0 |
| **Roll mode** | | | | | | |
| $\tau_R$, sec . . . . . | 1.689 | 0.850 | 0.270 | 0.241 | $\geq$1.4 | $\geq$3.0 |
| **Spiral mode** | | | | | | |
| $t_{1/2}$, sec . . . . | 23.1 | 15.5 | $\infty$ | $\infty$ | ---------- | ---------- |
| **Dutch roll mode** | | | | | | |
| $\omega_d$, rad/sec . . . | 0.805 | 0.522 | 0.741 | 0.562 | $\geq$0.4 | $\geq$0.4 |
| $\zeta_d$ . . . . . | 0.079 | 0.450 | 0.266 | 0.259 | $\geq$0.08 | $\geq$0.02 |
| $\zeta_d\omega_d$, rad/sec . . | 0.064 | 0.235 | 0.197 | 0.146 | $\geq$0.15 | $\geq$0.05 |
| $P_d$, sec . . . . . | 7.83 | 13.47 | 8.79 | 11.58 | ---------- | ---------- |
| $\phi/\beta$ . . . . . | 2.5 | 2.10 | 0.80 | 0.71 | ---------- | ---------- |
| **Roll-control parameters** | | | | | | |
| $\omega_\phi/\omega_d$ . . . . . | 0.565 | 0.874 | 1.004 | 1.025 | 0.30 to 1.15 | 0.65 to 1.35 |
| $\zeta_\phi/\zeta_d$ . . . . . | 3.12 | 0.589 | 0.962 | 0.987 | ---------- | ---------- |

* Autothrottle on.

TABLE X.- CONTROL RESPONSE CHARACTERISTICS

(a) AST-105-1

(Approach speed = 158 knots)

| Parameter | Augmentation | | | | Satisfactory Criterion | Acceptable Criterion |
|---|---|---|---|---|---|---|
| | None | HSAS * | SCAS * | Modified SCAS * | | |
| **Longitudinal** | | | | | | |
| $\ddot{\theta}_{max}$, rad/sec$^2$ . . | -.075** | -.053** | -.075** | Same as SCAS* | -0.08** | -0.05** |
| $\ddot{\theta}/\ddot{\theta}_{ss}$ . . . . . | ------ | ------ | See figure 34 | | See figure 34 | ---------- |
| **Lateral** | | | | | | |
| $\ddot{\phi}_{max}$, rad/sec$^2$. . . | .266 | .224 | .208 | .221 | See figure 35(a) | See figure 35(a) |
| $\dot{\phi}_{max}$, deg/sec . . . | 16.57 | 10.51 | 23.25 | 21.10 | ---------- | ---------- |
| $t_{\phi=30°}$, sec . . . . | 2.84 | 3.74 | 2.74 | 2.79 | ≦ 2.5 | ≦ 3.2 |

* Autothrottle on.

** Minimum demonstrated speed of 129 knots

TABLE X.- CONCLUDED

(b) Baseline concept, ref. 25
(Approach speed = 153 knots)

| Parameters | Augmentation | | | | Satisfactory Criterion | Acceptable Criterion |
|---|---|---|---|---|---|---|
| | None | HSAS * | SCAS * | Modified SCAS * | | |
| **Longitudinal** | | | | | | |
| $\ddot{\theta}_{max}$, rad/sec$^2$ . . | -0.06** | -0.05** | -0.06** | Same as SCAS* | -0.08** | -0.05** |
| $\dot{\theta}/\dot{\theta}_{ss}$ . . . . . | ------ | ------ | See figure 34 | | See figure 34 | ---------- |
| **Lateral** | | | | | | |
| $\ddot{\phi}_{max}$, rad/sec$^2$. . . | 0.211 | 0.188 | 0.190 | 0.190 | See figure 35(a) | See figure 35(a) |
| $\dot{\phi}_{max}$, deg/sec . . . | 14.94 | 9.3 | 19.9 | 15.7 | ---------- | See figure 35(b) |
| $p_2/p_1$ . . . . . | -0.155 | 0.803 | 0.940 | 0.992 | $\geq$0.60 | $\geq$0.25 |
| $\phi_{osc}/\phi_{av}$ . . . . . | 0.801 | 0.012 | 0.011 | 0.015 | See figure 43*** | See figure 43*** |
| $t_{\phi=30°}$, sec . . . . | 2.9 | 4.0 | 2.7 | 2.9 | $\leq$2.5 | $\leq$3.2 |

* Autothrottle on.

** Minimum demonstrated speed of 125 knots.

***In reference 25

# TABLE XI.- PILOT RATING SYSTEM

| | | | PILOT RATING | |
|---|---|---|---|---|
| | | SATISFACTORY | Excellent, highly desirable. | 1 |
| | | Meets all requirements and expectations; good enough without improvement. | Good, pleasant, well behaved. | 2 |
| | ACCEPTABLE | Clearly adequate for mission. | Fair. Some mildly unpleasant characteristics. Good enough for mission without improvement. | 3 |
| | May have deficiencies which warrant improvement, but adequate for mission. | | Some minor but annoying deficiencies. Improvement is requested. Effect on performance is easily compensated for by pilot. | 4 |
| | | UNSATISFACTORY | | |
| | Pilot compensation, if required to achieve acceptable performance, is feasible. | Reluctantly acceptable. Deficiencies which warrant improvement. Performance adequate for mission with feasible pilot compensation. | Moderately objectionable deficiencies. Improvement is needed. Reasonable performance requires considerable pilot compensation. | 5 |
| CONTROLLABLE | | | Very objectionable deficiencies. Major improvements are needed. Requires best available pilot compensation to achieve acceptable performance. | 6 |
| Capable of being controlled or managed in context of mission, with available pilot attention. | | | Major deficiencies which require improvement for acceptance. Controllable. Performance inadequate for mission, or pilot compensation required for minimum acceptable performance in mission is too high. | 7 |
| | UNACCEPTABLE | | Controllable with difficulty. Requires substantial pilot skill and attention to retain control and continue mission. | 8 |
| | Deficiencies which require improvement. Inadequate performance for mission even with maximum feasible pilot compensation. | | Marginally controllable in mission. Requires maximum available pilot skill and attention to retain control. | 9 |
| | UNCONTROLLABLE | | Uncontrollable in mission. | 10 |
| | Control will be lost during some portion of mission. | | | |

TABLE XII.- WEIGHT SUMMARY

| ITEM | kN | lbf |
|---|---|---|
| STRUCTURE | 778.910 | 175106 |
| PROPULSION | 197.719 | 44449 |
| SYSTEMS | 234.964 | 52822 |
| WEIGHT EMPTY | 1211.593 | 272377 |
| OPERATING ITEMS | 69.339 | 15588 |
| OPERATING WEIGHT | 1280.932 | 287965 |
| PAYLOAD | 253.802 | 57057 |
| ZERO FUEL WEIGHT | 1534.734 | 345022 |
| MISSION FUEL | 1516.746 | 340978 |
| TAKE-OFF GROSS WEIGHT | 3051.480 | 686000 |
| NORMAL LANDING WEIGHT | 1744.815 | 392250 |

TABLE XIII.- GROUP WEIGHT SUMMARY

| | kN | lbf |
|---|---|---|
| WING | 337.887 | 75960 |
| HORIZONTAL TAIL | 29.456 | 6622 |
| VERTICAL TAIL | 18.167 | 4084 |
| VERTICAL FIN | 9.510 | 2138 |
| CANARD | 0 | 0 |
| FUSELAGE | 222.491 | 50018 |
| LANDING GEAR | 118.309 | 26597 |
| NACELLE | 43.090 | 9687 |
| STRUCTURE TOTAL | (778.910) | (175106) |
| ENGINES | 157.200 | 35340 |
| THRUST REVERSERS | 0 | 0 |
| MISCELLANEOUS SYSTEMS | 7.918 | 1780 |
| FUEL SYSTEM - TANKS AND PLUMBING | 32.601 | 7329 |
| - INSULATION | 0 | 0 |
| PROPULSION TOTAL | (197.719) | (44449) |
| SURFACE CONTROLS | 39.967 | 8985 |
| AUXILIARY POWER | 0 | 0 |
| INSTRUMENTS | 7.820 | 1758 |
| HYDRAULICS | 25.559 | 5746 |
| ELECTRICAL | 22.090 | 4966 |
| AVIONICS | 11.992 | 2696 |
| FURNISHINGS AND EQUIPMENT | 88.048 | 19794 |
| AIR CONDITIONING | 38.553 | 8667 |
| ANTI-ICING | .934 | 210 |
| SYSTEMS AND EQUIPMENT TOTAL | (234.964) | (52822) |
| WEIGHT EMPTY | 1211.593 | 272377 |
| CREW AND BAGGAGE - FLIGHT, 3 | 3.003 | 675 |
| - CABIN, 9 | 6.606 | 1485 |
| UNUSABLE FUEL | 9.021 | 2028 |
| ENGINE OIL | 2.028 | 456 |
| PASSENGER SERVICE | 36.760 | 8264 |
| CARGO CONTAINERS, 6 | 11.921 | 2680 |
| OPERATING WEIGHT | 1280.932 | 287965 |
| PASSENGERS, 273 | 200.370 | 45045 |
| PASSENGER BAGGAGE | 53.432 | 12012 |
| CARGO | 0 | 0 |
| ZERO FUEL WEIGHT | 1534.740 | 345022 |
| MISSION FUEL | 1516.734 | 340978 |
| TAKE-OFF GROSS WEIGHT | 3051.480 | 686000 |

TABLE XIV.- MASS DATA SUMMARY

| ITEM DESCRIPTION | CONDITION: TAKE-OFF GROSS WEIGHT | CONDITION: NORMAL LANDING WEIGHT |
|---|---|---|
| WEIGHT, kN | 3051.480 | 1744.815 |
| , klbf | 686.000 | 392.250 |
| HORIZONTAL c.g., m | 52.992 | 52.733 |
| , in | 2086.3 | 2076.1 |
| percent of $\bar{c}_{ref}$ | 59.98 | 59.02 |
| ROLL INERTIA, $I_x$, kg-m$^2$ | 10.22 x $10^6$ | 5.67 x $10^6$ |
| , slug-ft$^2$ | 7.54 x $10^6$ | 4.18 x $10^6$ |
| PITCH INERTIA, $I_y$, kg-m$^2$ | 74.58 x $10^6$ | 67.97 x $10^6$ |
| , slug-ft$^2$ | 54.91 x $10^6$ | 50.70 x $10^6$ |
| YAW INERTIA, $I_z$, kg-m$^2$ | 82.48 x $10^6$ | 71.57 x $10^6$ |
| , slug-ft$^2$ | 60.73 x $10^6$ | 53.35 x $10^6$ |
| PRODUCT OF INERTIA, $I_{xz}$, kg-m$^2$ | -2.09 x $10^6$ | -1.59 x $10^6$ |
| , slug-ft$^2$ | -1.54 x $10^6$ | -1.17 x $10^6$ |
| PRINCIPAL AXIS ANGLE OF INCLINATION, $\theta$, deg. | -1.66 | -1.38 |

TABLE XV. - EFFECTIVE PERCEIVED NOISE LEVELS

| | JET EPNdB |
|---|---|
| 1. Takeoff, normal throttle setting, climb at $V_2$* + 5 m/sec (10 Kt), no power cutback: | |
| Centerline noise | 119.8 |
| Maximum sideline noise | 114.8 |
| 2. Takeoff, normal throttle setting, climb at $V_2$ + 5 m/sec (10 Kt), power cutback 5944 m (19,500 ft) from brake release: | |
| Centerline noise | 115.8 |
| Maximum sideline noise | 113.8 |
| 3. Takeoff, normal throttle setting, accelerating climb, power cutback 5944 m (19,500 ft) from brake release, alt. $\geq$ 213 m (700 ft): | |
| Centerline noise | 113.4 |
| Maximum sideline noise | 112.6 |
| 4. Approach, std. $3^{o}$ glide slope, constant speed 81.3 m/sec (158 Kt): | |
| Centerline noise | 106.6 |

* $V_2$ - speed of aircraft at 10.7 m (35 ft) obstacle

TABLE XVI.- MISSION PERFORMANCE

MISSION: Supersonic Cruise @ Mach 2.62

MODEL NO.: AST-105-1

AIRCRAFT CHARACTERISTICS

| | | | |
|---|---|---|---|
| Design gross weight | kN (lbf) | 3051.480 | (686000) |
| Operating weight empty | kN (lbf) | 1280.932 | (287965) |
| Payload - Passengers, 273 | kN (lbf) | 200.370 | (45045) |
| - Pass. baggage | kN (lbf) | 53.432 | (12012) |
| Total payload weight | kN (lbf) | 253.802 | (57057) |
| Wing area - reference | $m^2$ ($ft^2$) | 777 | (8366) |
| - gross | $m^2$ ($ft^2$) | 824 | (8866) |
| P&W VSCE-516 Engines (4); sea level static (std. +8°C day) installed thrust per engine, N (lbf) | | 193769 | 43561 |
| Initial installed thrust to weight ratio | | .254 | .254 |
| Initial wing loading - reference | kPa ($lbf/ft^2$) | 3.926 | (82.0) |
| - gross | kPa ($lbf/ft^2$) | 3.704 | (77.4) |

| MISSION SEGMENT OR CONDITION | OPERATING WEIGHTS kN, (lbf) | ΔFUEL kN, (lbf) | ΔRANGE km, (n.mi.) | ΔTIME min. |
|---|---|---|---|---|
| RAMP GROSS WT. | 3051.486 (686000) | | | |
| .Warm-Up & Taxi-Out | | 12.913 (2903) | 0 (0) | 10 |
| TAKE-OFF GROSS WT. | 3038.571 (683097) | | | |
| Take-Off Run | | 22.980 (5166) | 6 (3) | 1 |
| BEGIN ASCENT | 3015.594 (677931) | | | |
| Climb & Accelerate | | 338.385 (76072) | 641 (346) | 26 |
| BEGIN CRUISE | 2677.206 (601859) | | | |
| Cruise Segment | | 911.854 (204993) | 7019 (3790) | 149 |
| END CRUISE | 1765.354 (396866) | | | |
| Descent & Decelerate | | 20.764 (4668) | 574 (310) | 29 |
| END DESCENT | 1744.593 (392198) | | | |
| Landing & Taxi-In | | | | |
| END MISSION | 1744.593 (392198) | | | |
| TRIP FUEL, RANGE, & TIME | | 1271.000 (285732) | 8234 (4446) | 204 |
| BLOCK FUEL, RANGE, & TIME | | 1306.896 (293802) | 8240 (4449) | 215 |

TABLE XVI.- CONCLUDED

Model No.: AST-105-1

Reserve Fuel Breakdown, kN (lbf):

| | |
|---|---|
| 1. 5% Trip Fuel | 64.690 (14543) |
| 2. Missed Approach | 6.775 (1523) |
| 3. 463 km, (250 n.mi.) to alternate airport | 80.499 (18097) |
| 4. 30 min. holding at 3048 m (10000 ft) | 57.885 (13013) |
| Total Reserves | 209.849 (47176) |

Cruise Conditions:

| | Begin Cruise | End Cruise |
|---|---|---|
| Lift Coefficient | .0929 | .0929 |
| Drag Coefficient | .0101 | .0104 |
| Lift/Drag | 9.2267 | 8.9480 |
| TSFC, kg/hr/N, (lbm/hr/lbf) | .1564 (1.5343) | .1584 (1.5542) |
| Altitude, m, (ft) | 18032 (59160) | 20695 (67896) |

NOTES: 1. Taxi-in fuel taken out of reserves at destination.

2. C.A.B. range corresponding to block time and fuel equals trip range minus traffic allowances as will be specified for supersonic aircraft.

TABLE XVII.- BASELINE DATA FOR DIRECT OPERATING COST ANALYSIS

| | |
|---|---|
| Gross takeoff weight, KN (lbf) | 3051.5 (686,000) |
| Range, km (n.mi.) | 8,240 (4449) |
| Cruise speed, Mach number | 2.62 |
| Number of engines | 4 |
| Thrust per engine, KN (lbf) | 193.8(43561) |
| Seats (passengers) | 273 |
| Load factor, % | 100 |
| Fuel cost, cents/liter (cents/gal) | 10.22 (38.57) |
| Insurance rate, % of purchase price | 1.0 |
| Year dollars | 1976 |
| Depreciation period, years | 16 |
| Residual value, % | 10 |
| Utilization rate, hrs/yr | 4000 |
| Crew | 3 |
| Purchase price: | |
| Aircraft (complete), millions of dollars | 83.69 |
| Airframe, millions of dollars | 71.11 |
| Engines, millions of dollars | 12.58 |
| Spares, millions of dollars | 8.04 |
| Crew pay relative to subsonic flight, % | 117 |

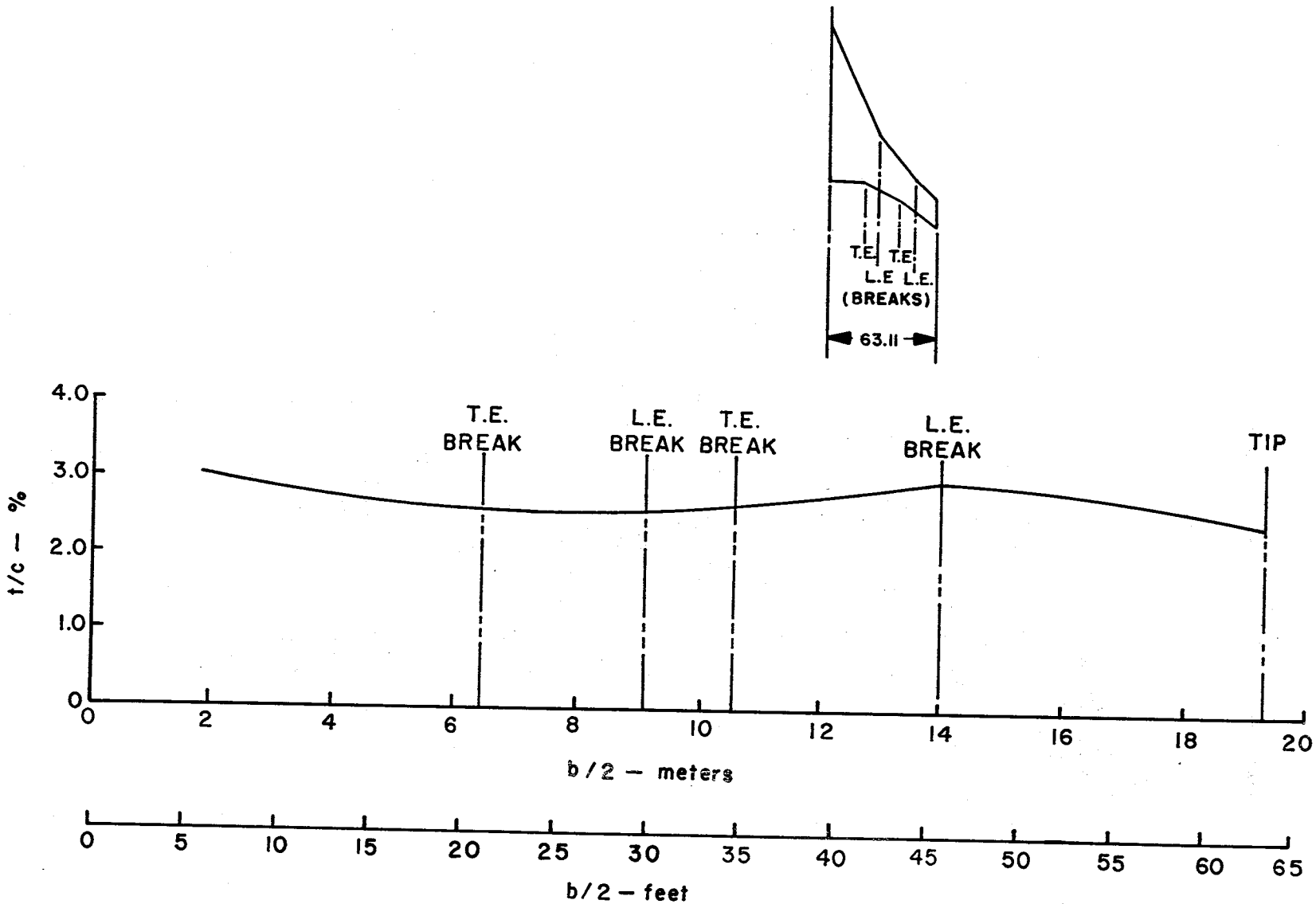


Figure 1.- Spanwise thickness distribution.

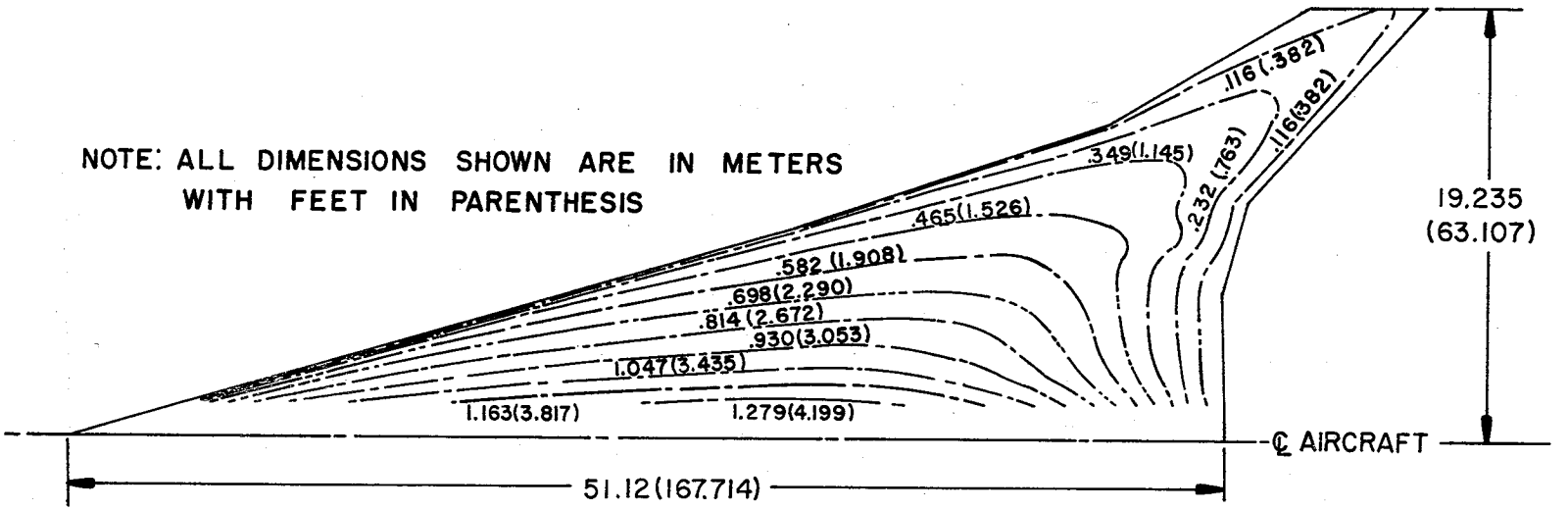


Figure 2.- Wing thickness map.

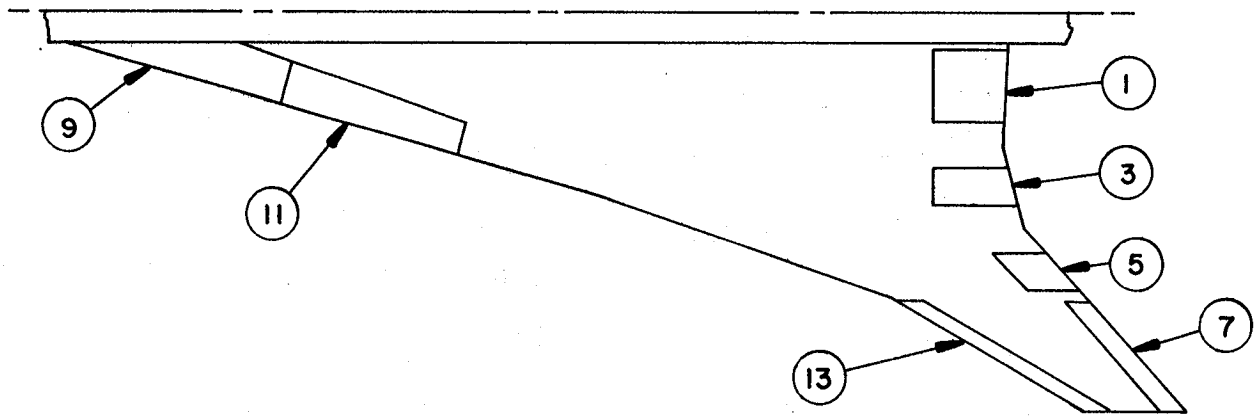


| W. T. MODEL DESIGNATION | NUMBER | AREA, $m^2$ ($ft^2$) EACH |
|---|---|---|
| $t_1$ | 1–2 | 11.734 (126.3) |
| $t_2$ | 3–4 | 8.101 (87.2) |
| $t_3$ | 5–6 | 4.692 (50.5) |
| $t_4$ | 7–8 | 7.665 (82.5) |
| $L_1$ | 9–10 | 15.440 (166.2) |
| $L_2$ | 11–12 | 16.397 (176.5) |
| $L_6$ | 13–14 | 8.454 (91.0) |

NOTE: ODD NUMBERS LEFT WING EVEN NUMBERS RIGHT WING

Figure 3.- Wing control surfaces.

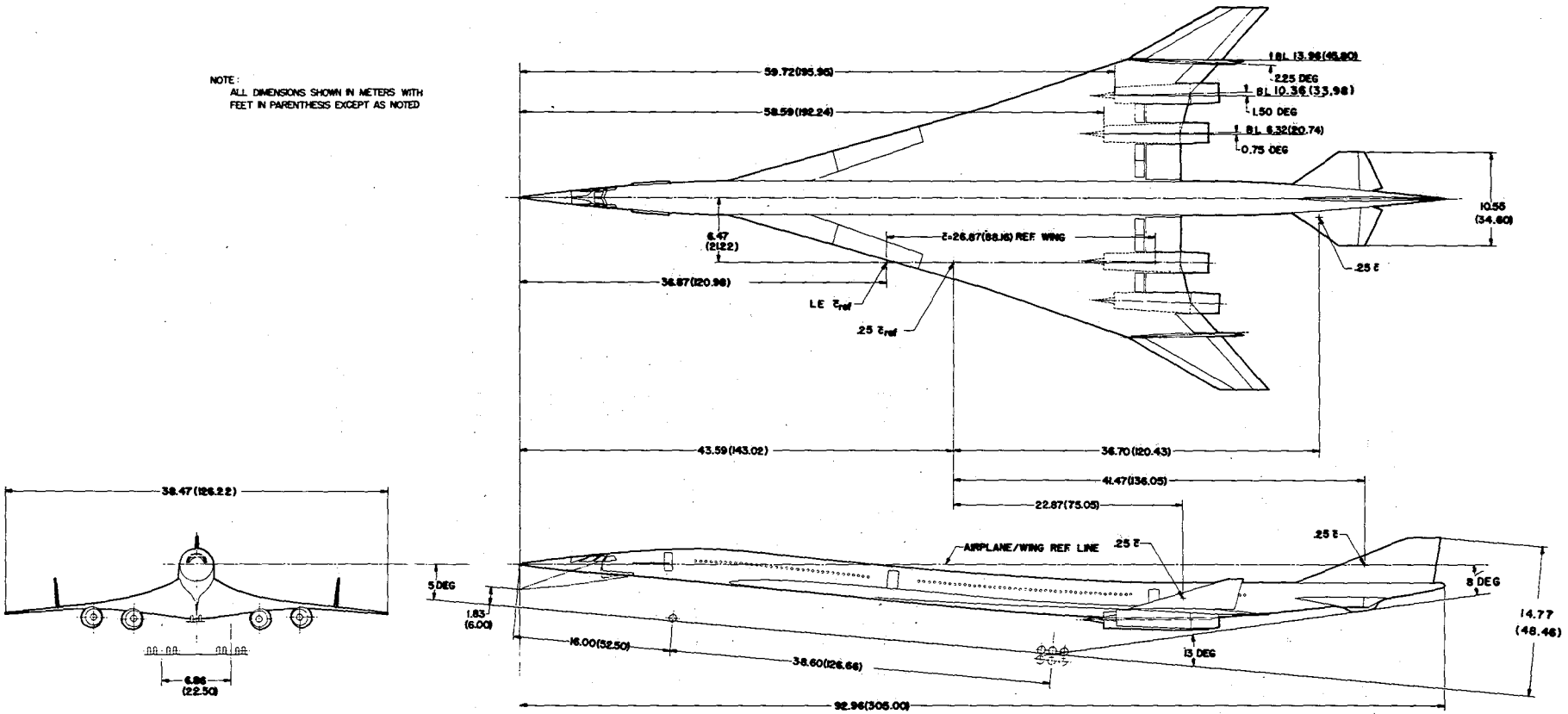


Figure 4.- General arrangement.

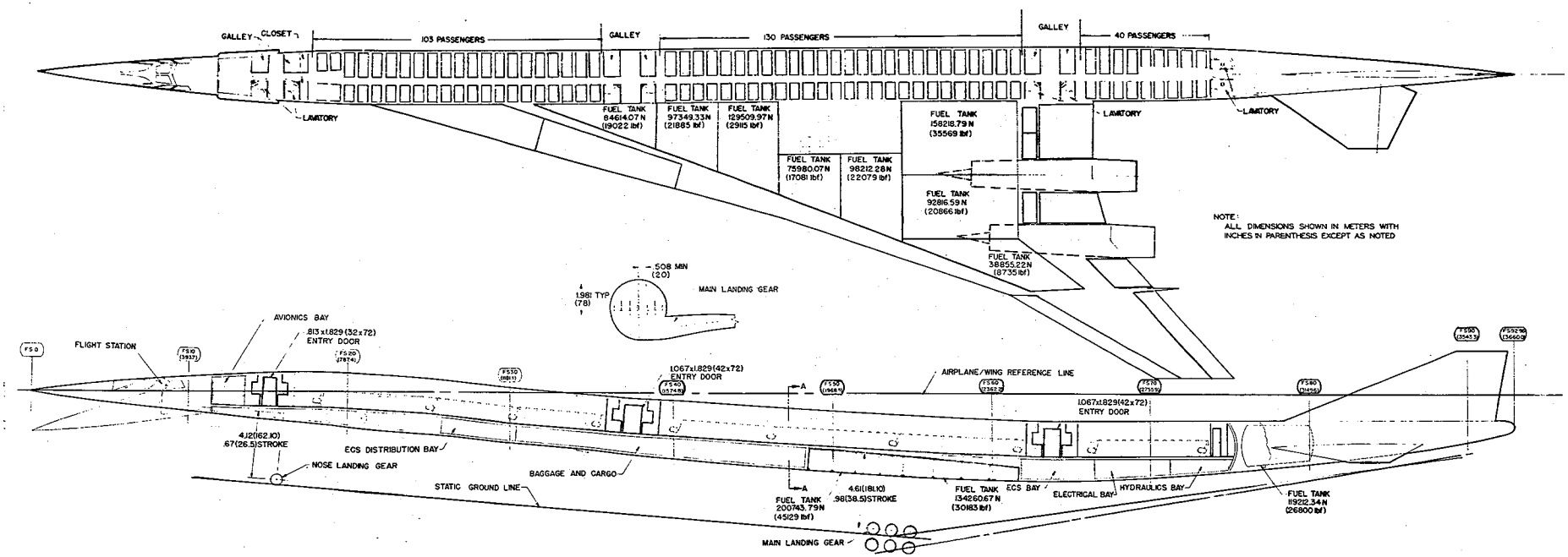


Figure 5.- Inboard profile.

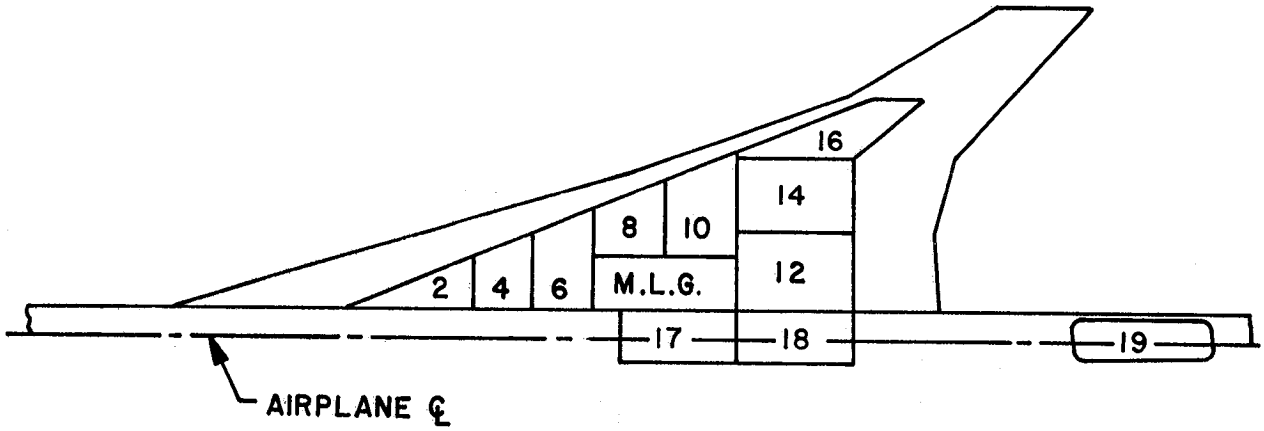


| TANK NUMBER | FUEL WEIGHT PER TANK | |
|---|---|---|
| | kN | lbf |
| 1–2 | 84.612 | 19022 |
| 3–4 | 97.351 | 21885 |
| 5–6 | 129.507 | 29115 |
| 7–8 | 75.982 | 17081 |
| 9–10 | 98.214 | 22079 |
| 11–12 | 158.220 | 35569 |
| 13–14 | 92.820 | 20866 |
| 15–16 | 38.854 | 8735 |
| 17 | 200.754 | 45129 |
| 18 | 134.263 | 30183 |
| 19 | 119.210 | 26800 |
| TOTAL | 2005.335 | 450816 |

NOTE: ODD NUMBER TANK LEFT WING
EVEN NUMBER TANK RIGHT WING
M.L.G. — MAIN LANDING GEAR

Figure 6.- Fuel tank locations and capacities.

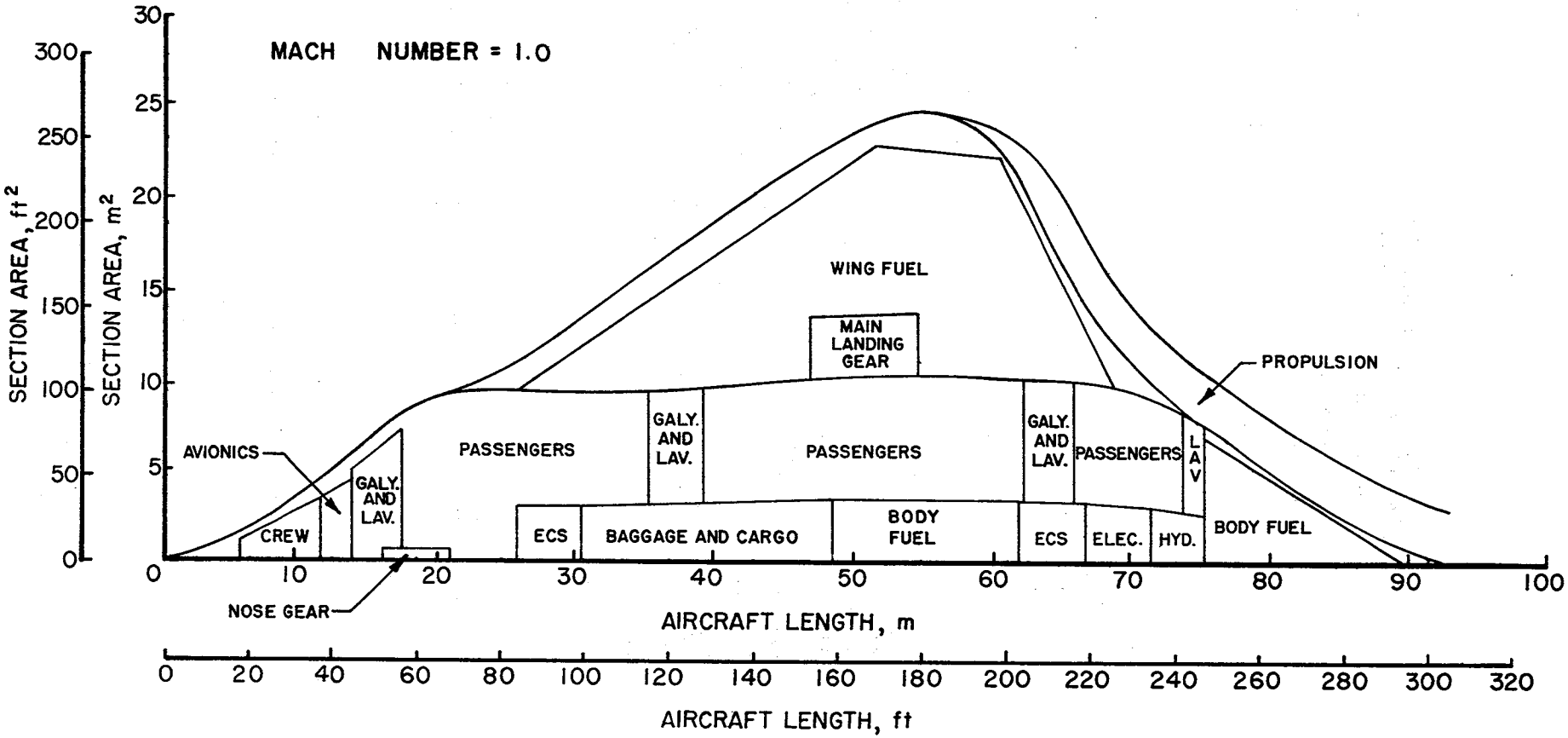


Figure 7.- Area distribution for M = 1.0.

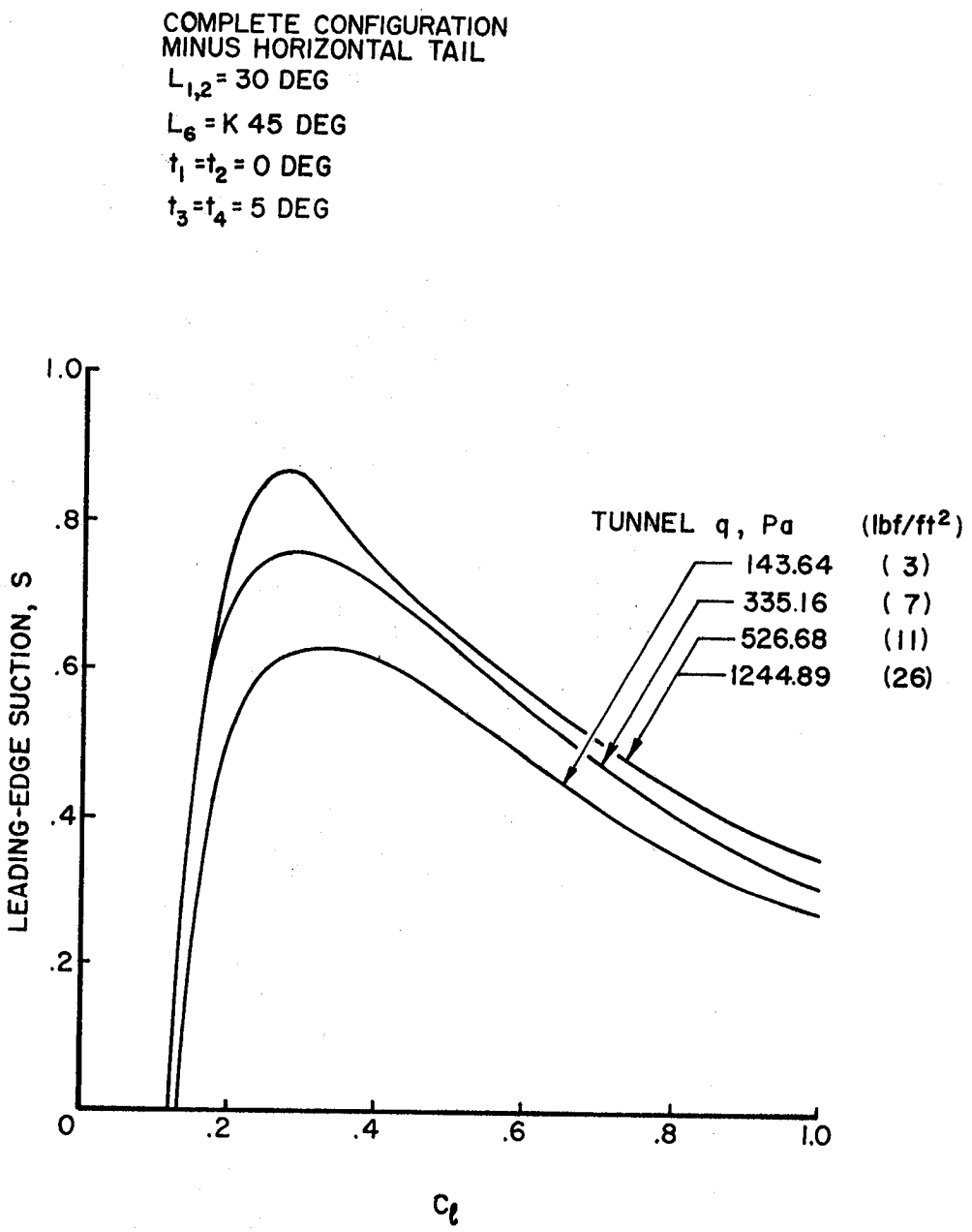


Figure 8.- Reynolds number effect on leading-edge suction.

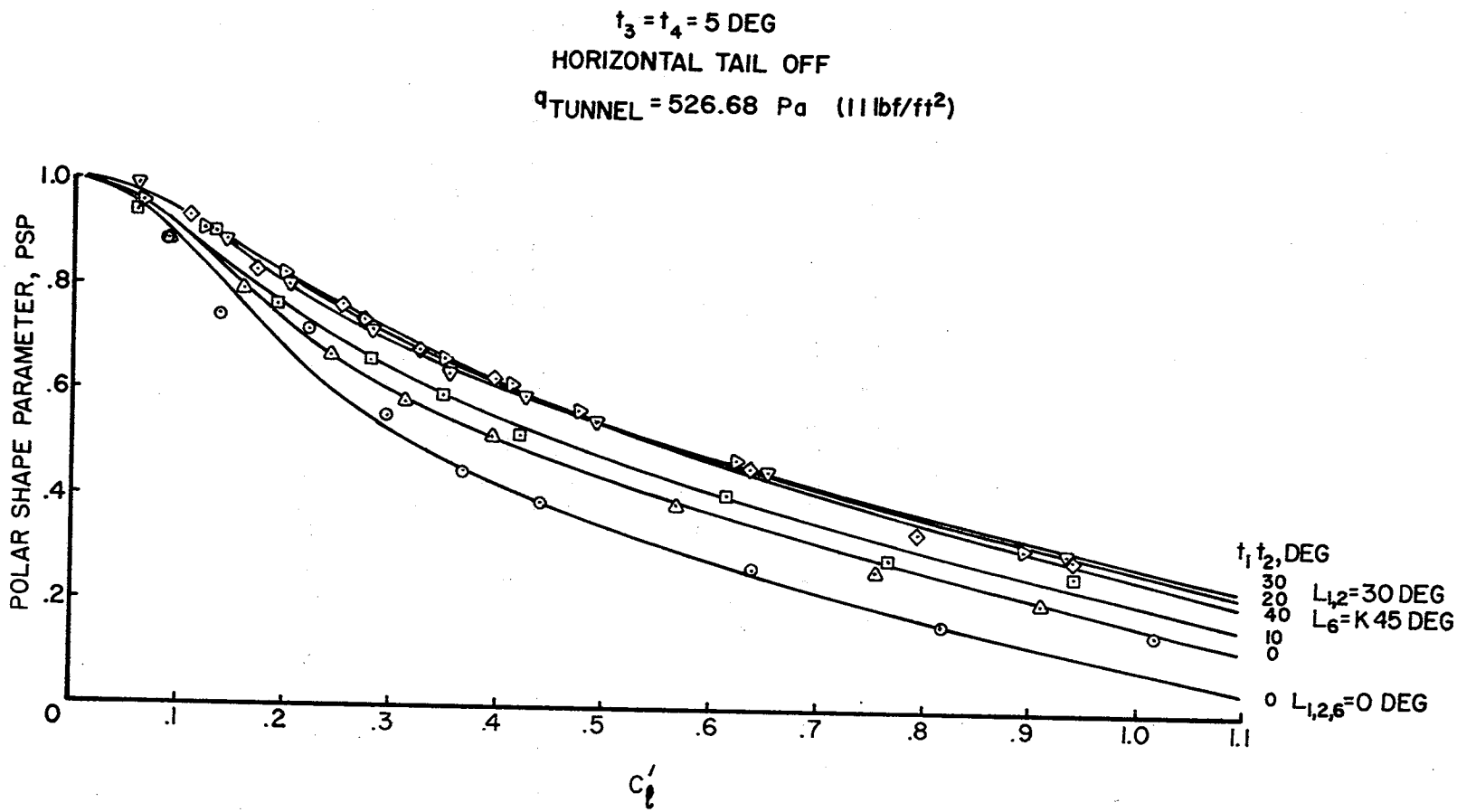


Figure 9.- Effect of high-lift devices on polar shape parameter.

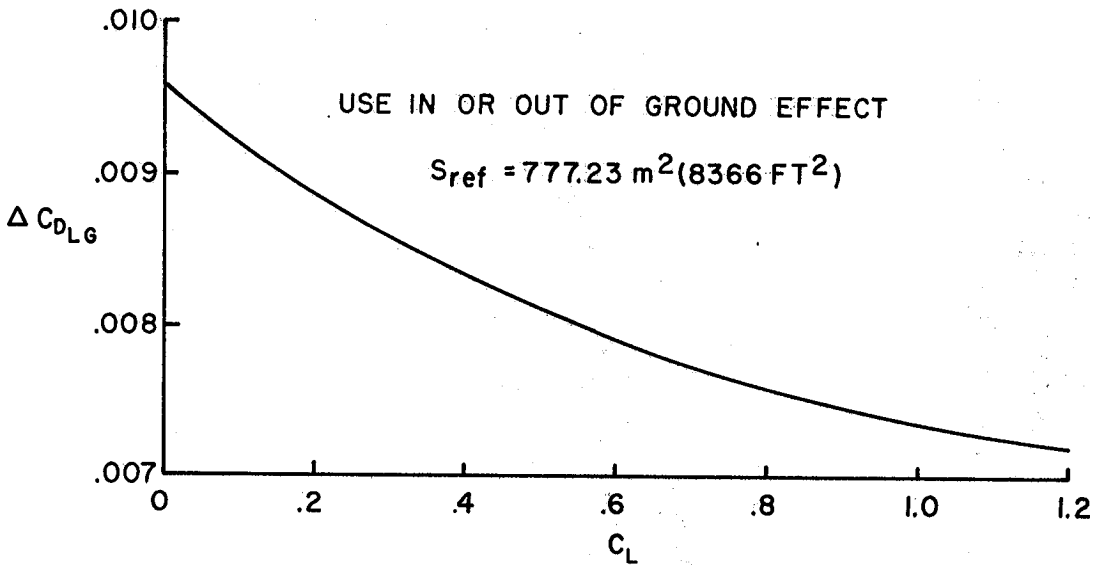


Figure 10.- Landing gear drag coefficient.

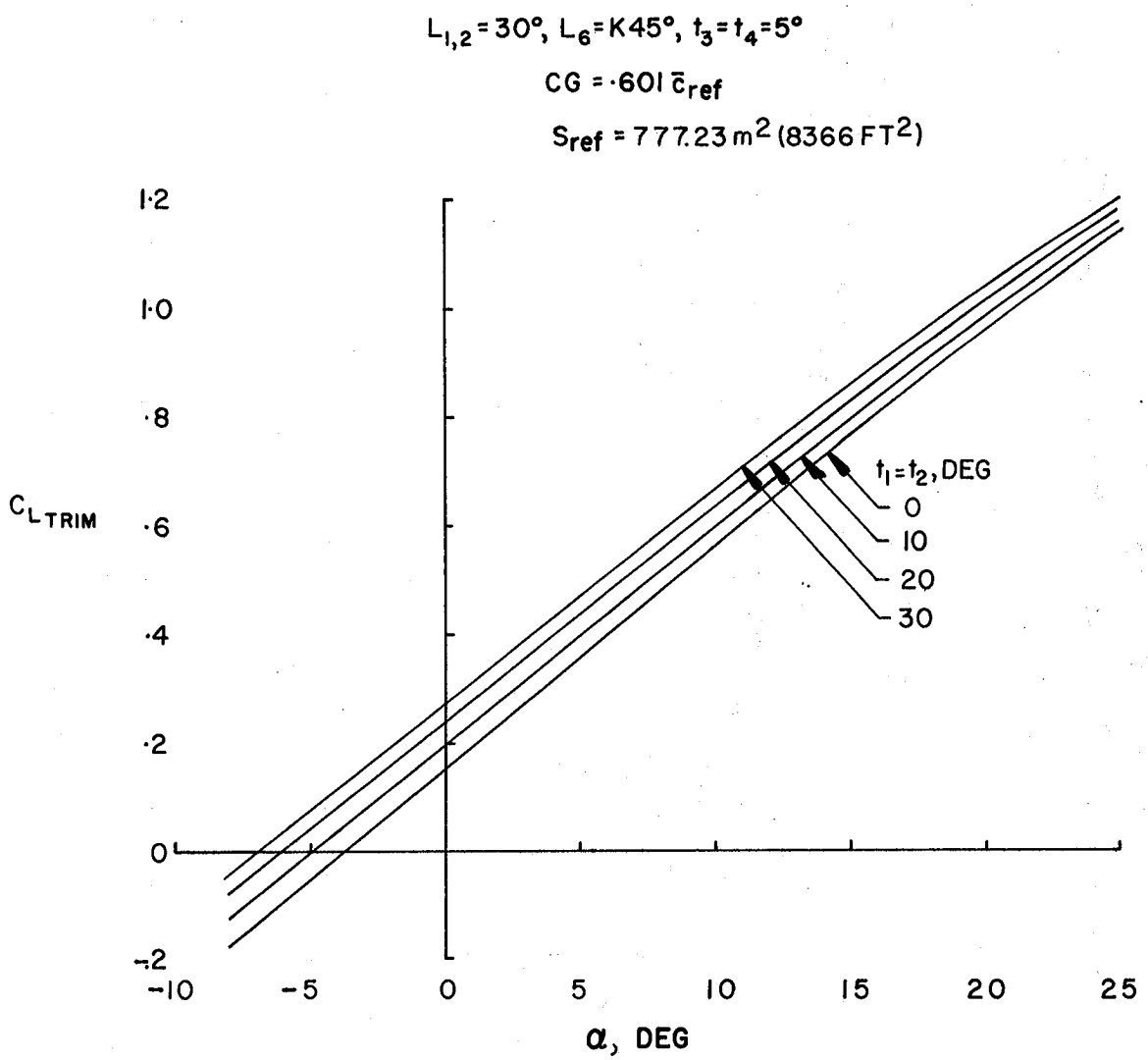


Figure 11.- Trimmed lift curves (out of ground effect).

$L_{1,2}=30°$, $L_6=K45°$, $t_3=t_4=5°$

$S_{ref}=777.23\ m^2(8366\ FT^2)$, $CG=.601\bar{c}$, LANDING GEAR RETRACTED

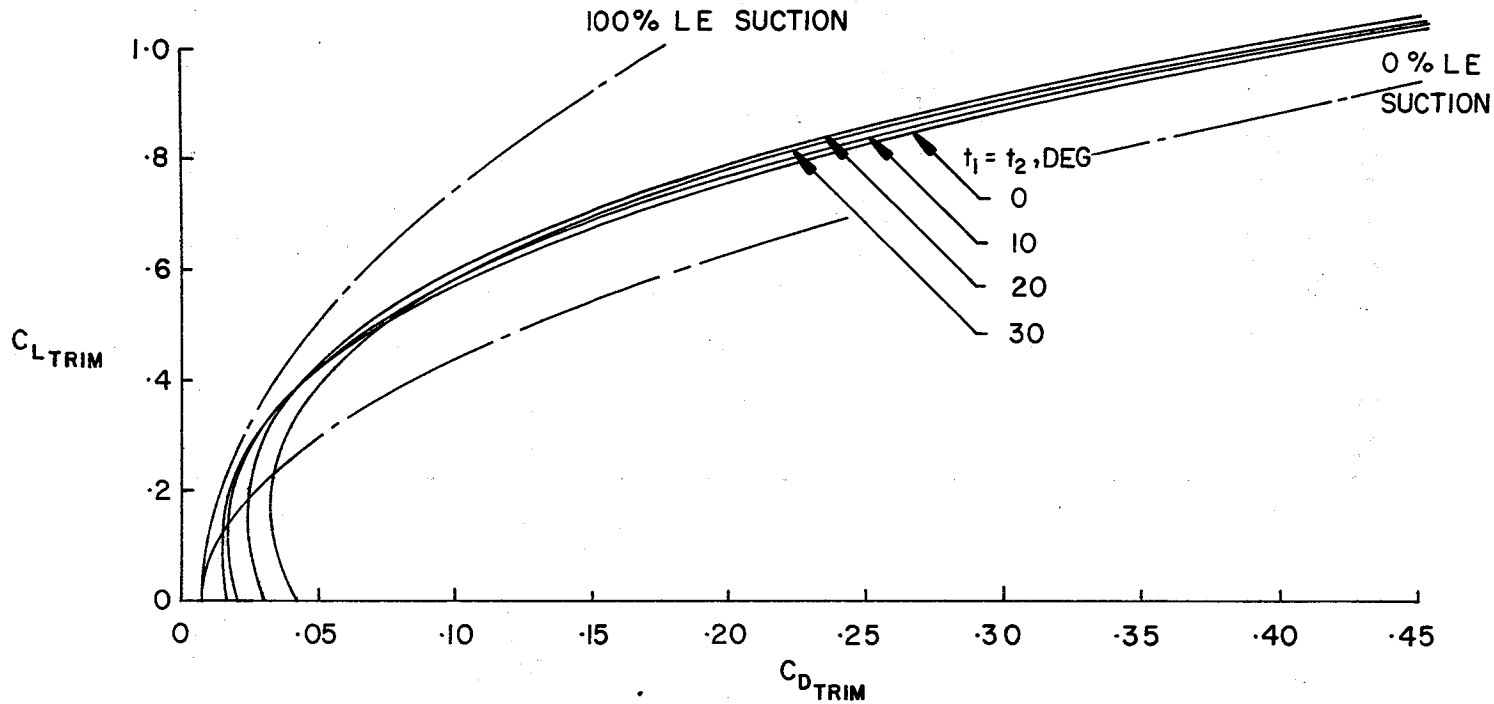


Figure 12.- Trimmed drag polar (out of ground effect).

$L_{1,2} = 30°$, $L_6 = K\,45°$, $t_3 = t_4 = 5°$, $S_{ref} = 777.23\ m^2 (8366\ FT^2)$ $CG = .601\ \bar{c}_{ref}$

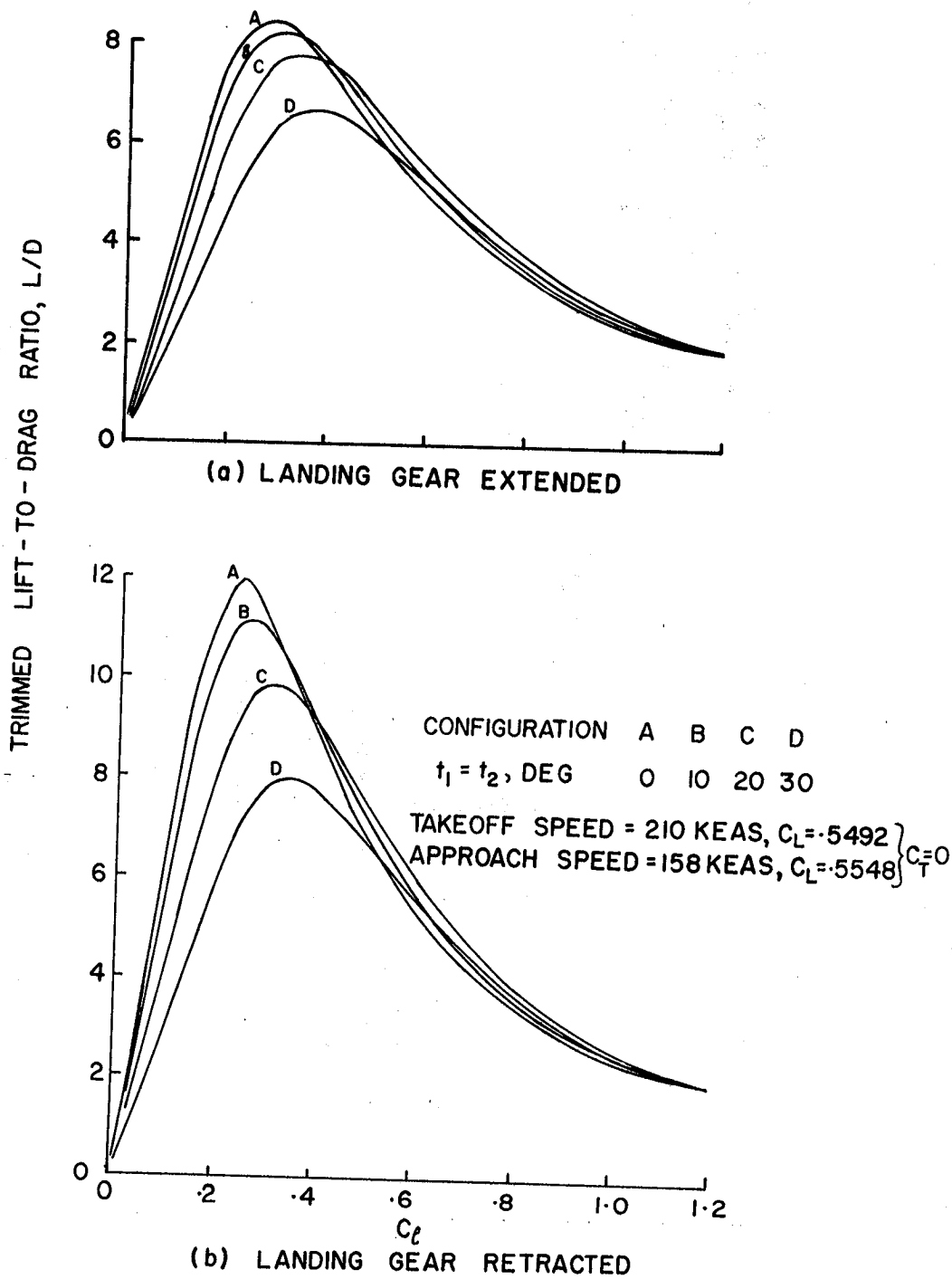


Figure 13.- High-lift configuration aerodynamic performance (out of ground effect).

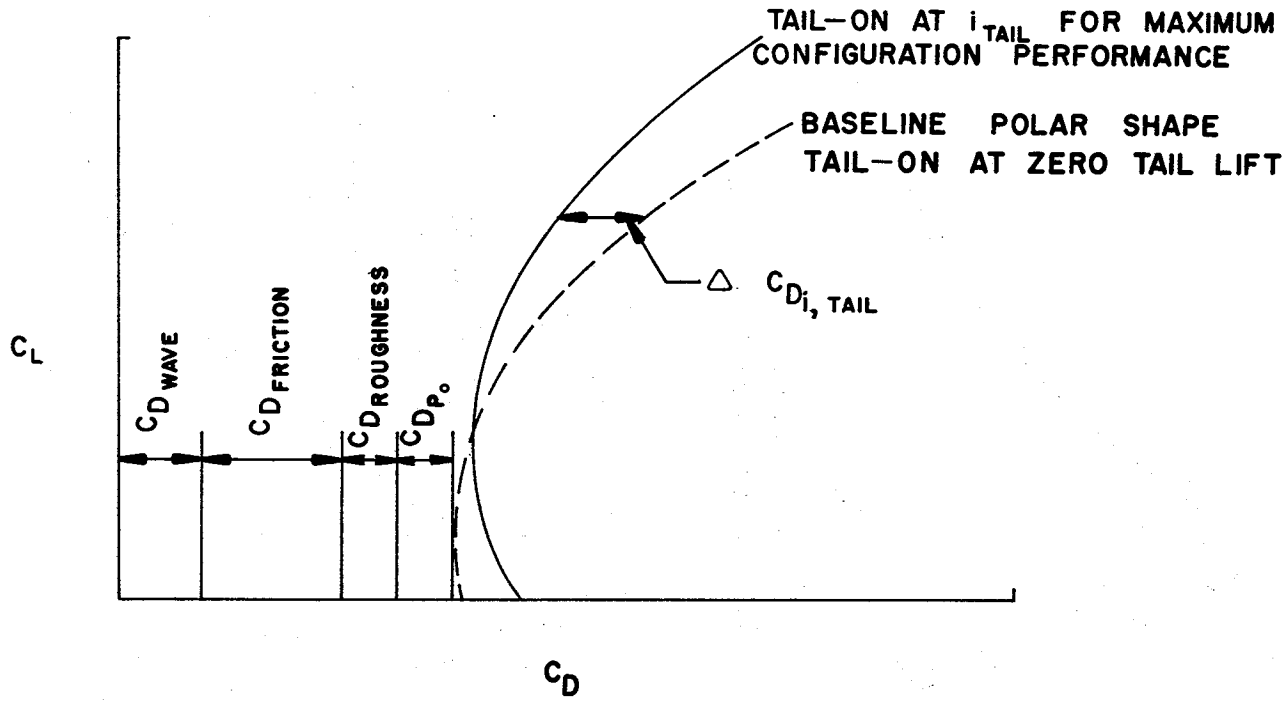


Figure 14.- High-speed drag build-up procedure.

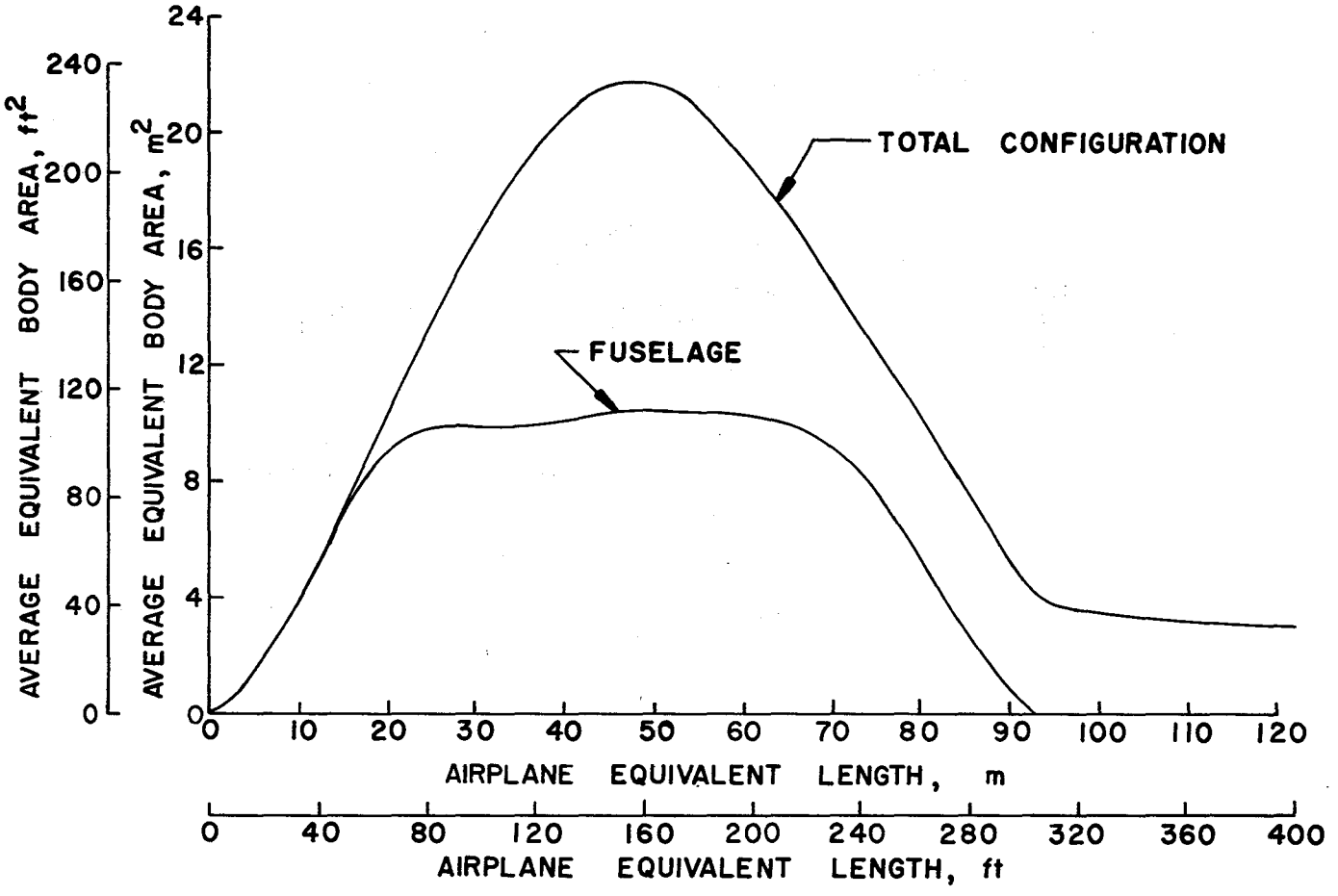


Figure 15.- Equivalent area distribution, M = 2.62.

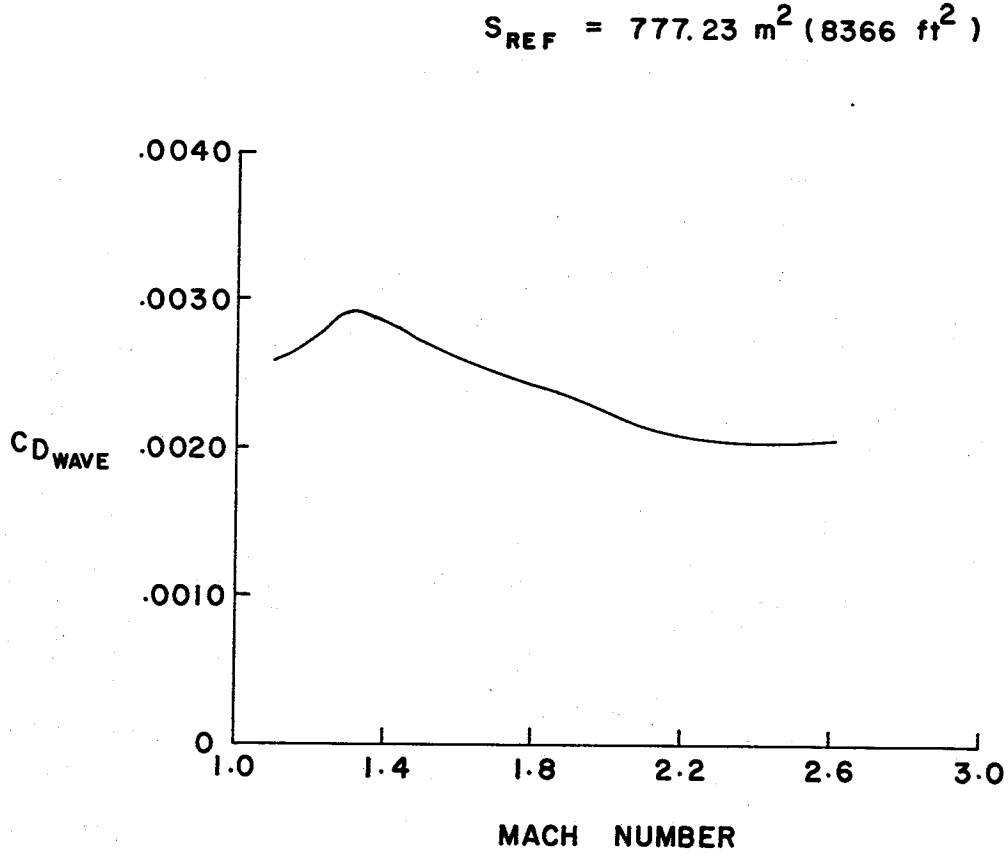


Figure 16.- Wave drag variation with Mach number.

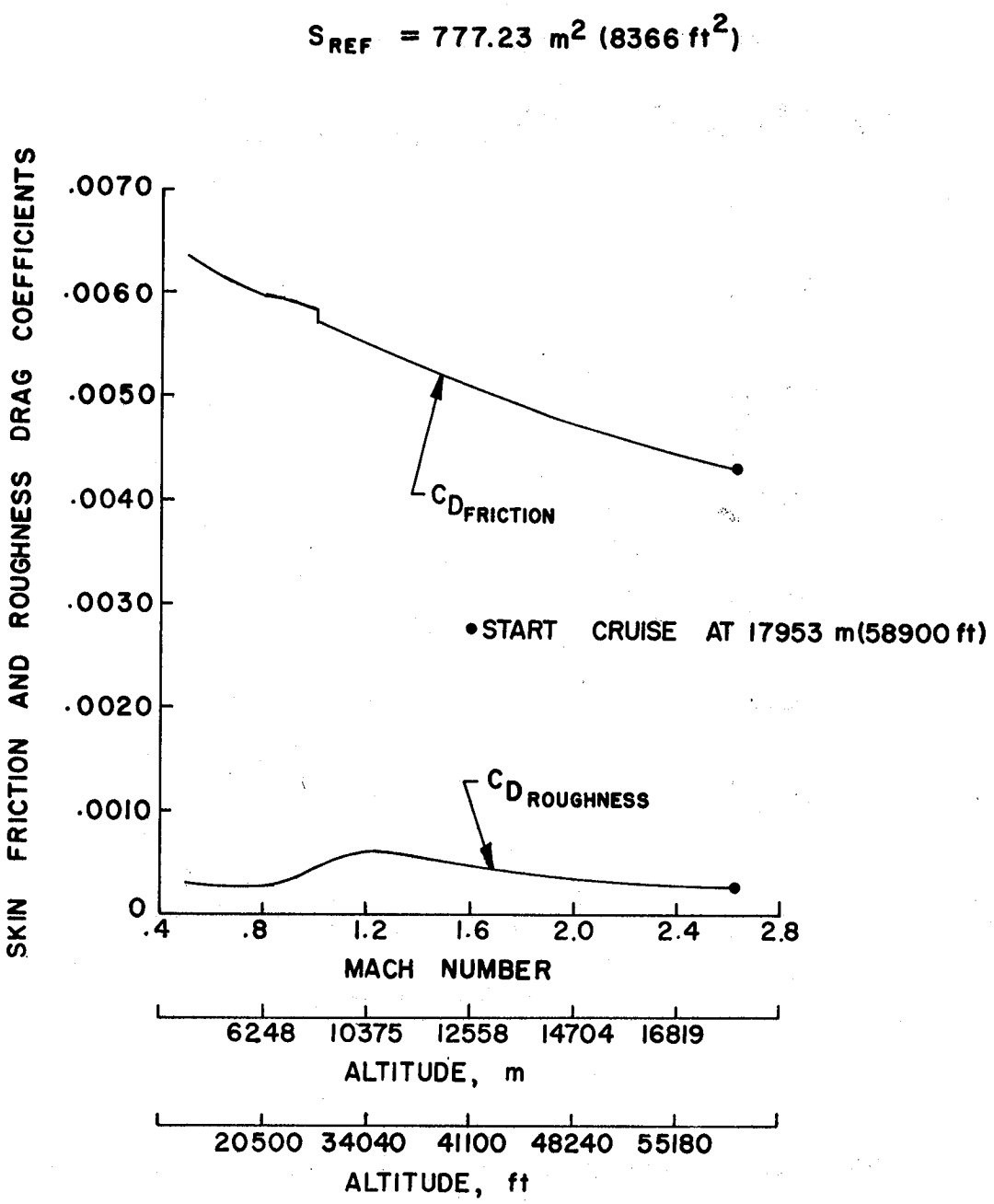


Figure 17.- Skin friction and roughness drag coefficients variation with altitude.

REFERENCE CONFIGURATION

$$C_{D_{P_o}} = C_{D_{MIN}} - (C_{D_{WAVE}} + C_{D_{FRICTION}} + C_{D_{ROUGHNESS}})$$

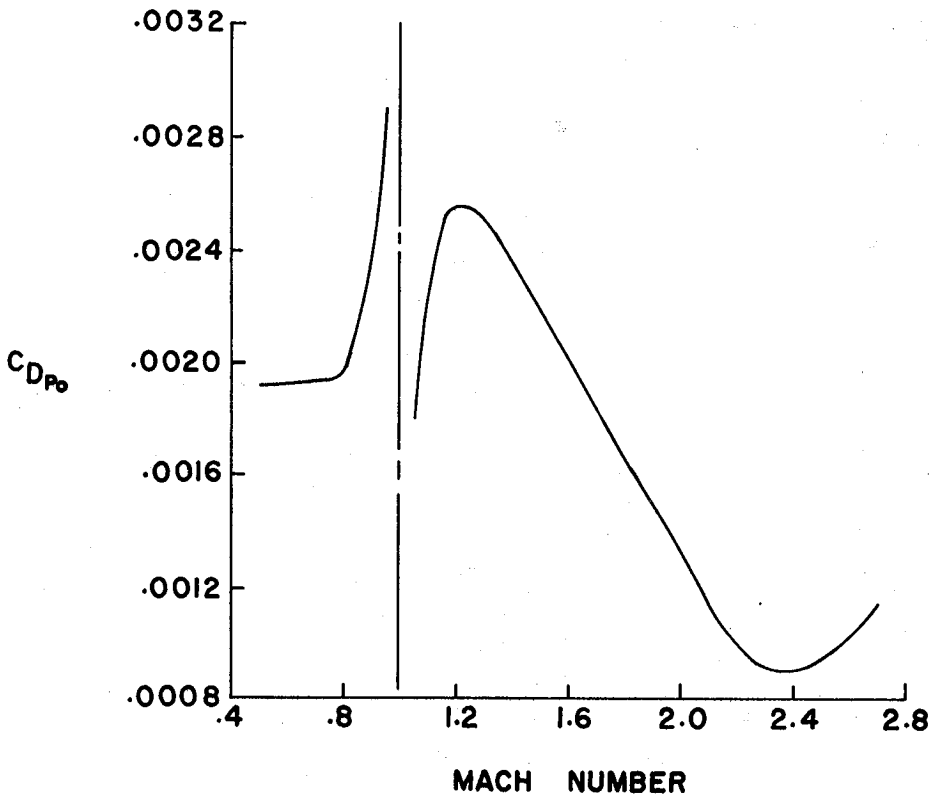


Figure 18.- Profile drag coefficient variation with Mach number.

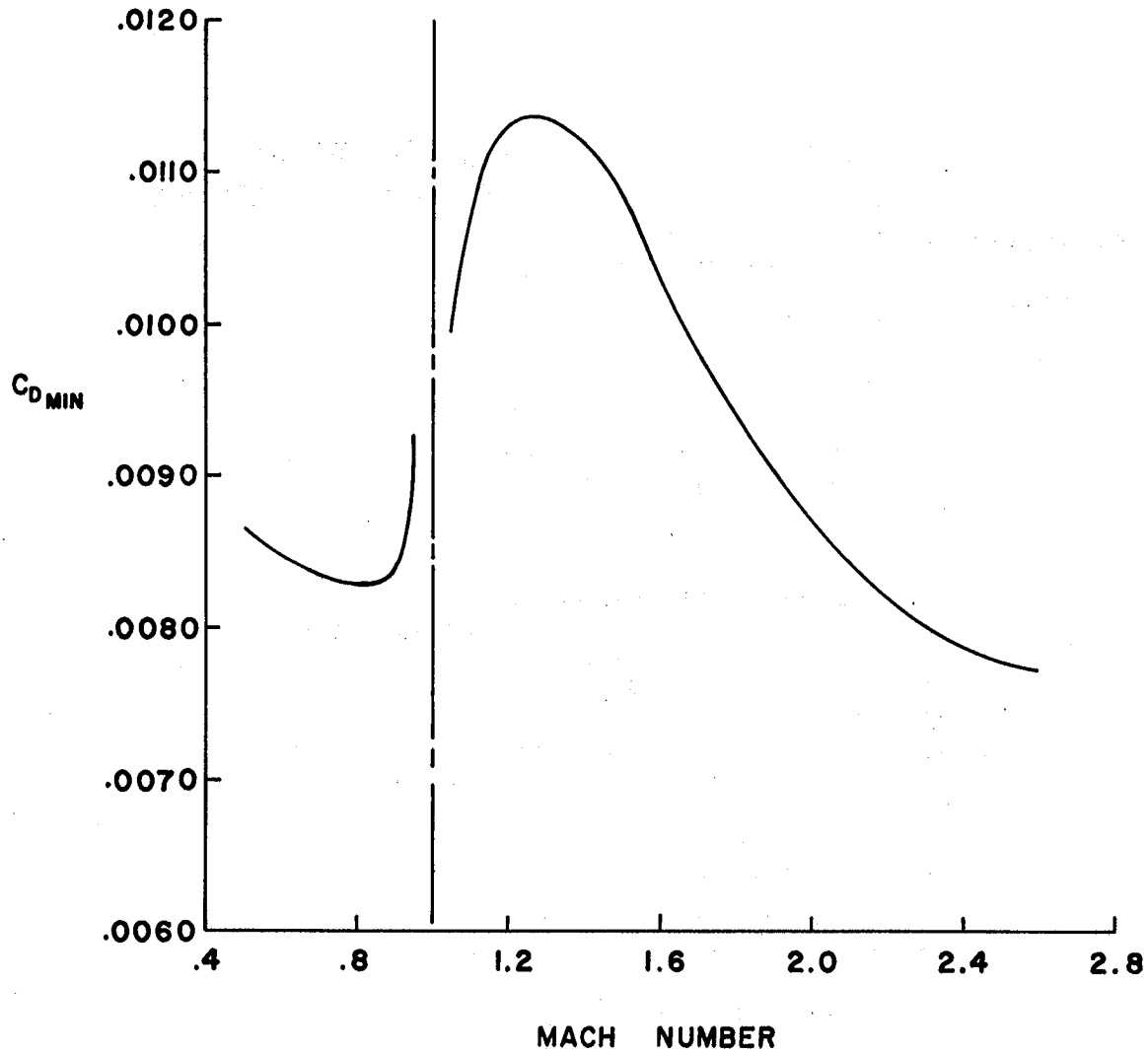


Figure 19.- Minimum drag coefficient variation.

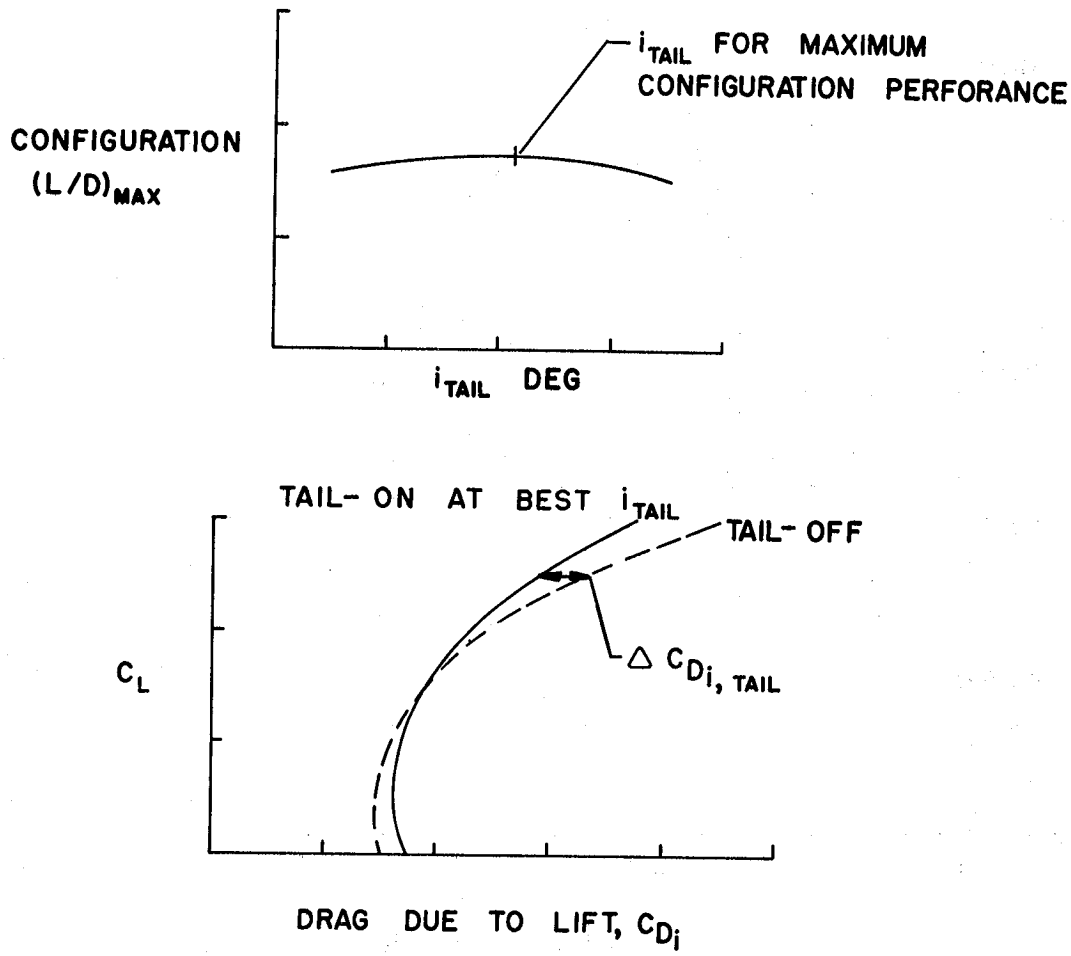


Figure 20.- Horizontal tail incidence for optimum configuration performance.

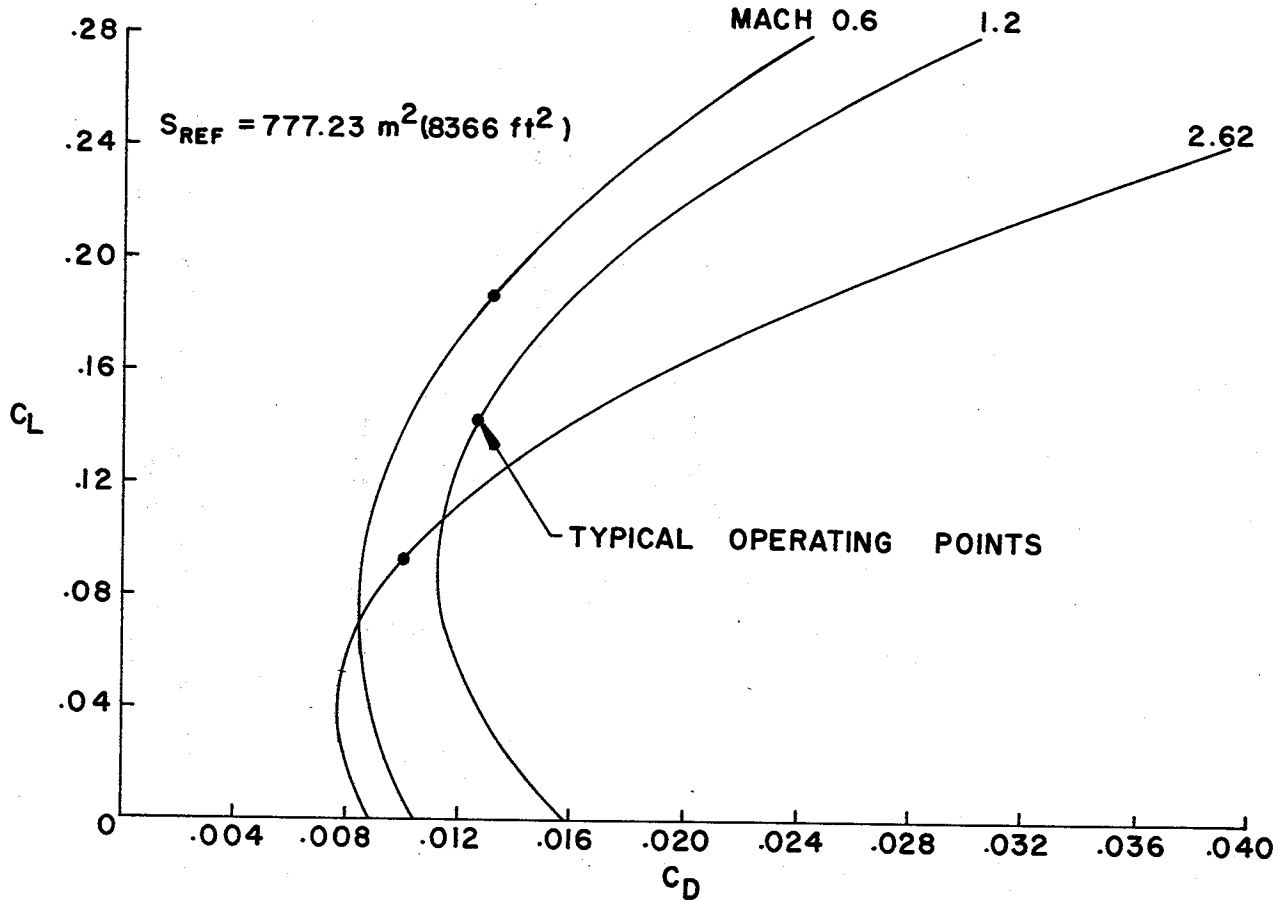


Figure 21.- Typical drag polars.

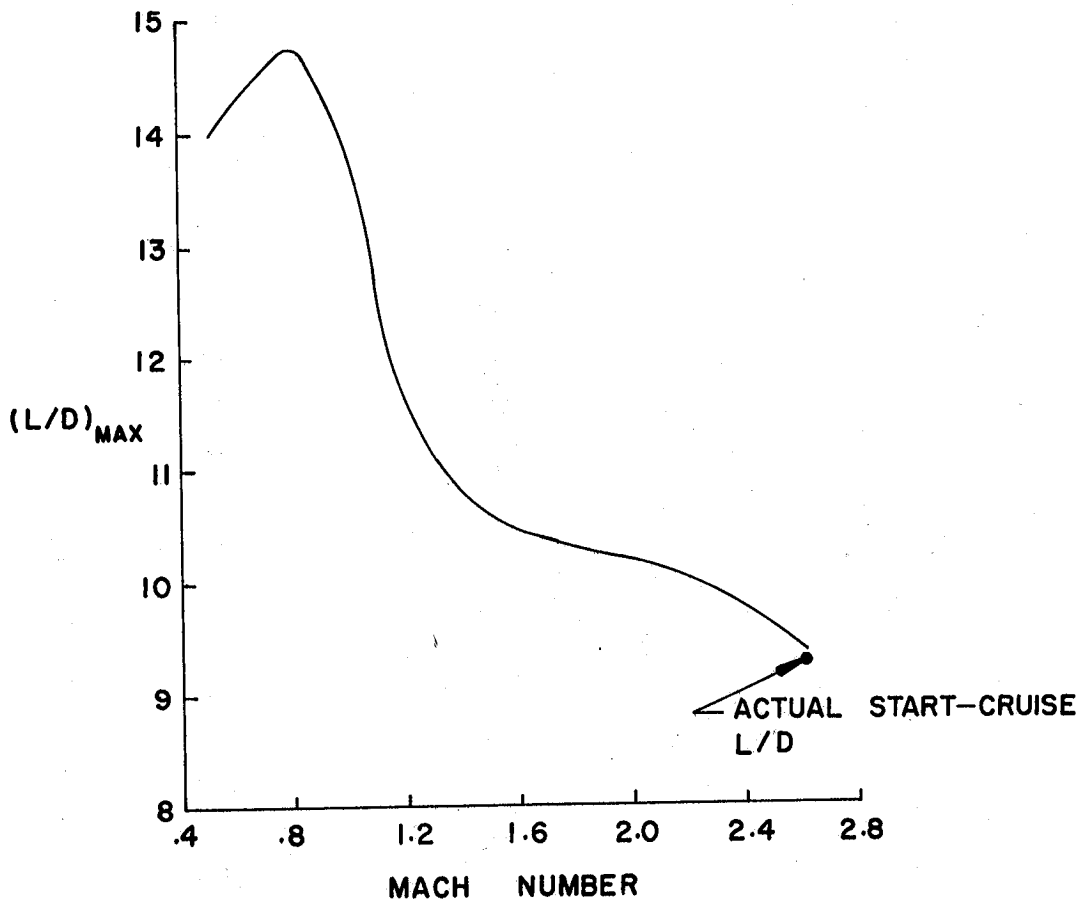


Figure 22.- Maximum lift-to-drag ratio variation with Mach number.

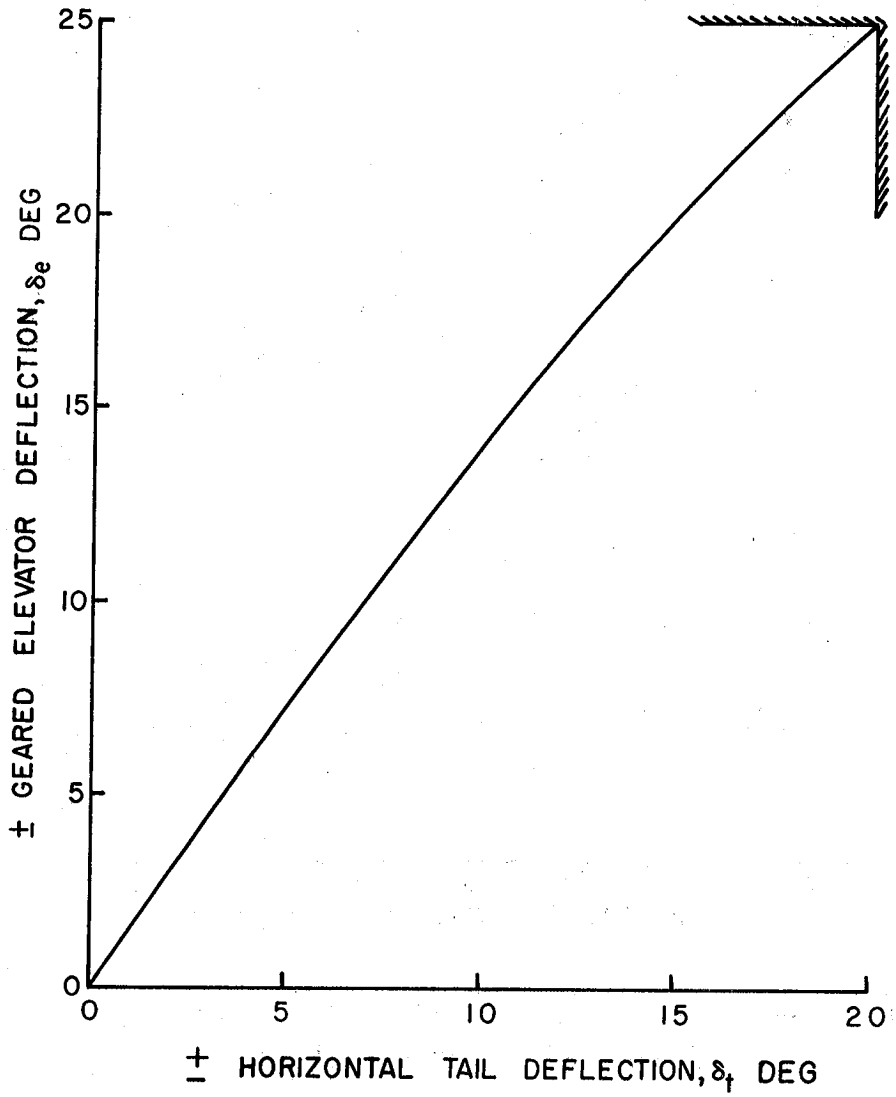


Figure 23.- Assumed horizontal tail/elevator deflection relationship.

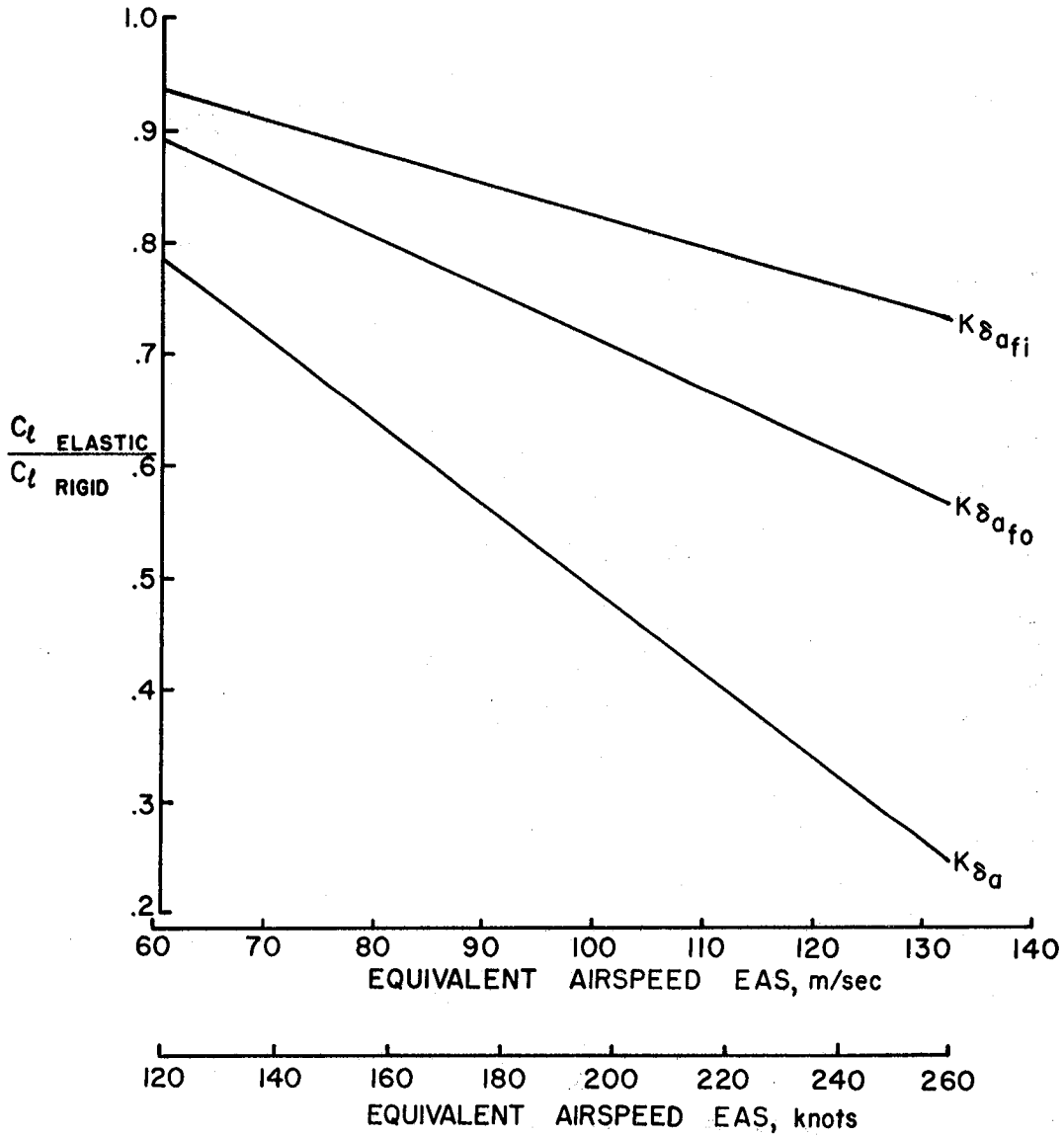


Figure 24.- Estimated lateral control-flexibility factors.

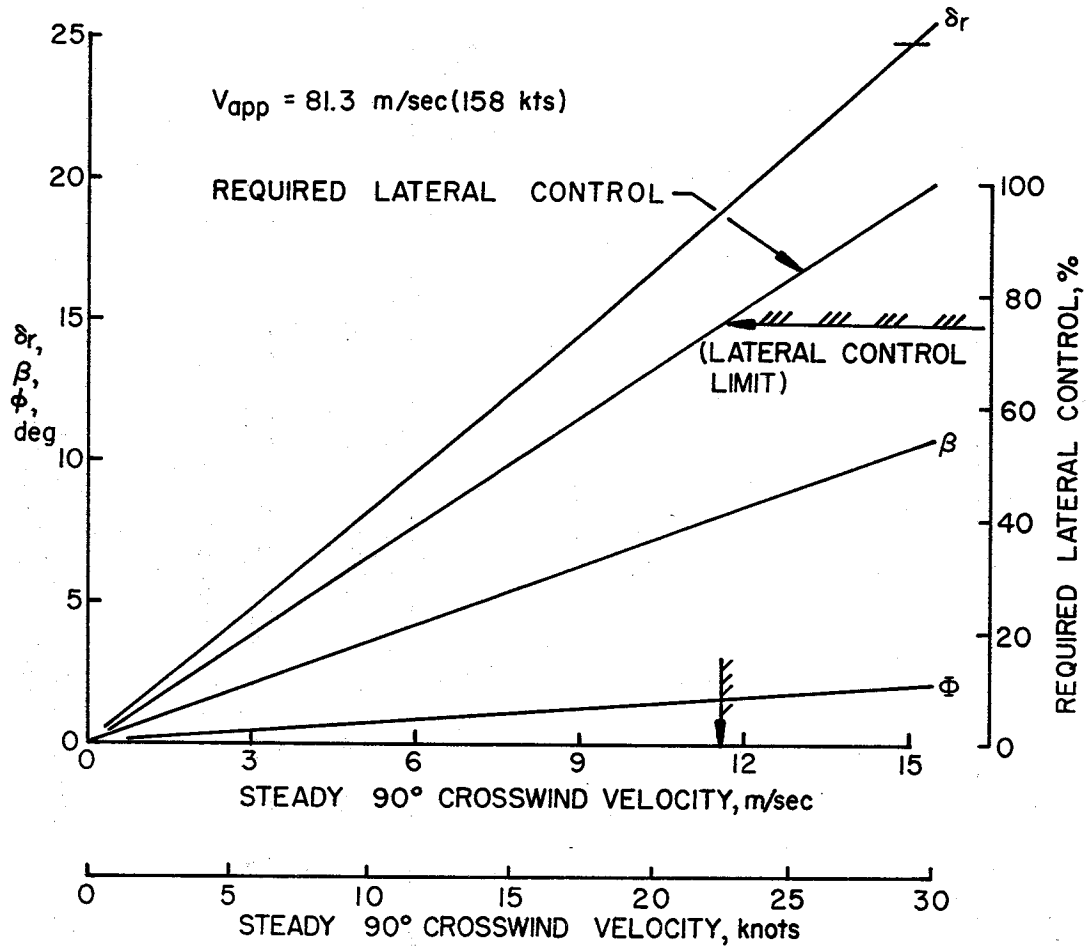


Figure 25.- Crosswind trim capability.

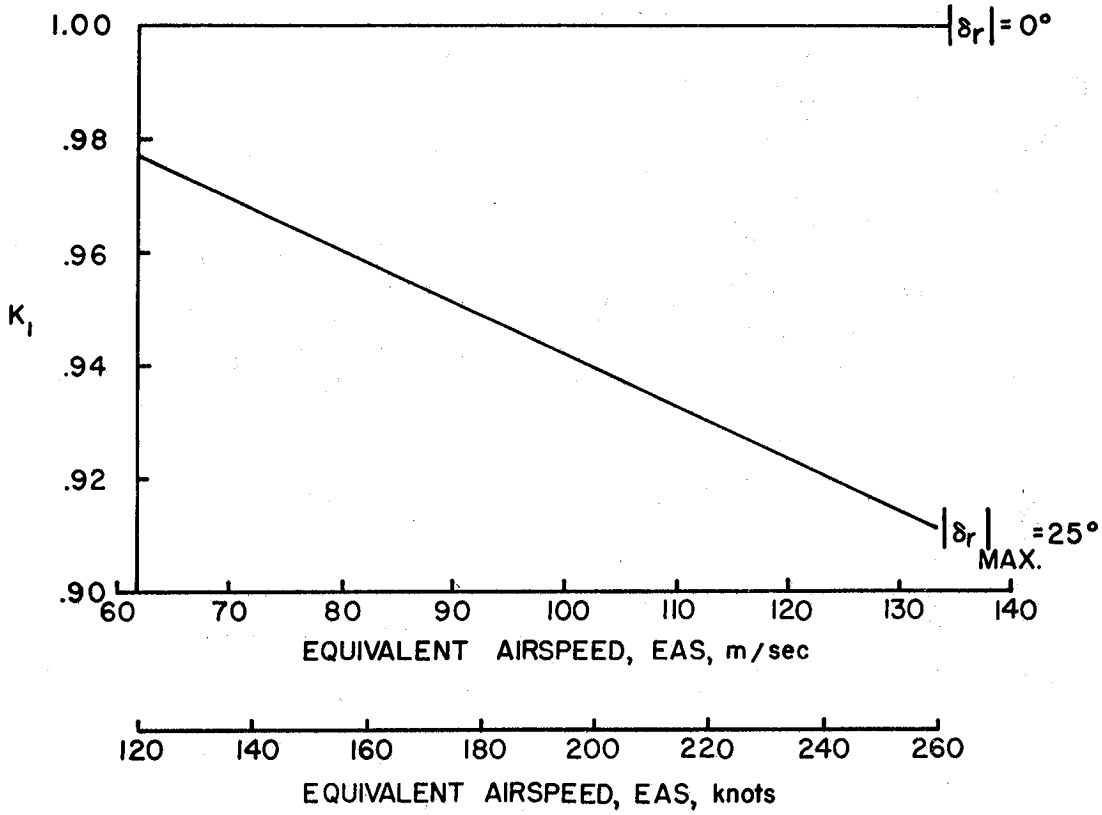


Figure 26.- Estimated directional control flexibility factors due to fuselage bending.

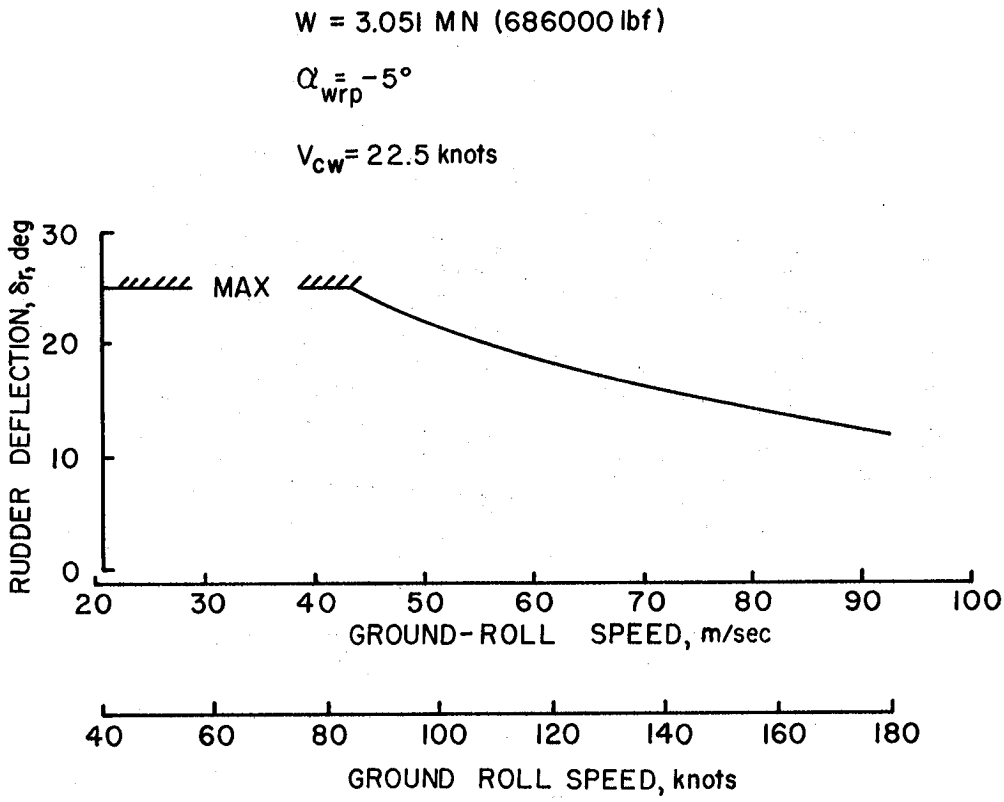


Figure 27.- Directional trim required in 90-degree crosswind.

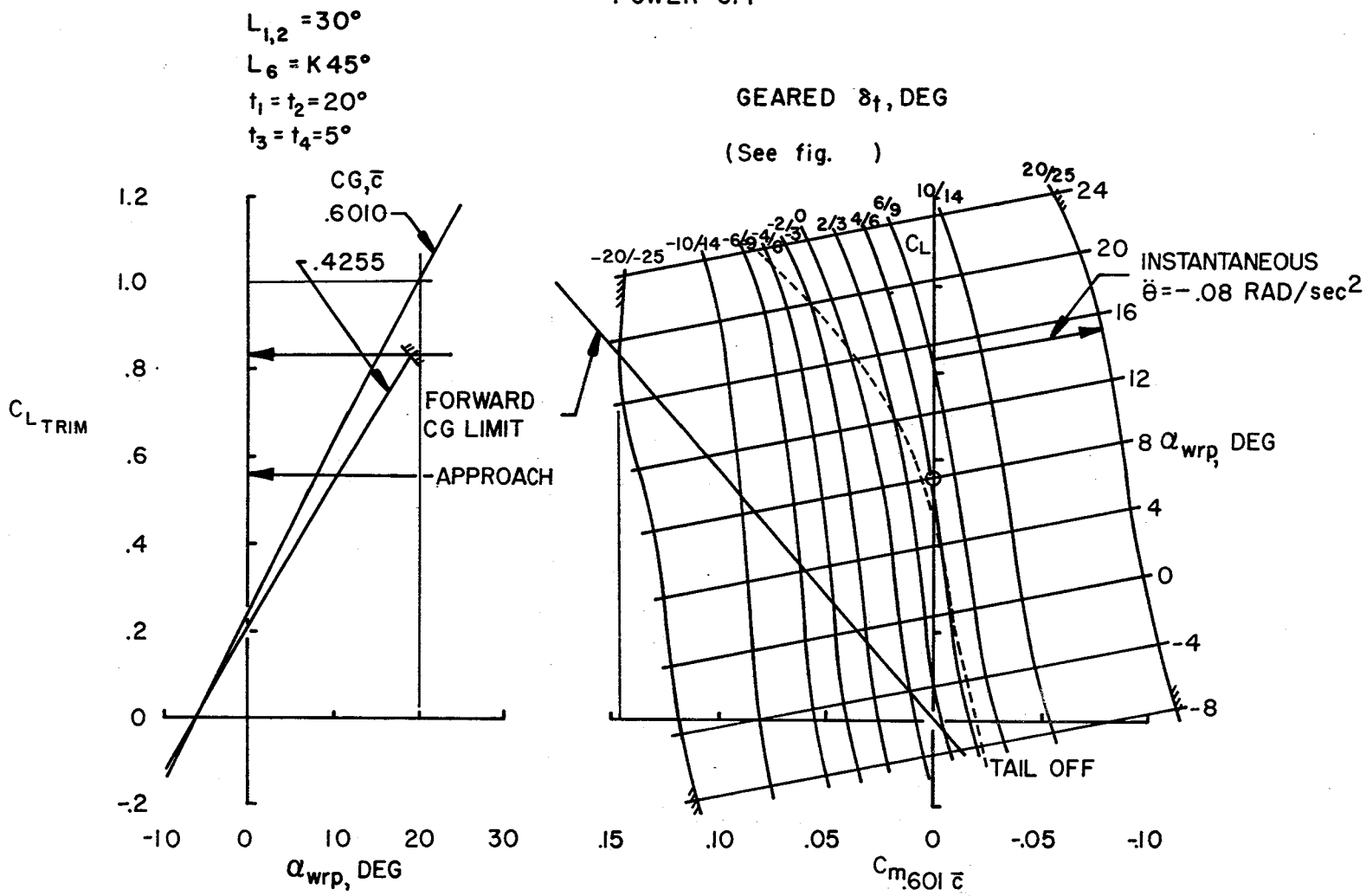


Figure 28.- High-lift trim and stability (out-of-ground effect).

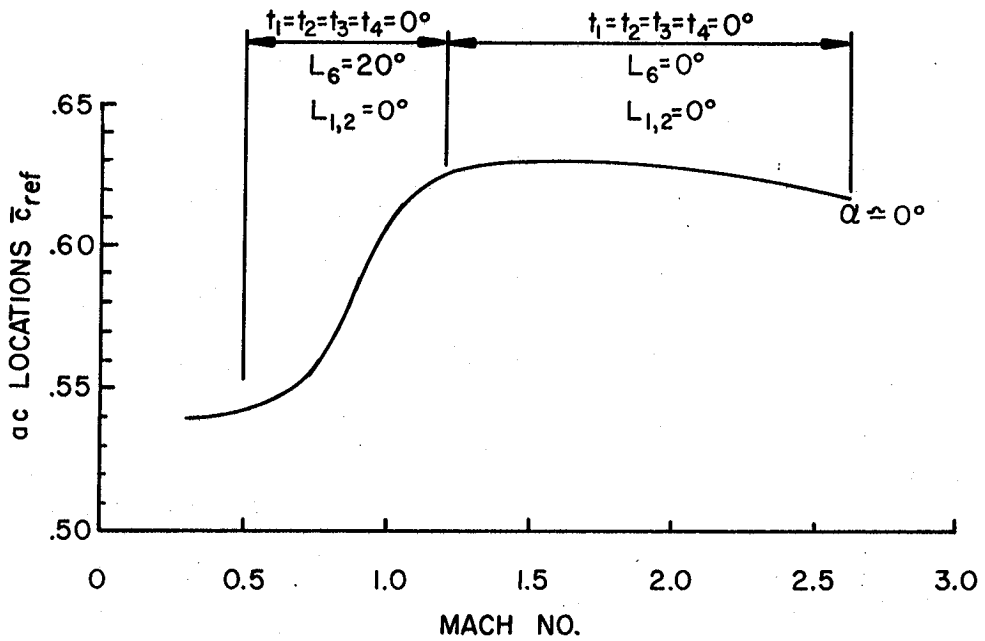


Figure 29.- Flexible airplane aerodynamic center location variation with Mach number.

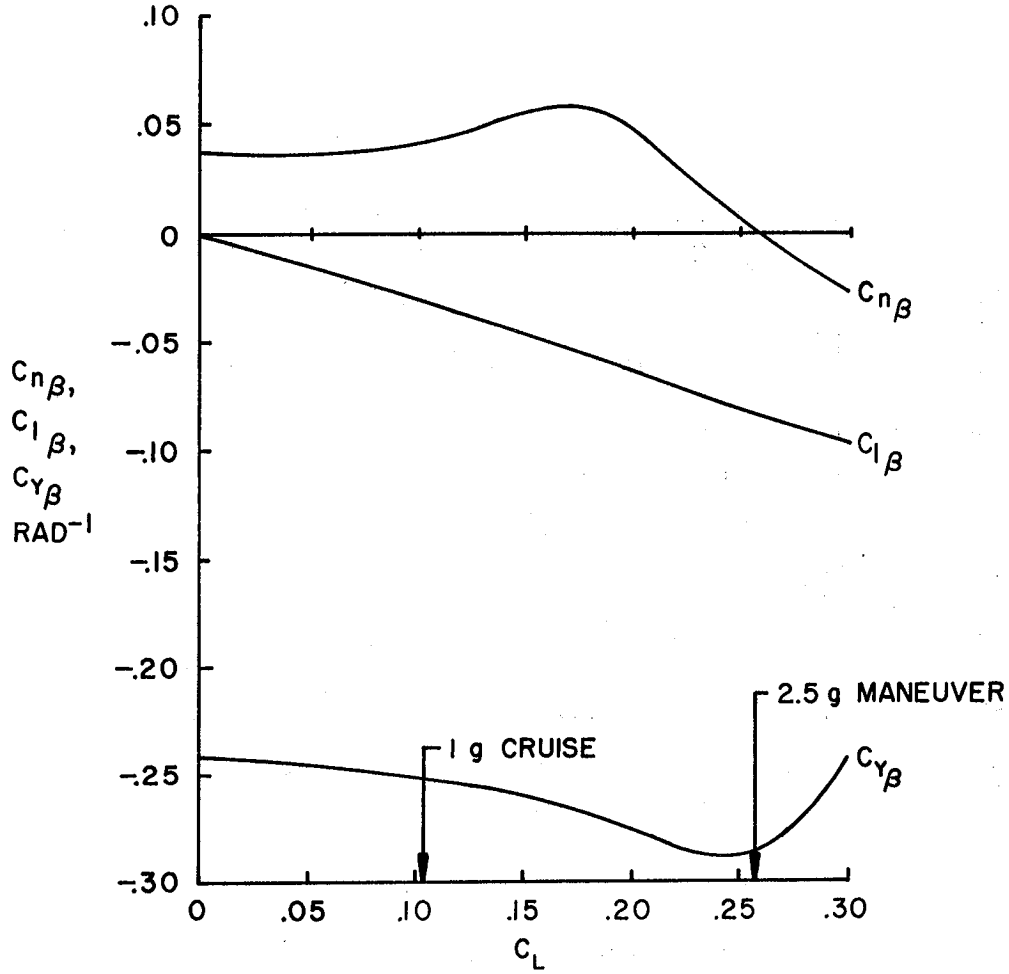


Figure 30.- Flexible static lateral-directional stability at M = 2.62.

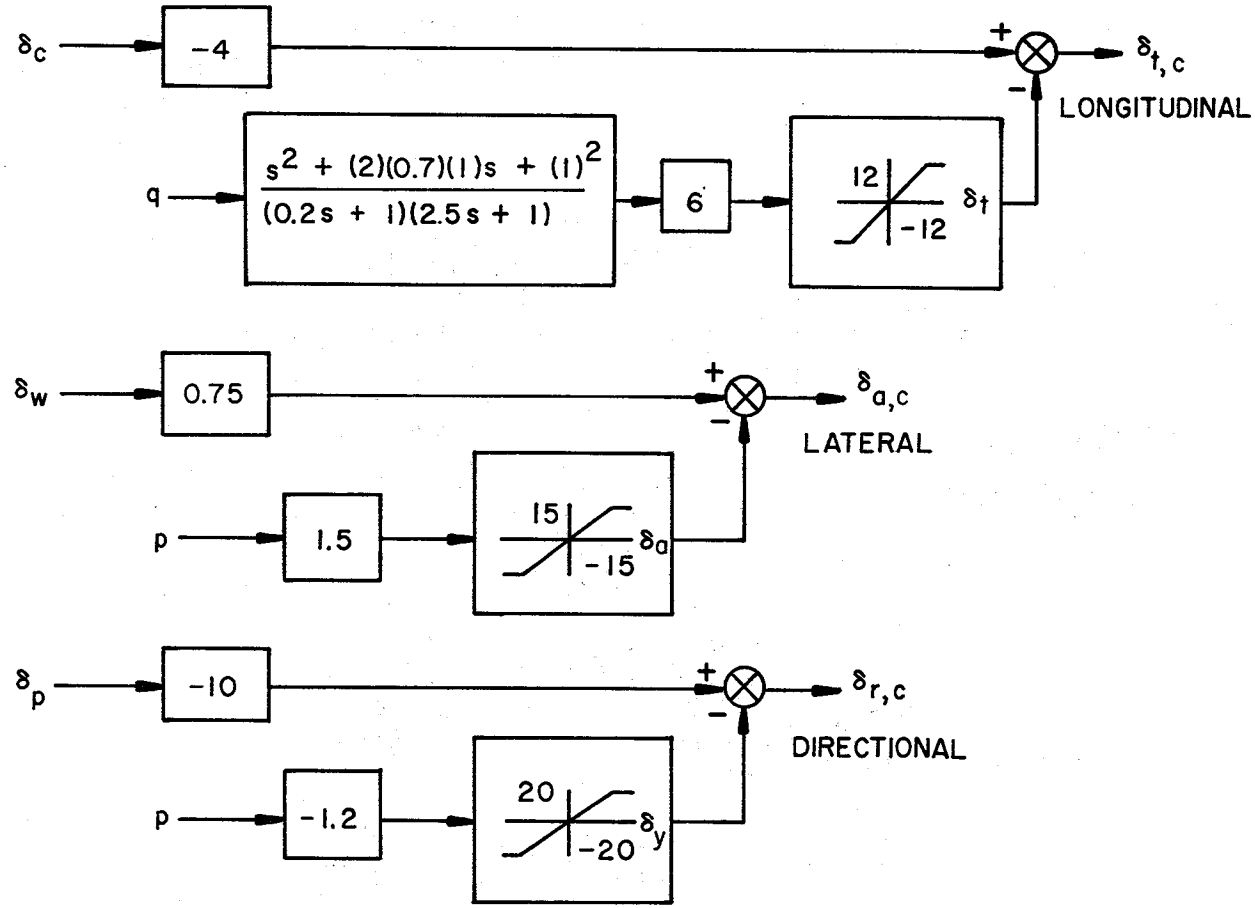


Figure 31.- Hardened stability augmentation system (HSAS). All control surface deflections had 0.1-second lag due to actuator servo.

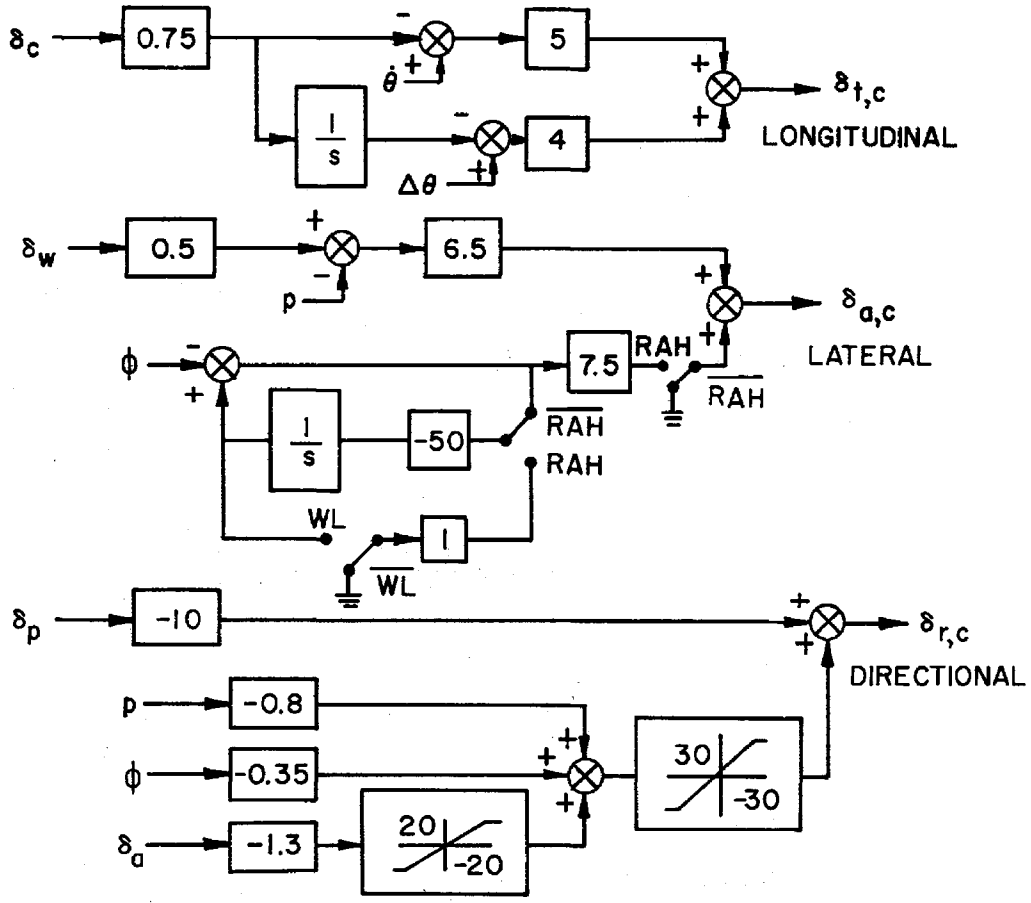


Figure 32.- Normal stability and control augmentation system (SCAS). All control surface deflections had 0.1-second lag due to actuator servo.

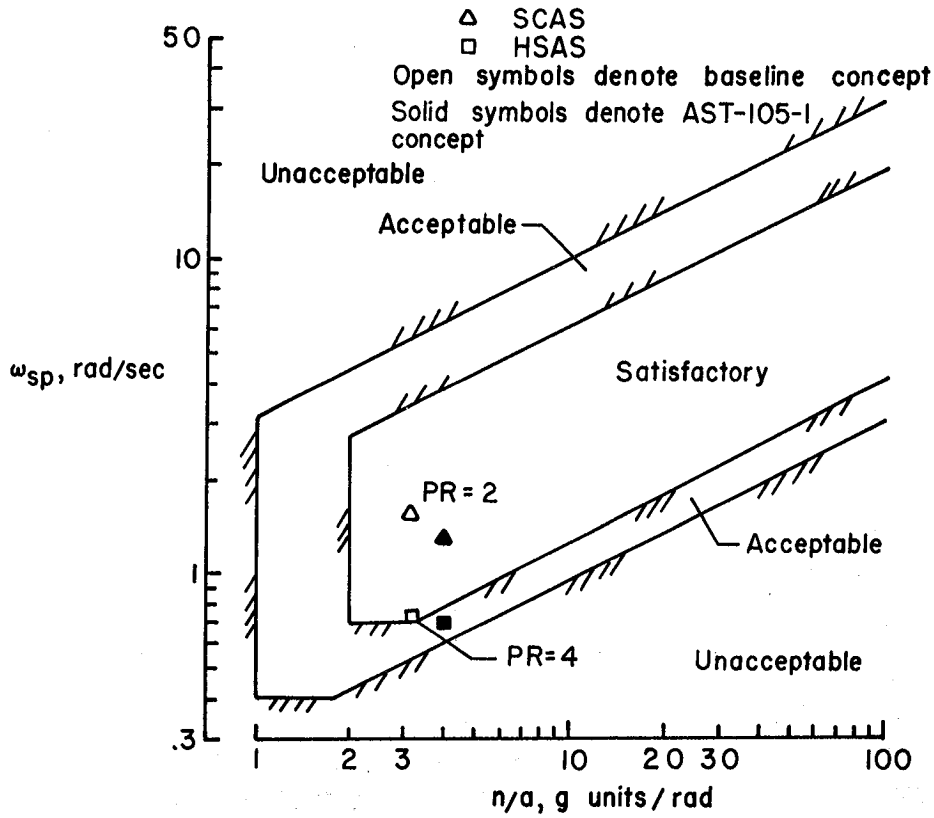


(a) Longitudinal short-period frequency requirements of reference 21 (Unaugmented configurations fell outside of plotted range.)

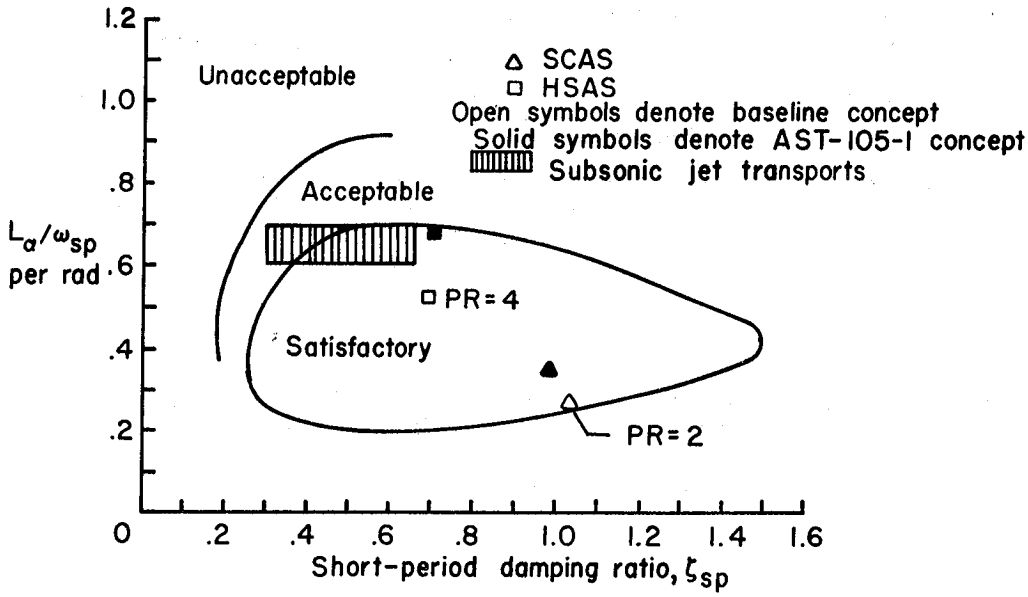


(b) Shomber-Gertsen longitudinal handling qualities criteria of reference 22 (Unaugmented configurations fell outside of plotted range.)

Figure 33.- Comparison of longitundinal short-period characteristics with handling qualities criteria.

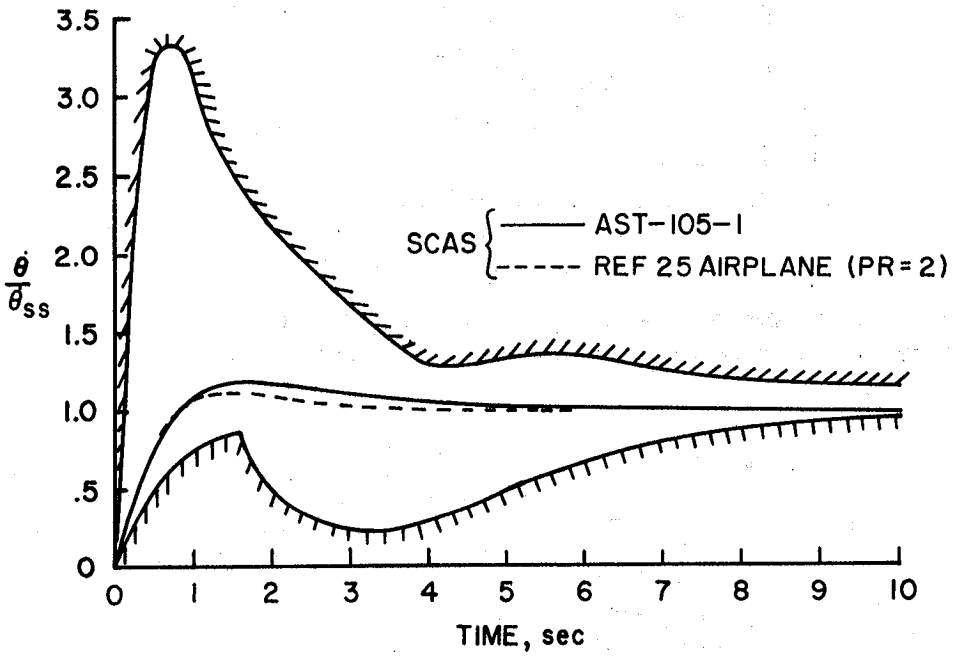


Figure 34.- Comparison of low-speed pitch rate response with criteria boundaries from reference 23.

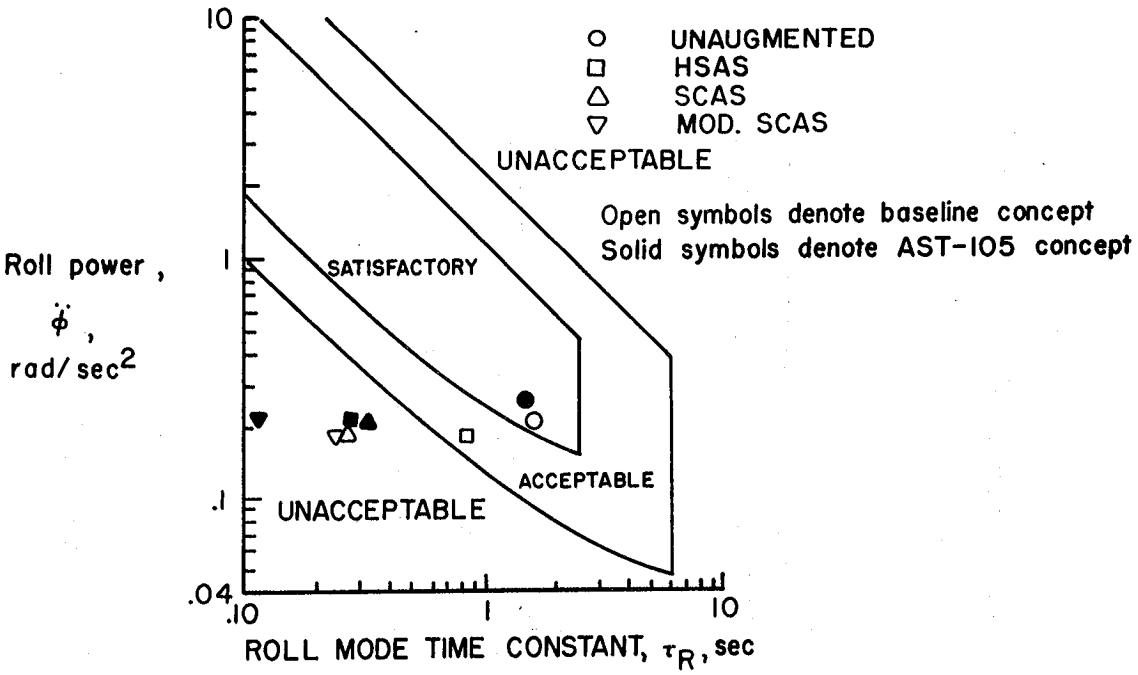


(a) Roll acceleration response boundaries for large aircraft
Boundaries from reference 24

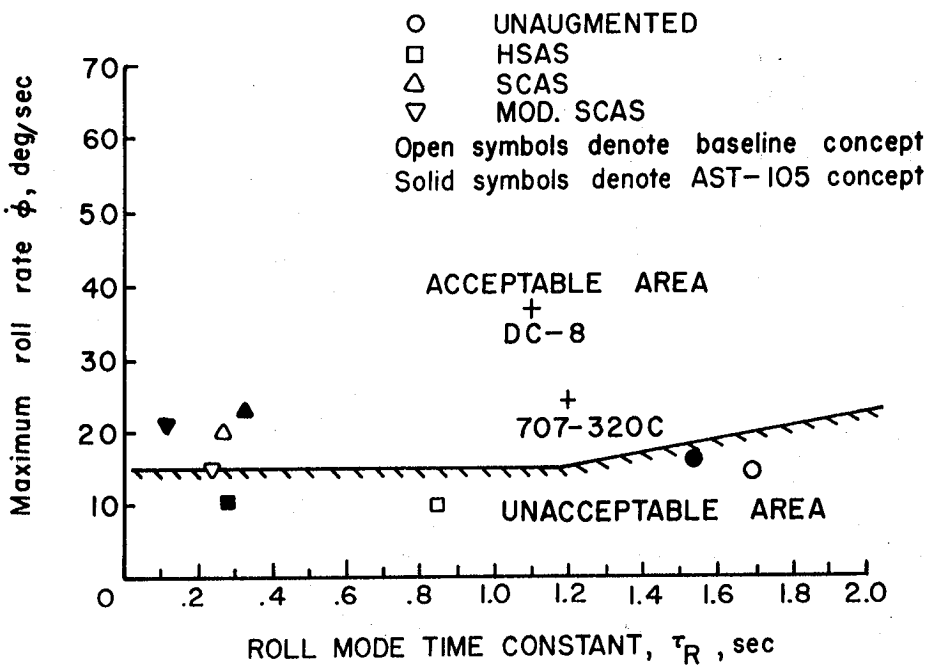


(b) Roll-rate capability criterion for transport aircraft
Boundaries from reference 26

Figure 35.- Comparison of roll response with criteria boundaries.

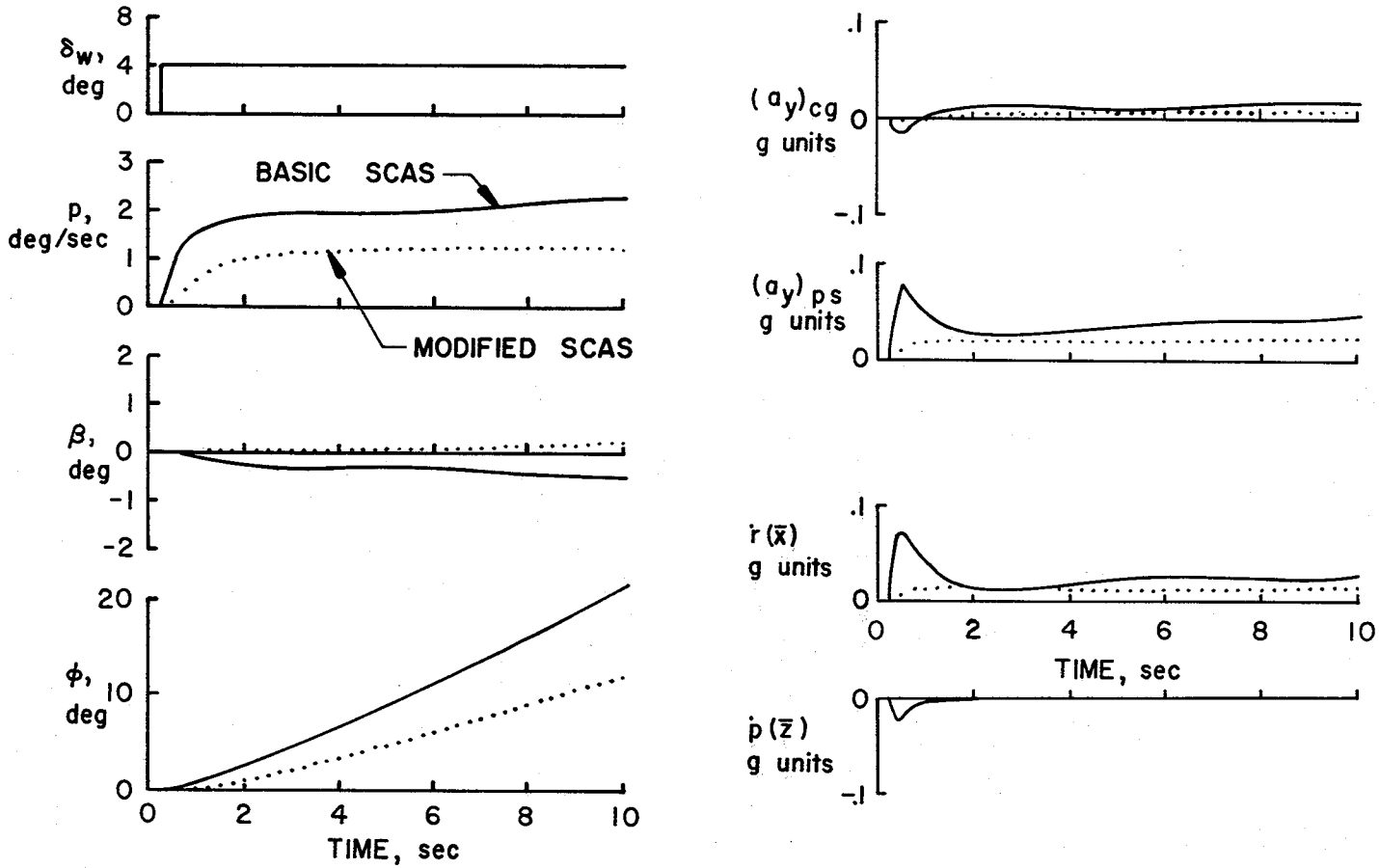


Figure 36.- Comparison of lateral response to control wheel step input for SCAS and modified SCAS configurations.

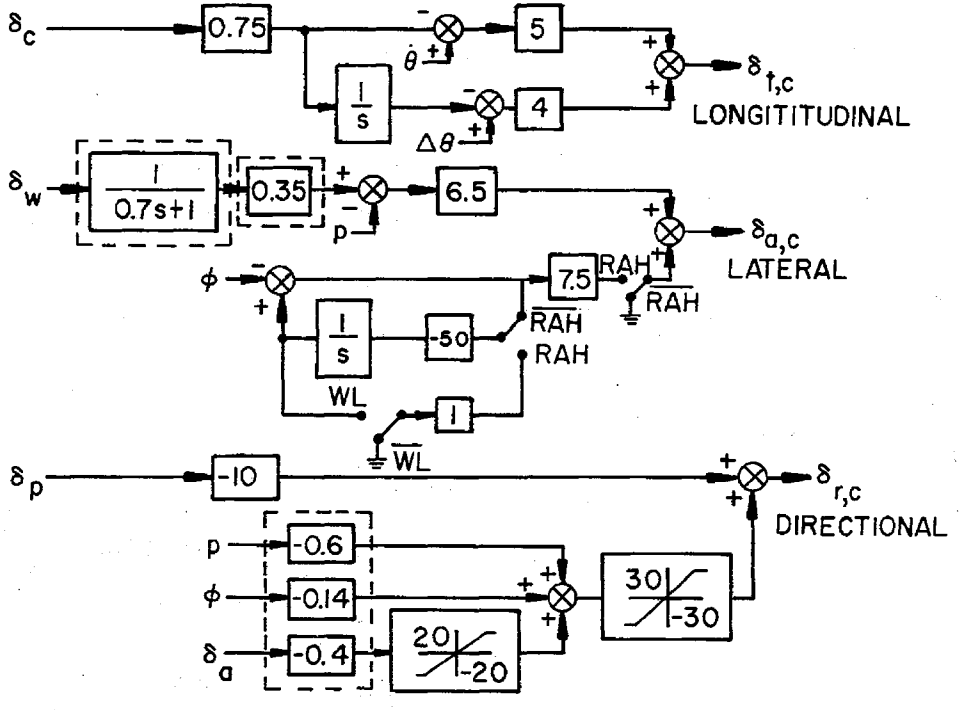


Figure 37.- Modified stability and control augmentation system (SCAS). Modifications to SCAS of figure 32 are indicated with dashed lines.

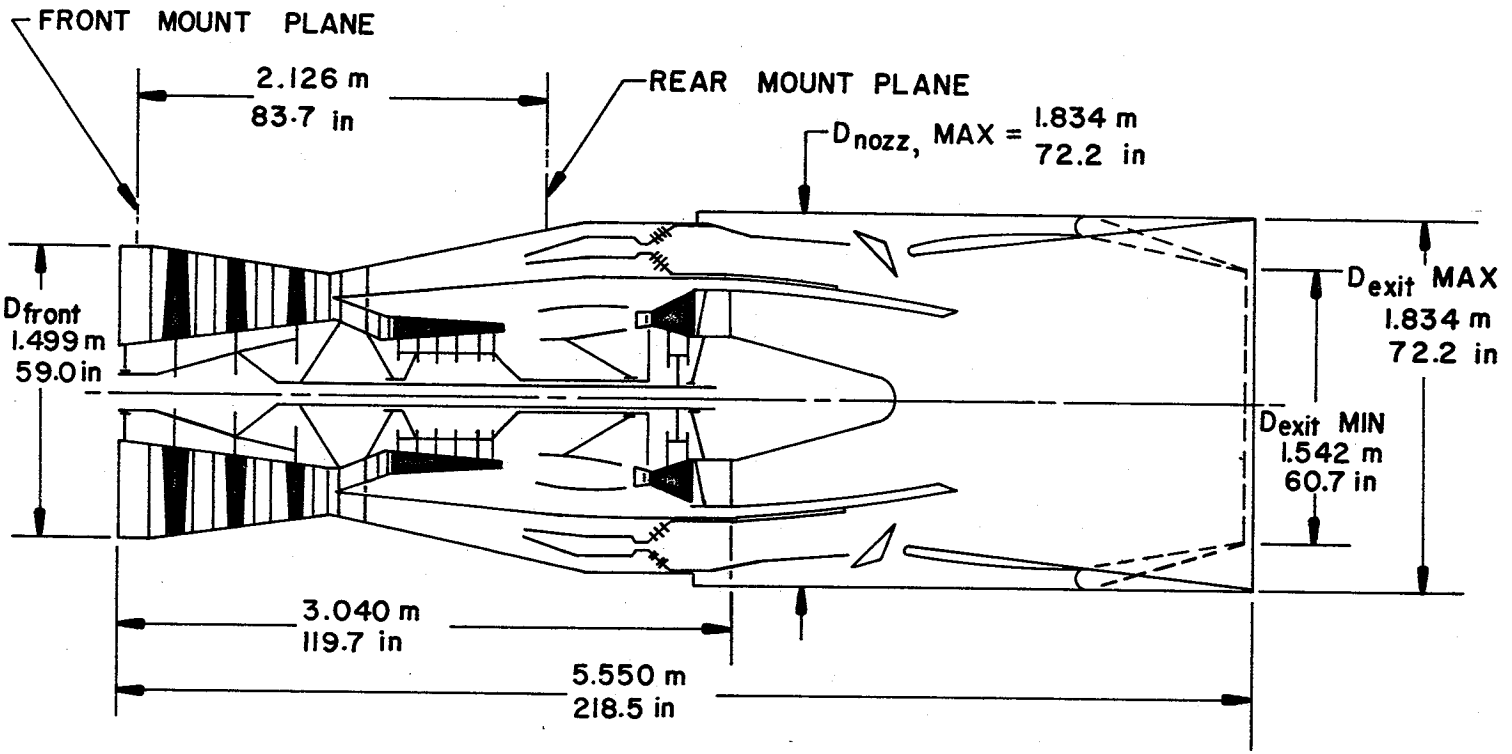


Figure 38.- Pratt and Whitney Aircraft VSCE-516 duct burning turbofan engine.

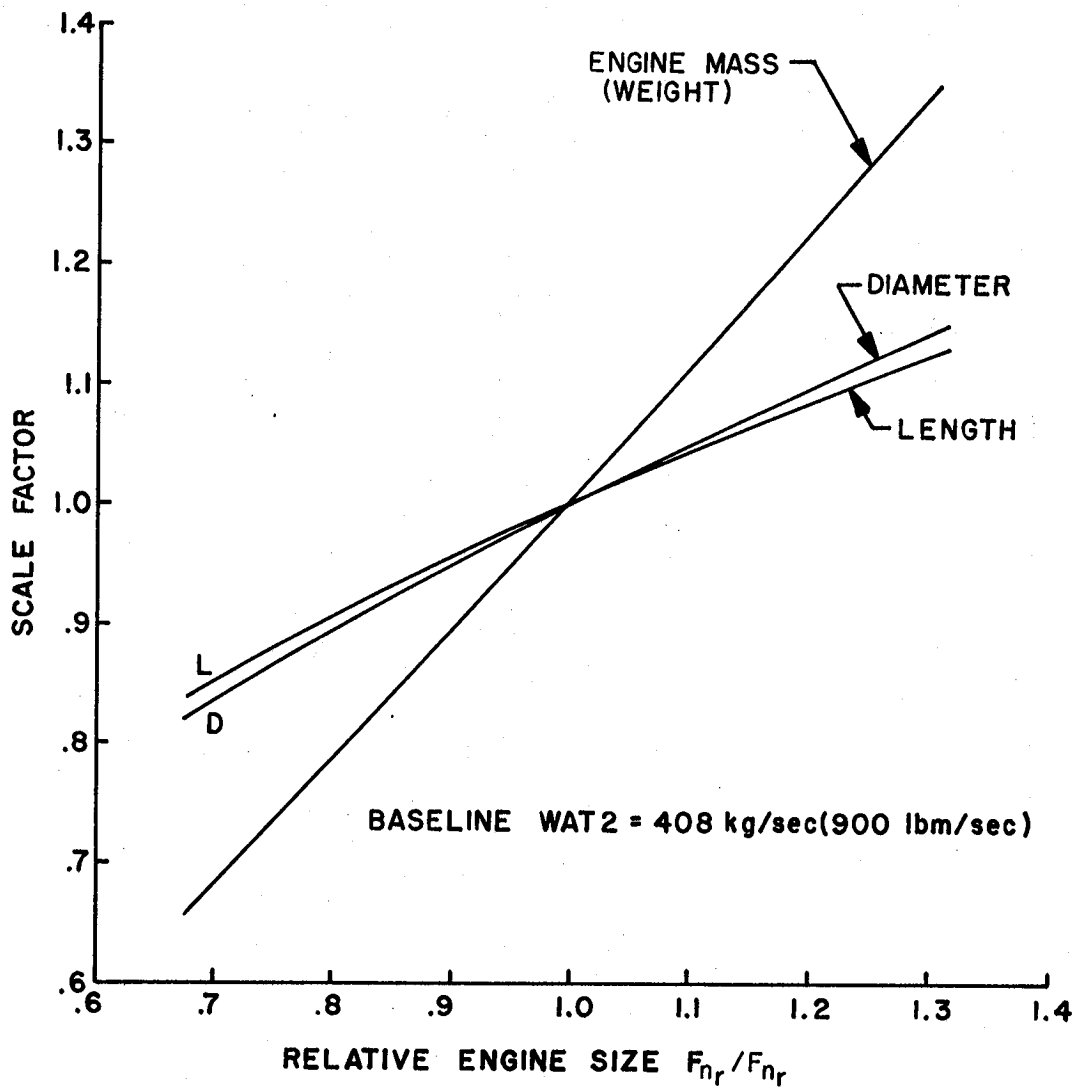


Figure 39.- Engine and nacelle scaling factors.

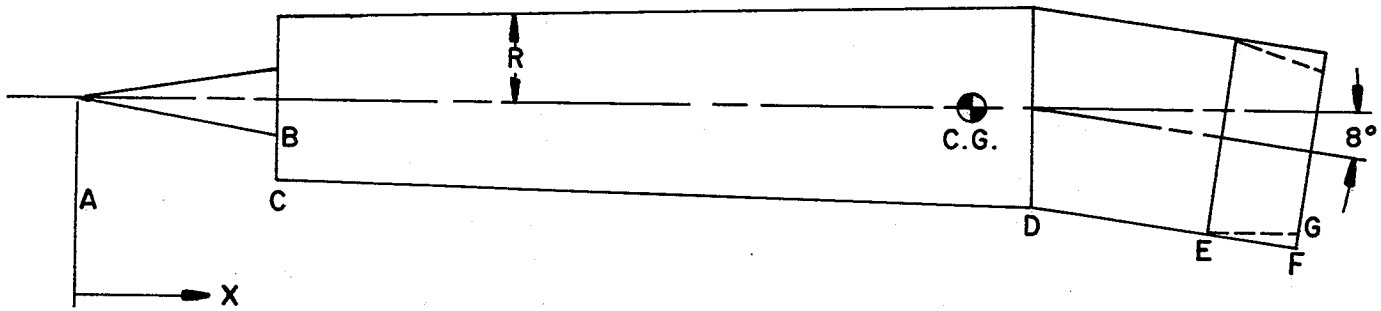


| STATION | X | | R | | AREA | |
|---|---|---|---|---|---|---|
| | m | ft | m | ft | $m^2$ | $ft^2$ |
| A | 0 | 0 | 0 | 0 | 0 | 0 |
| B | 1.911 | 6.271 | .296 | .972 | .276 | 2.968 |
| C | 1.911 | 6.271 | .770 | 2.526 | 1.862 | 20.045 |
| D | 9.123 | 29.931 | .915 | 3.003 | 2.632 | 28.331 |
| E | 11.044 | 36.233 | .915 | 3.003 | 2.632 | 28.331 |
| F(max R) | 11.917 | 39.099 | .915 | 3.003 | 2.632 | 28.331 |
| G(min R) | 11.917 | 39.099 | .770 | 2.526 | 1.862 | 20.045 |
| C.G(engine) | 8.543 | 28.028 | 0 | 0 | 0 | 0 |

Figure 40.- VSCE-516 engine nacelle.

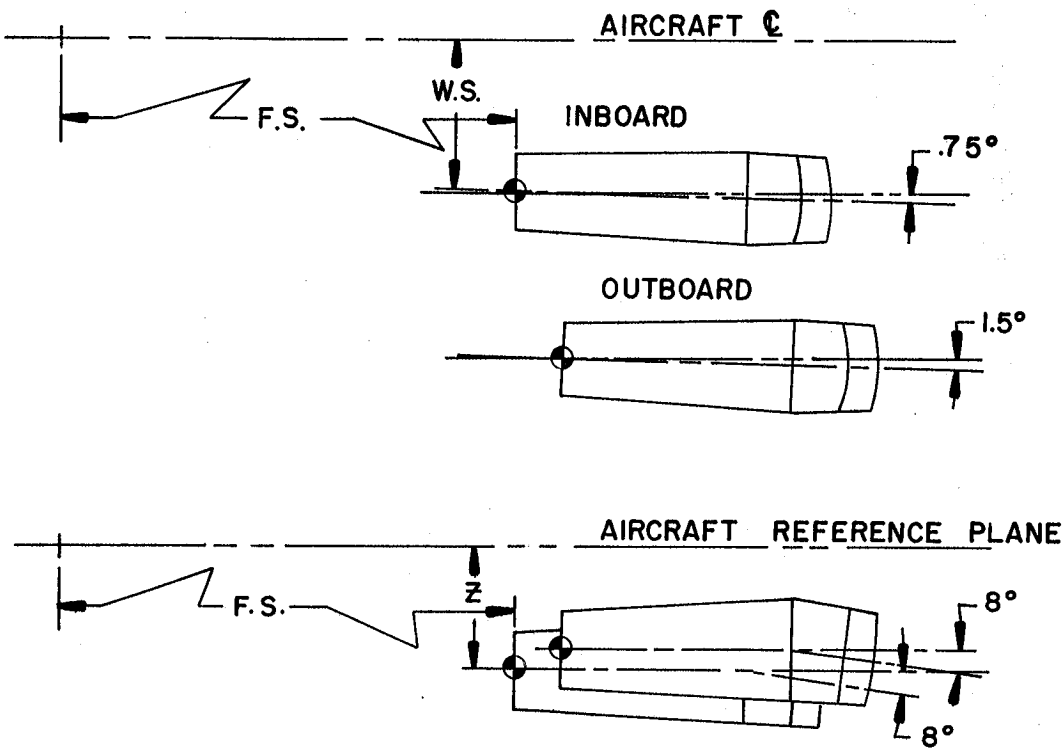


| INBOARD NACELLE | in | ft | m |
|---|---|---|---|
| FUSELAGE STATION(F.S.) | 2306.946 | 192.246 | 58.597 |
| WING STATION (W S ) | 248.929 | 20.744 | 6.323 |
| VERTICAL STATION (Z) | −216.926 | −18.077 | −5.510 |
| OUTBOARD NACELLE | | | |
| FUSELAGE STATION (F S ) | 2351.403 | 195.950 | 59.726 |
| WING STATION (W.S.) | 407.716 | 33.976 | 10.356 |
| VERTICAL STATION (Z) | −209.827 | −17.486 | −5.330 |

Figure 41.- Engine-nacelle location details.

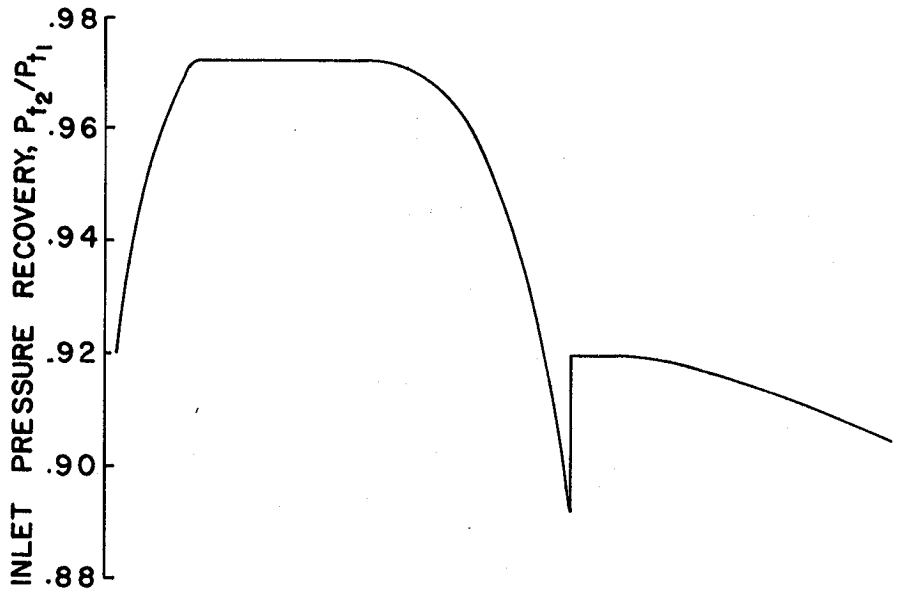


(a) "P" INLET PRESSURE RECOVERY

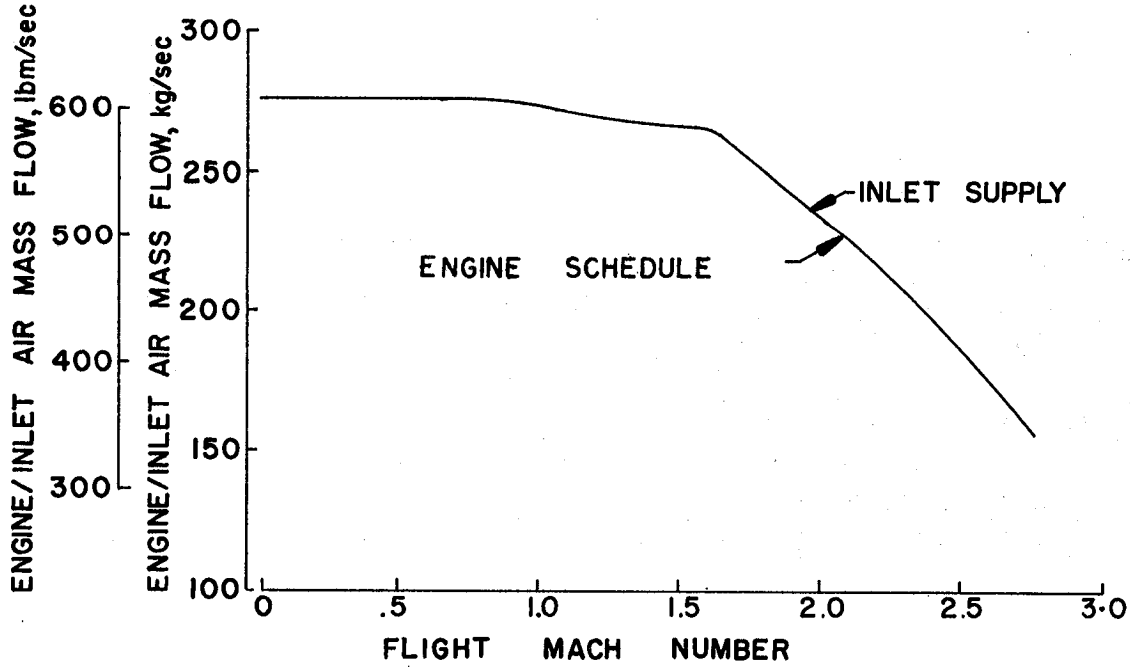


(b) AIR FLOW SCHEDULE

Figure 42.- NASA-Ames "P" inlet performance.

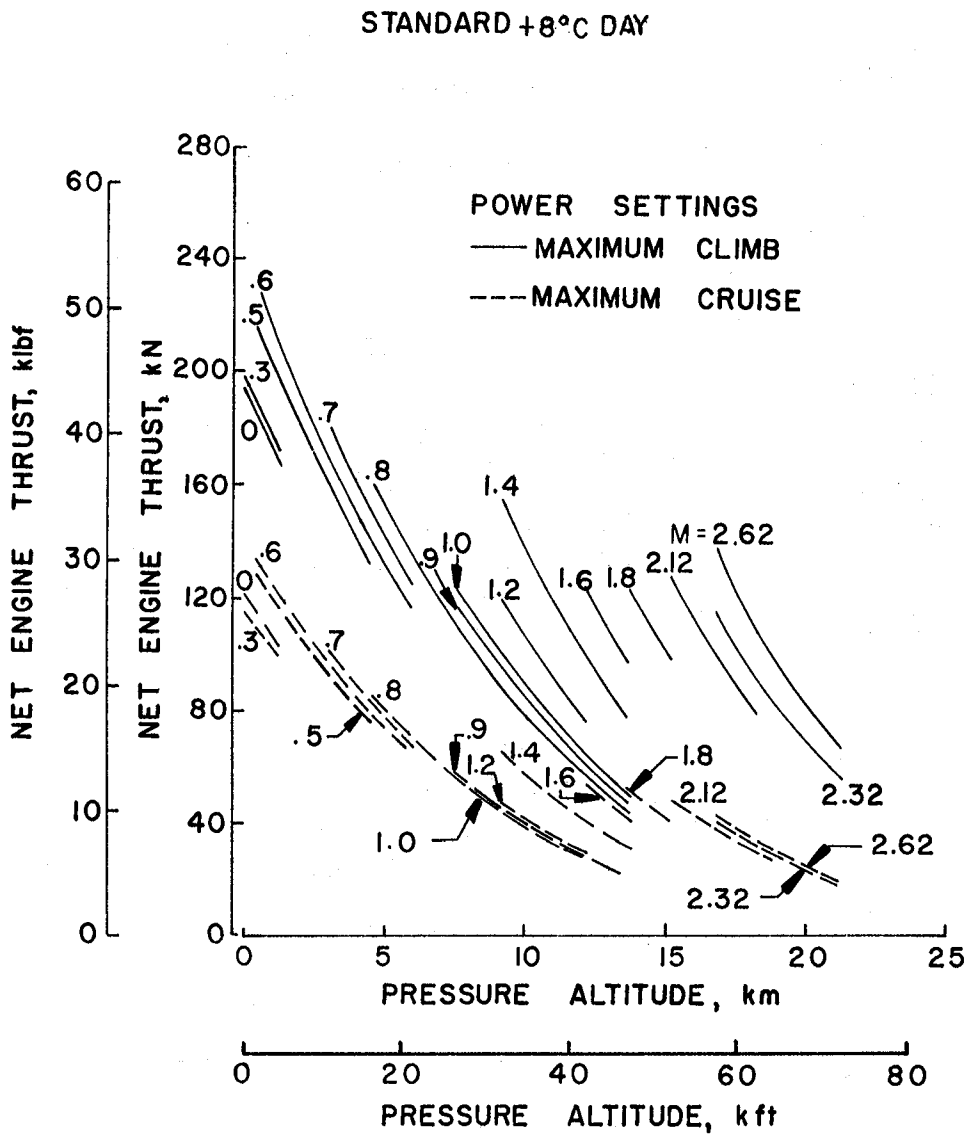


Figure 43.- Installed VSCE-516 net engine thrust.

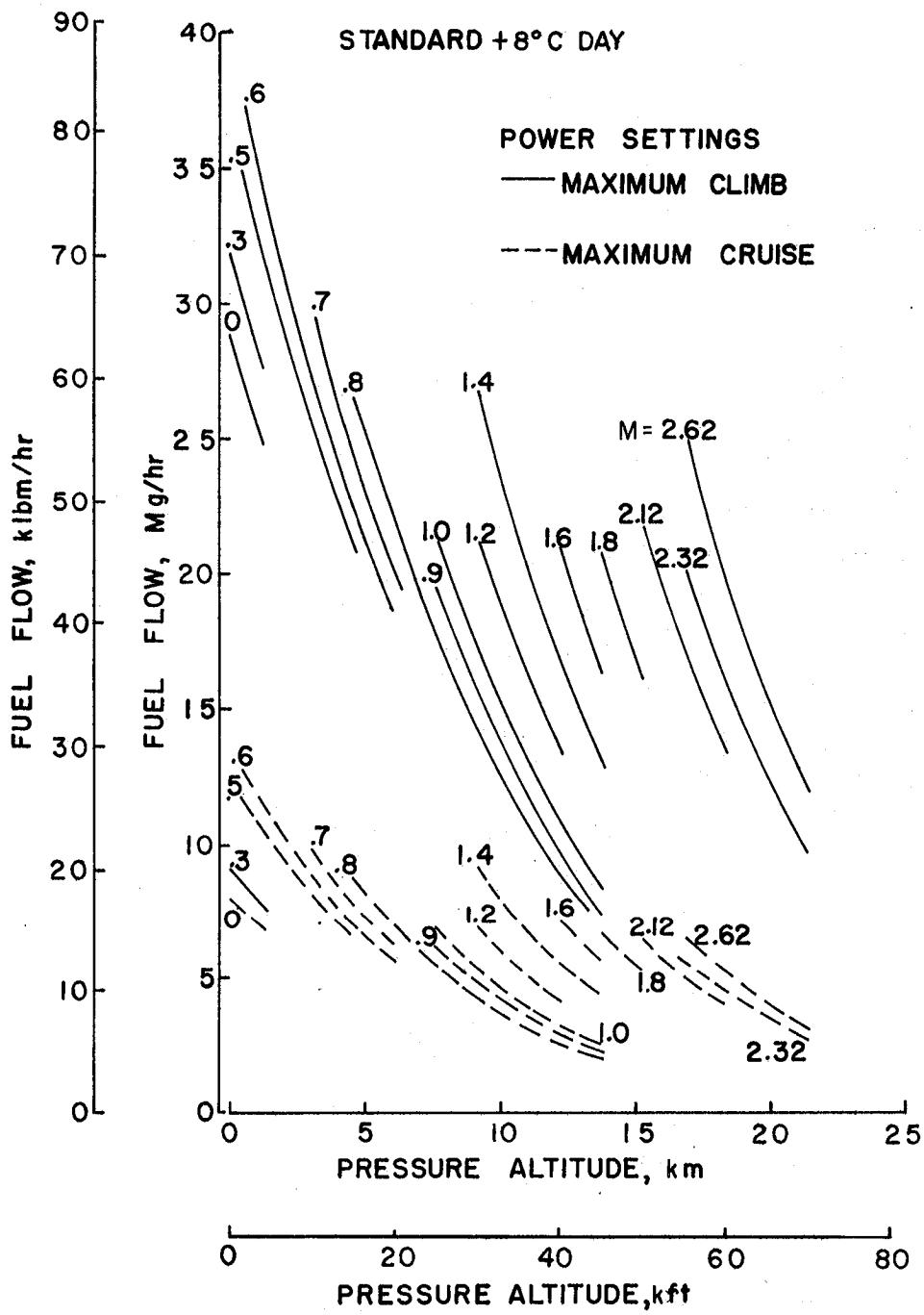


Figure 44.- Installed VSCE-516 fuel flow rate.

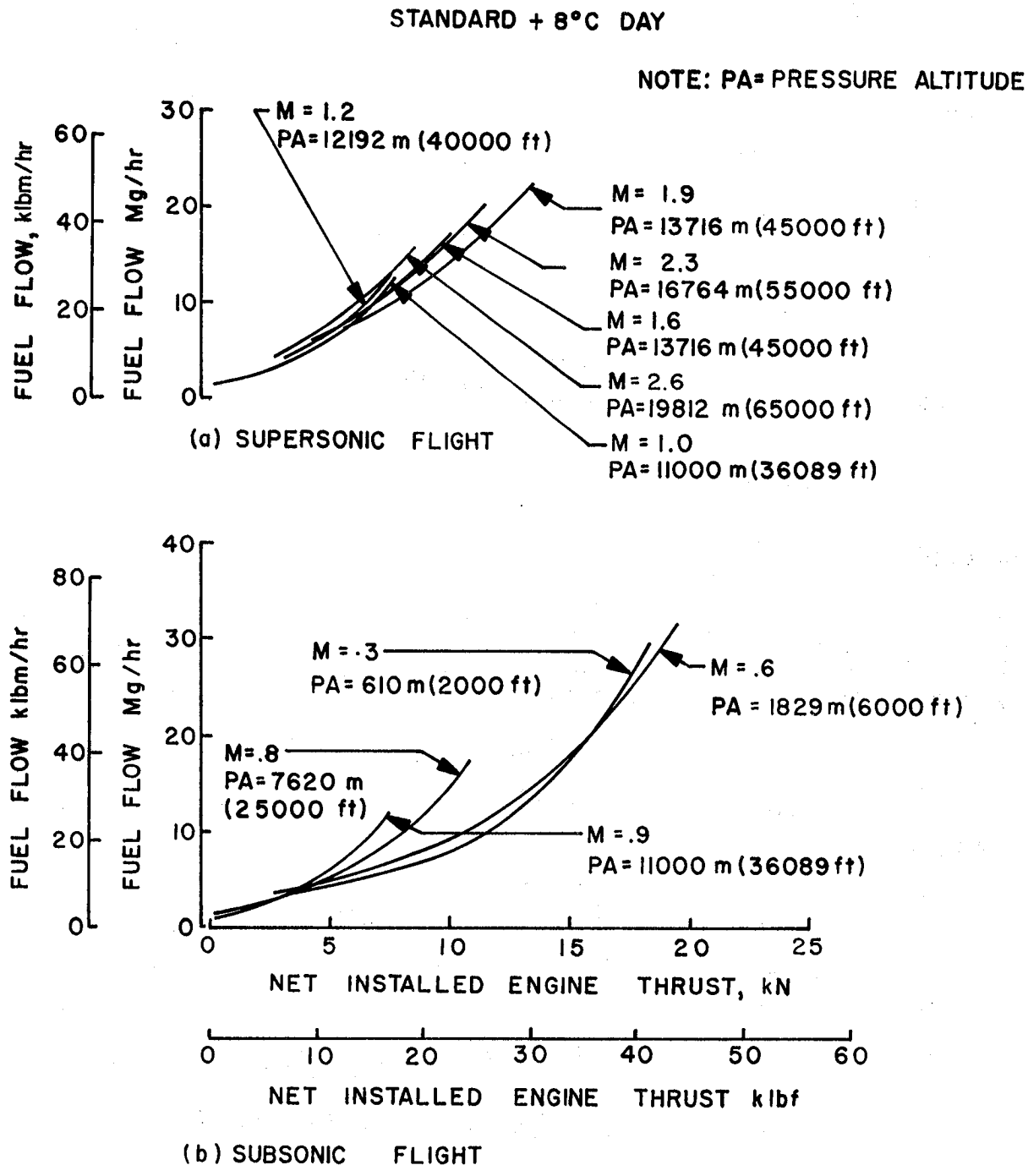


Figure 45.- Installed fuel flow for maximum and part power cruise.

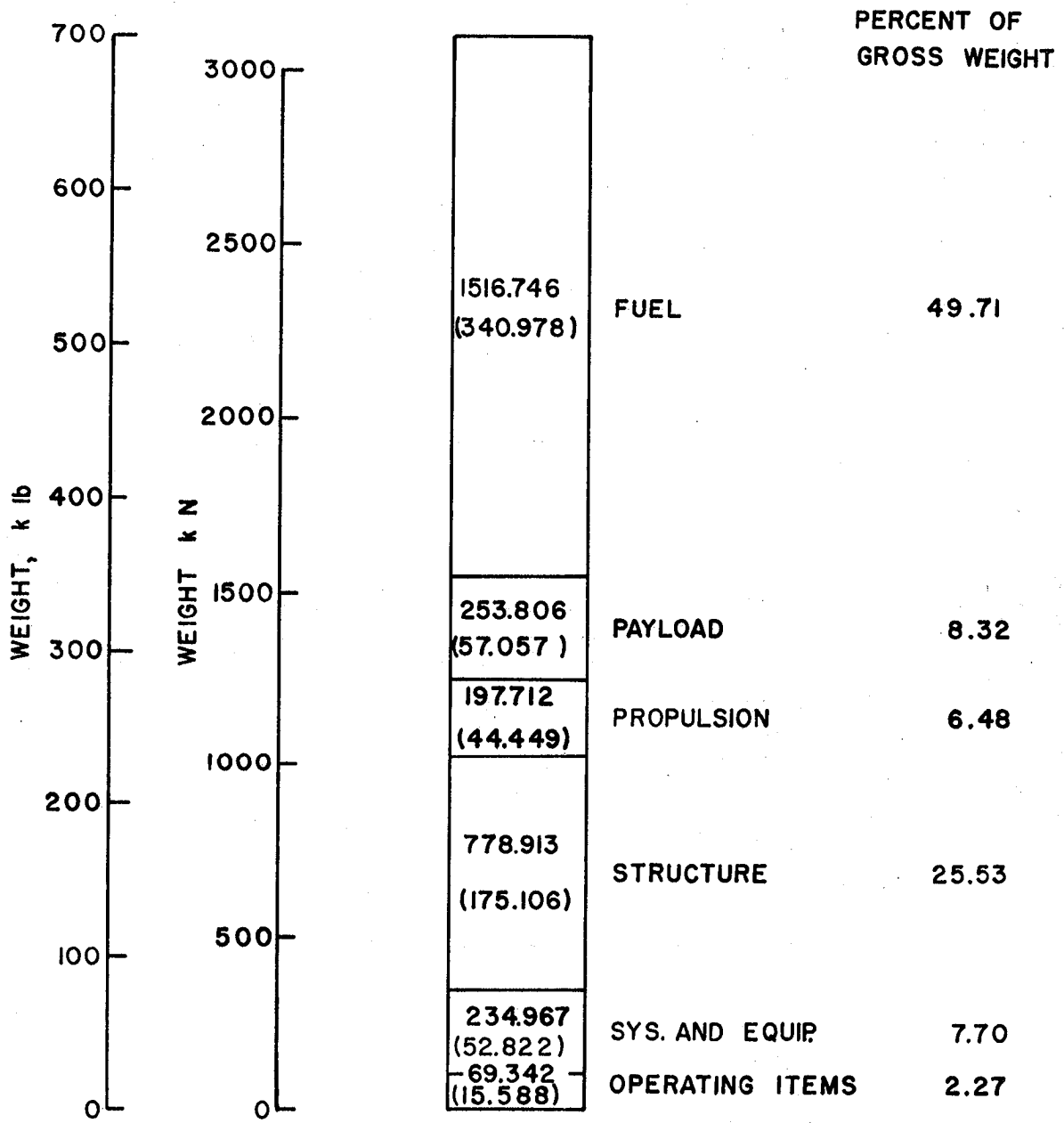


Figure 46.- Gross weight breakdown.

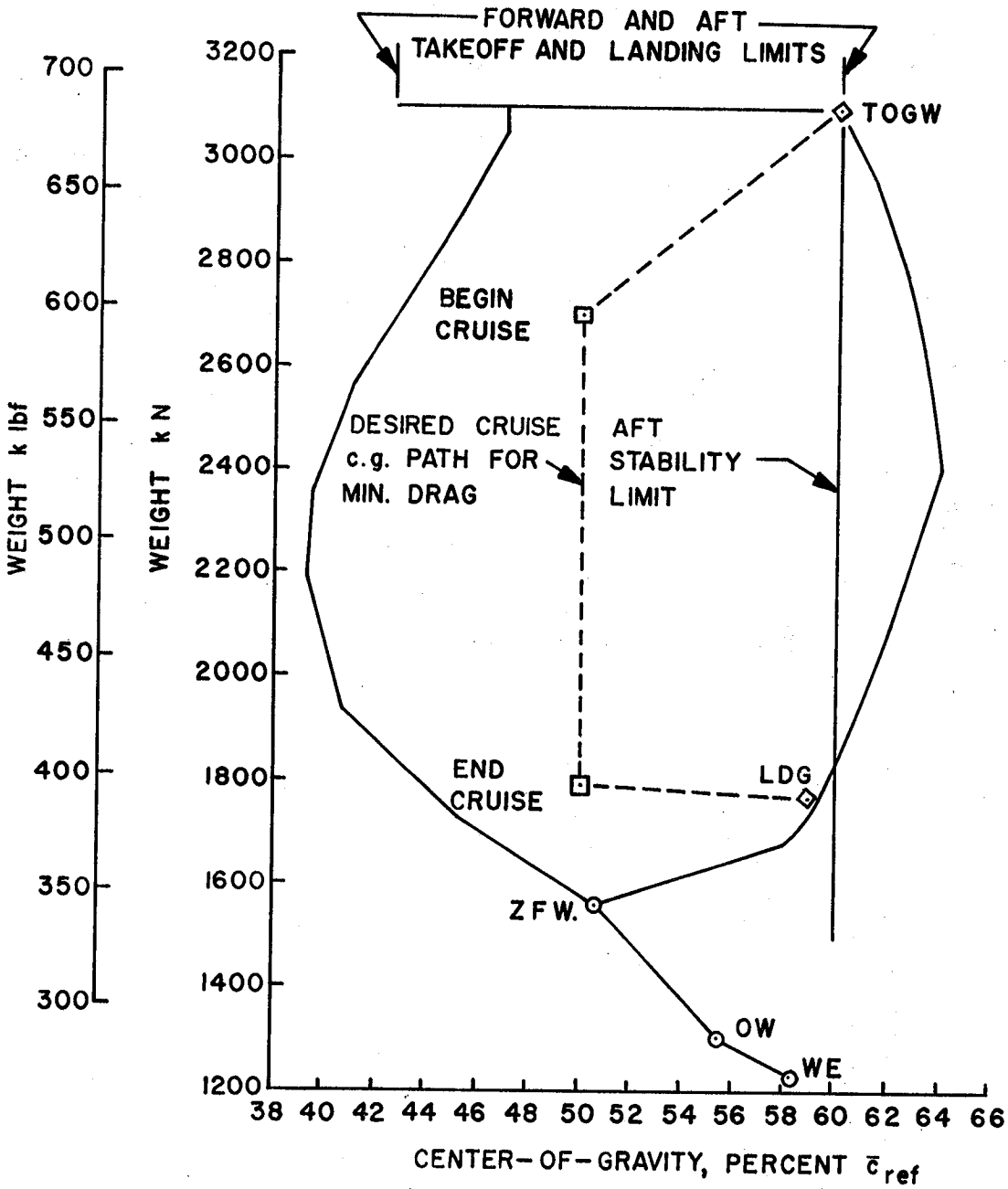


Figure 47.- Center-of-gravity travel diagram.

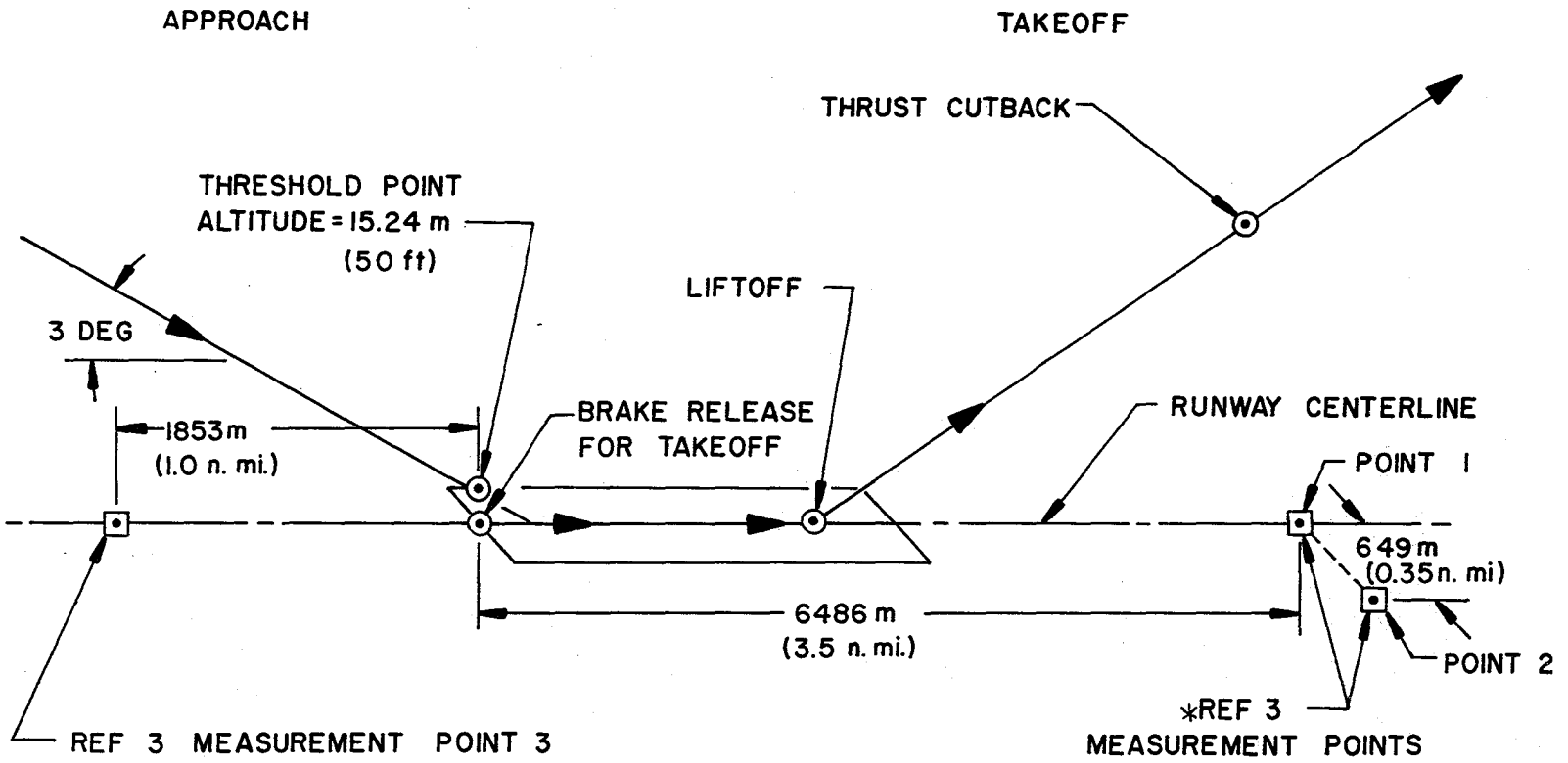


Figure 48.- Noise measurement locations for approach and takeoff.

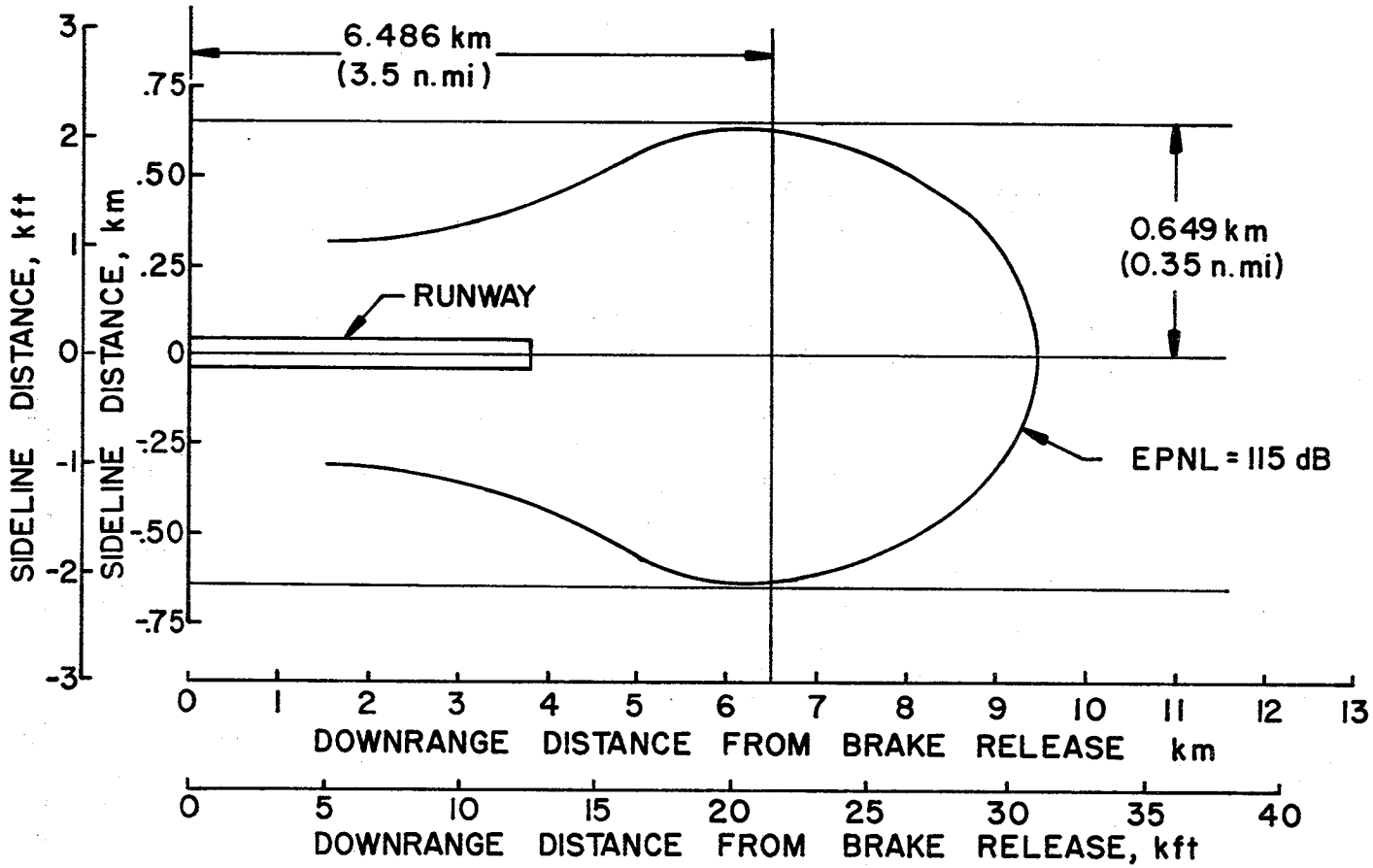


Figure 49.- Constant effective perceived noise level during takeoff without power cutback.

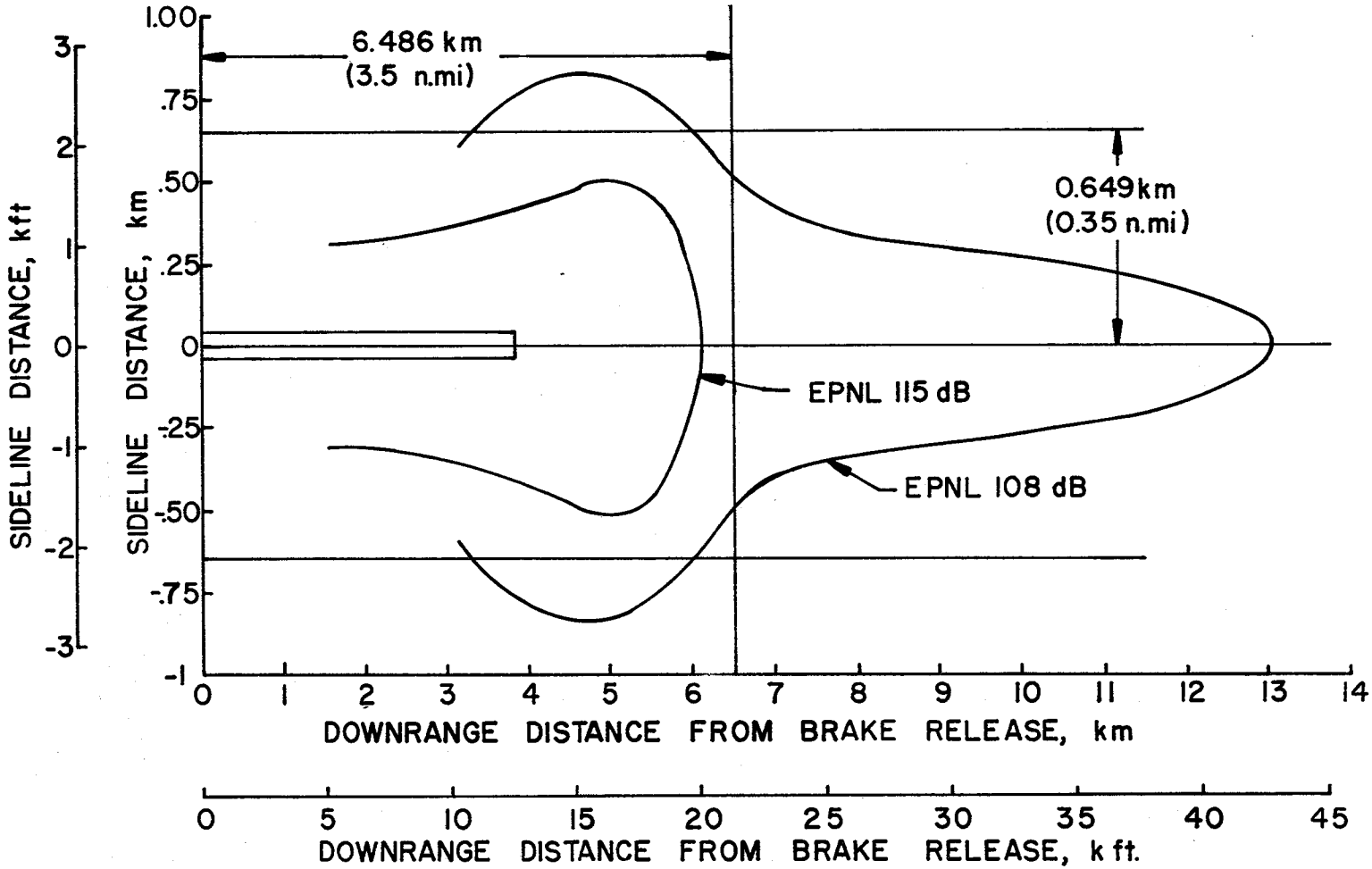


Figure 50.- Constant effective perceived noise level during takeoff with power cutback.

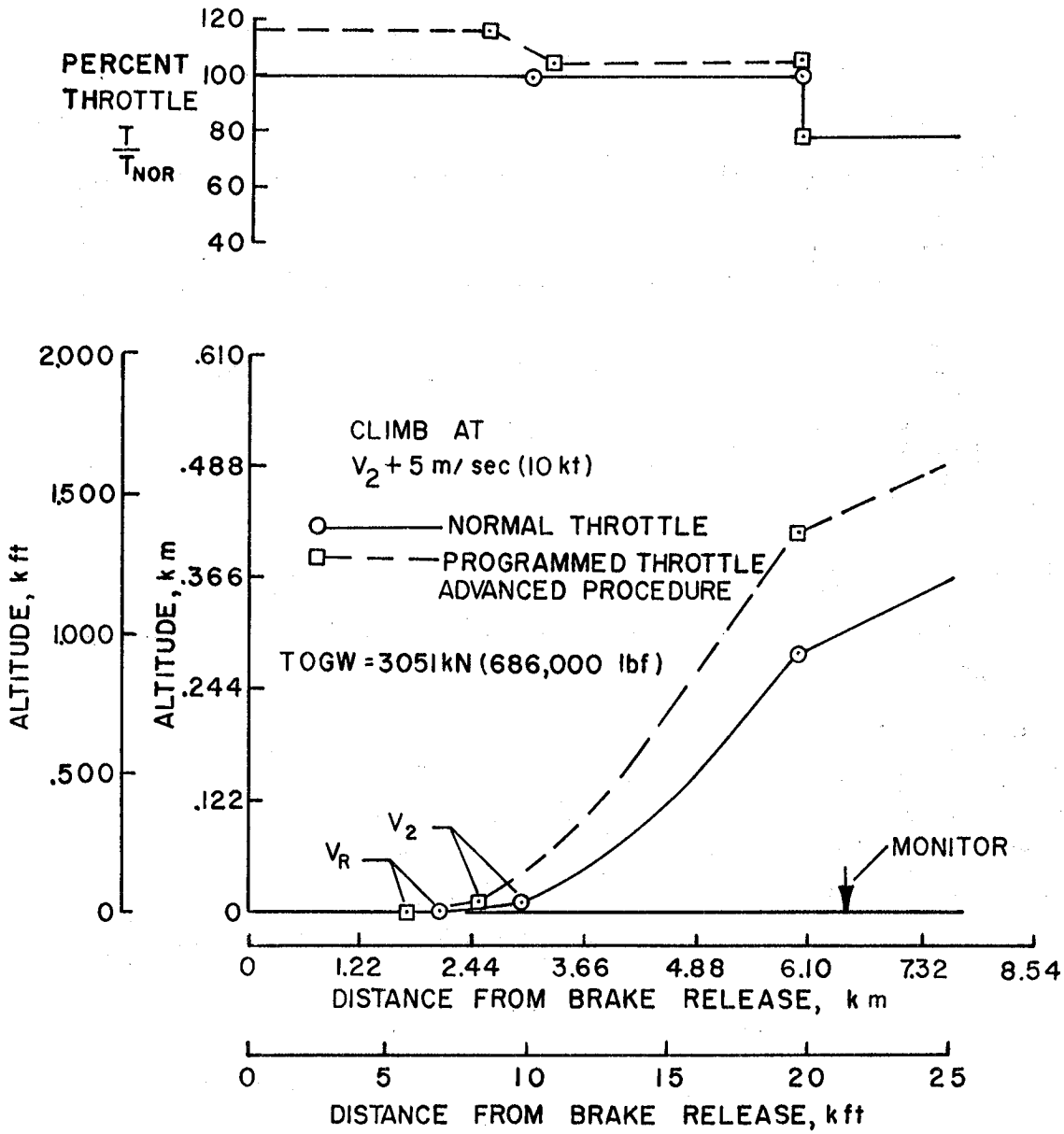


Figure 51.- Comparison of standard and advanced takeoff procedures.
$V_2$ is speed of aircraft at 10.7m (35 ft) obstacle.
For deflection of flaps see STABILITY and CONTROL.

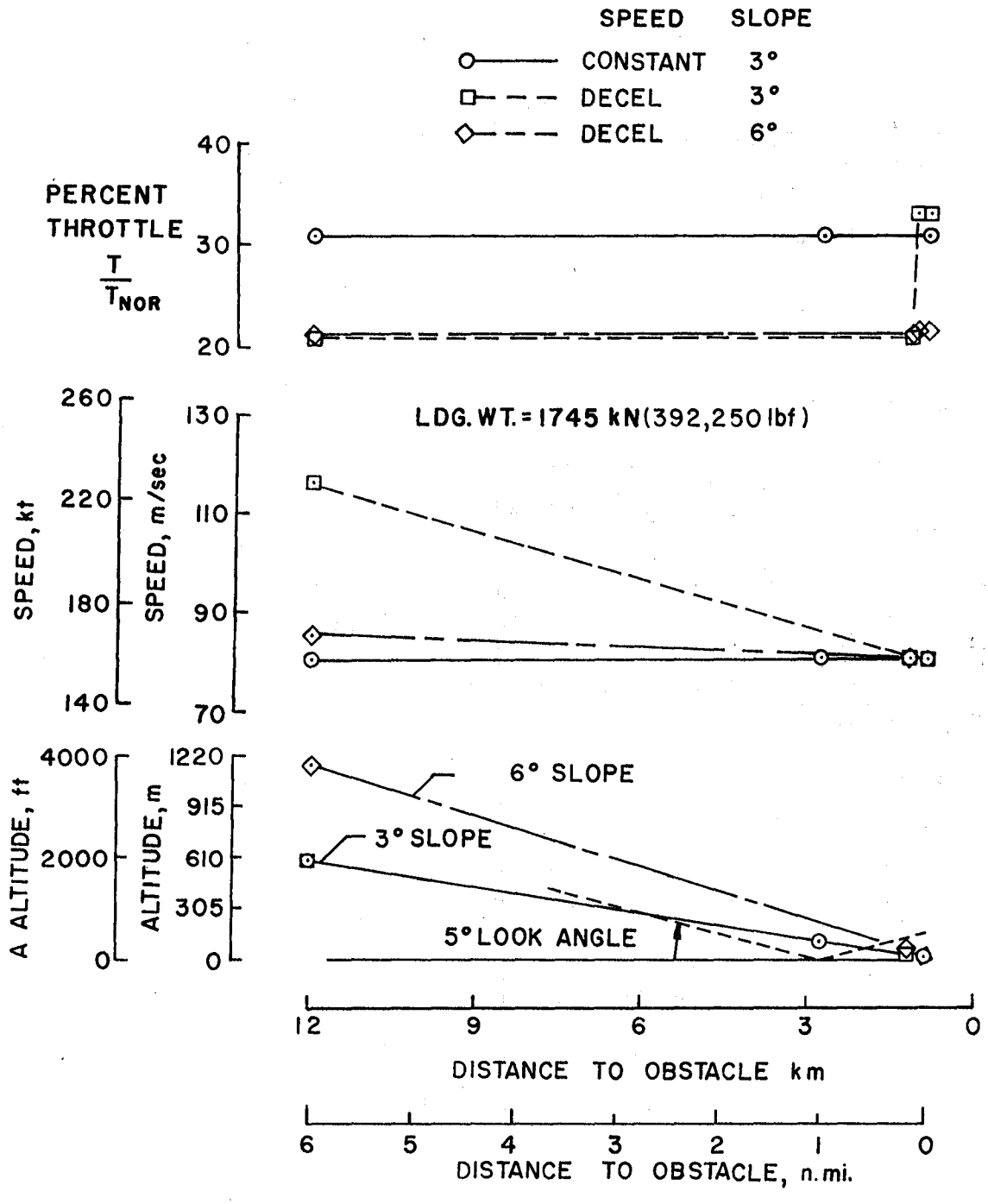


Figure 52.- Comparison of standard and advanced approach procedures. For deflection of flaps see STABILITY and CONTROL.

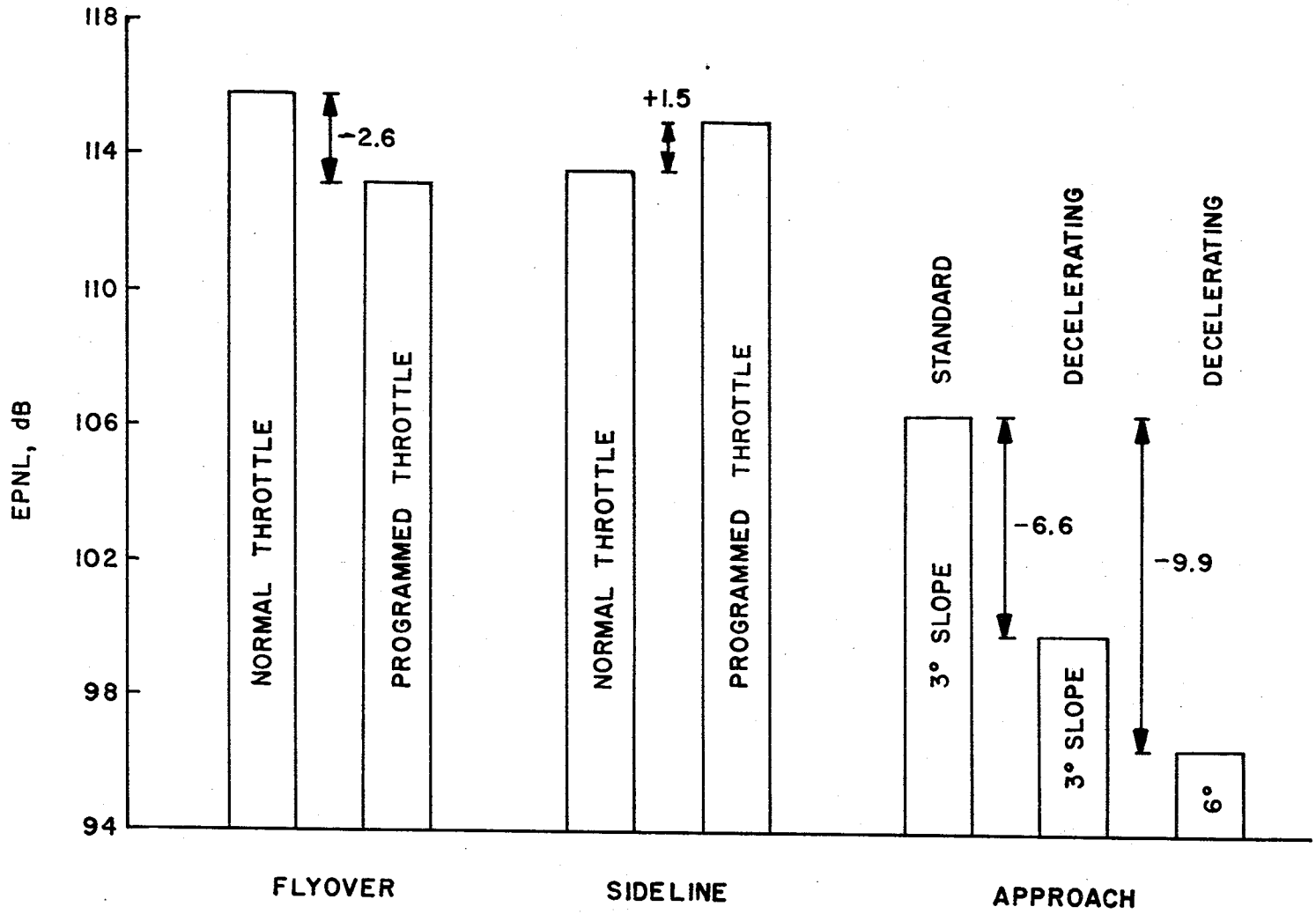


Figure 53.- Comparison of noise results (jet only) from standard and advanced procedures.

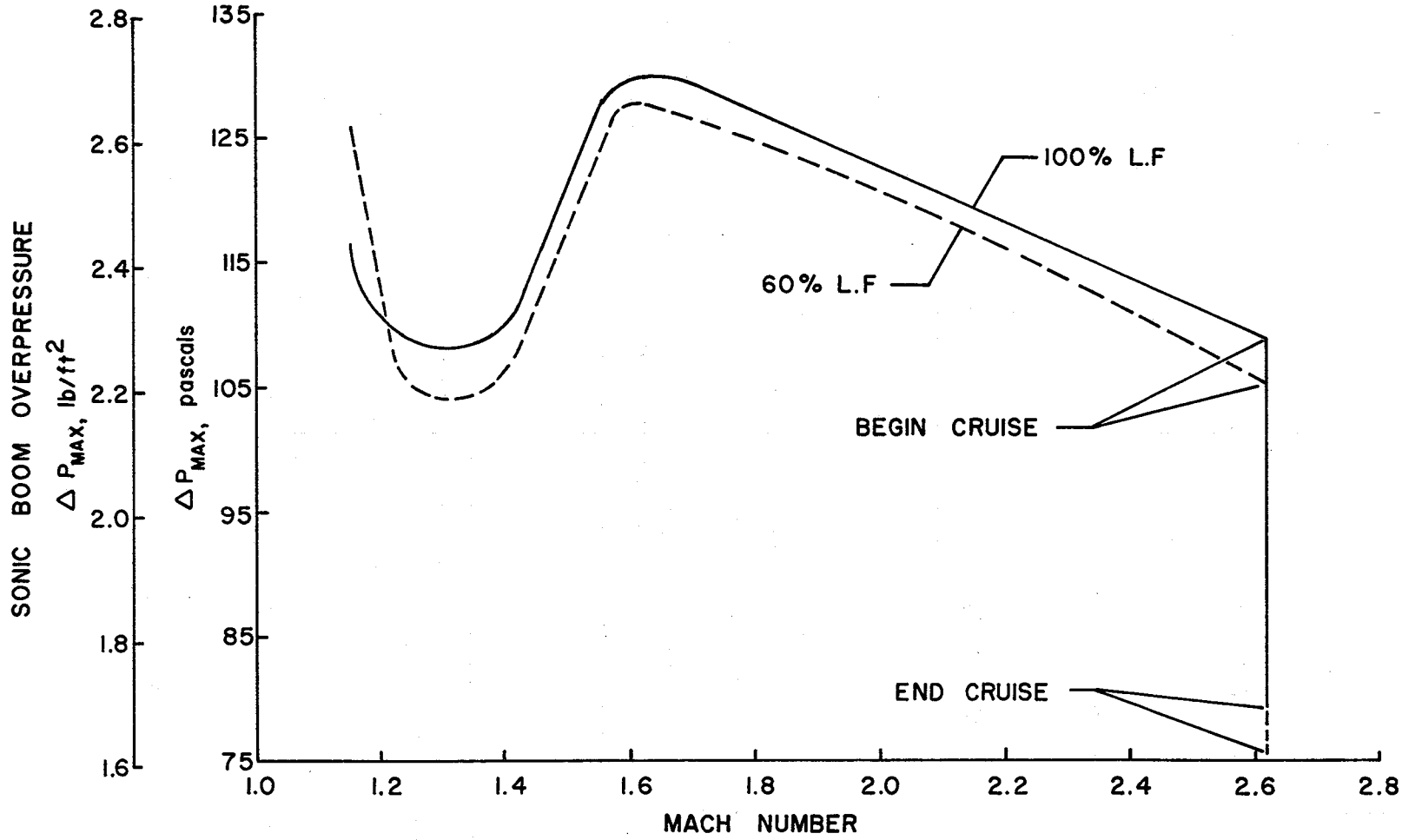


Figure 54.- Maximum over pressures during climb and cruise.

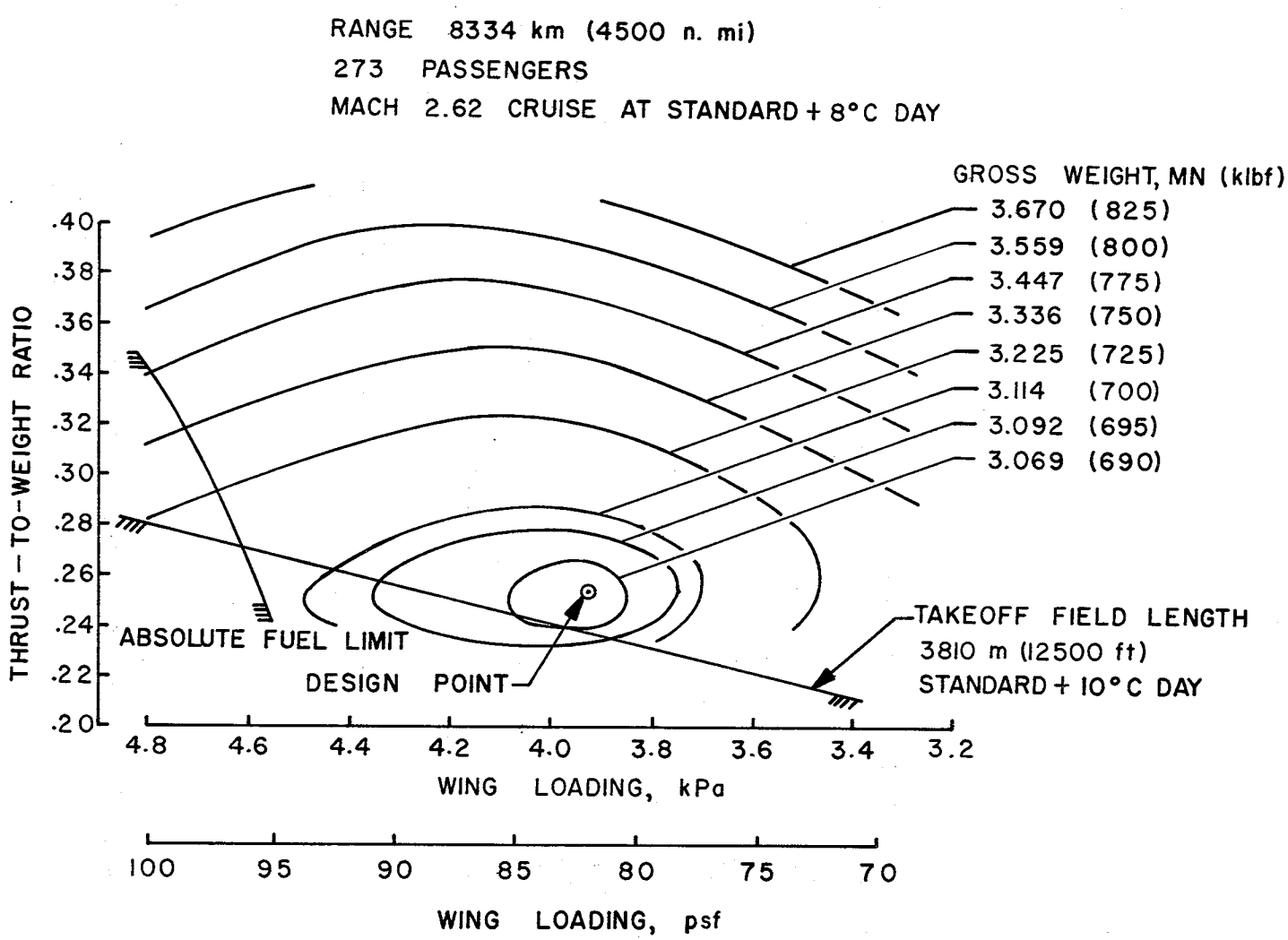


Figure 55.- Aircraft sizing "thumbprint."

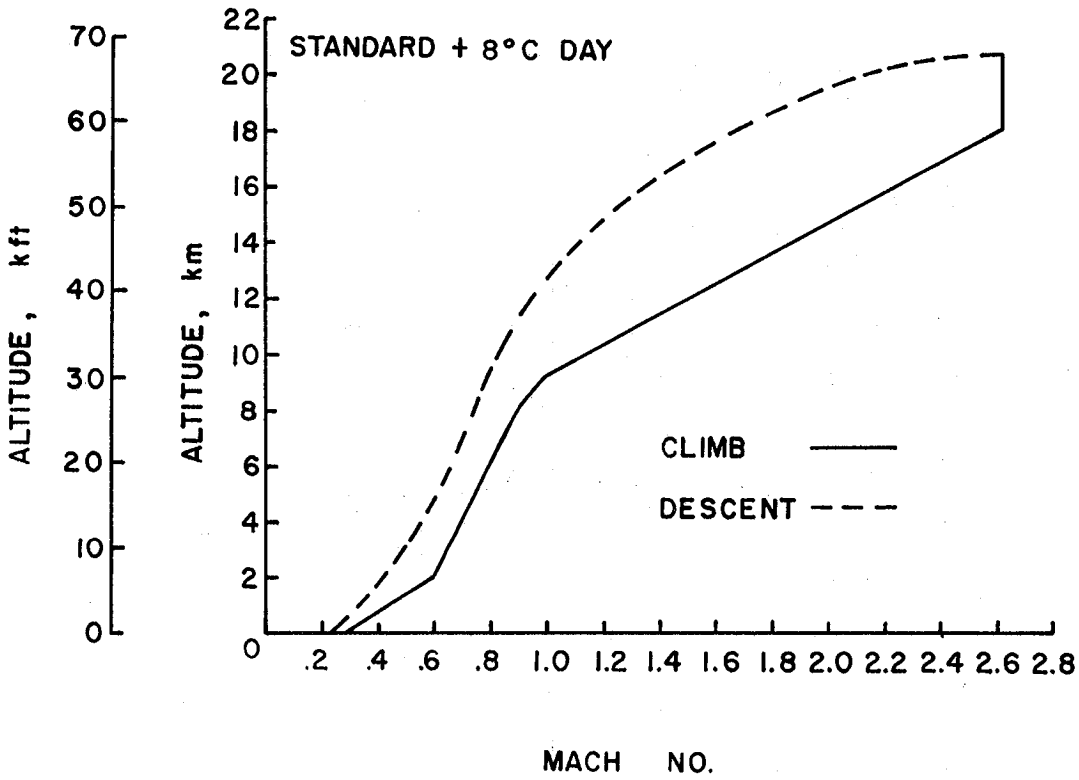


Figure 56.- Climb and descent schedule.

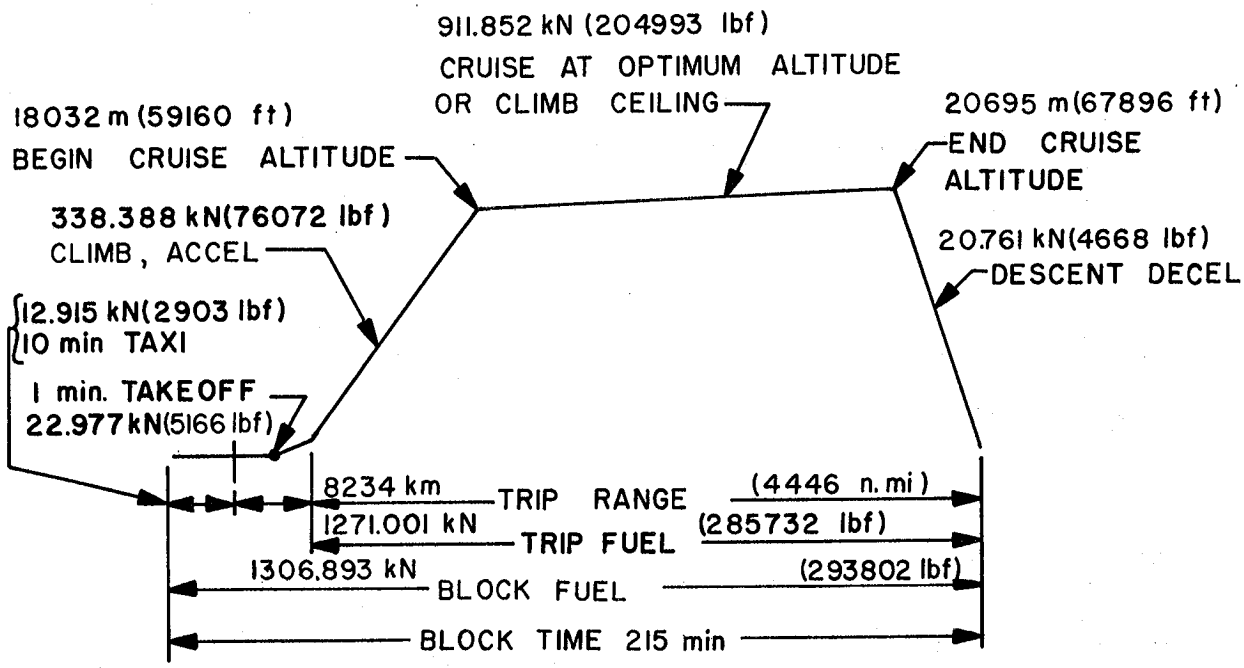


NOTE: CAB RANGE = TRIP RANGE MINUS TRAFFIC ALLOWANCE AS SPECIFIED FOR SUPERSONIC AIRCRAFT

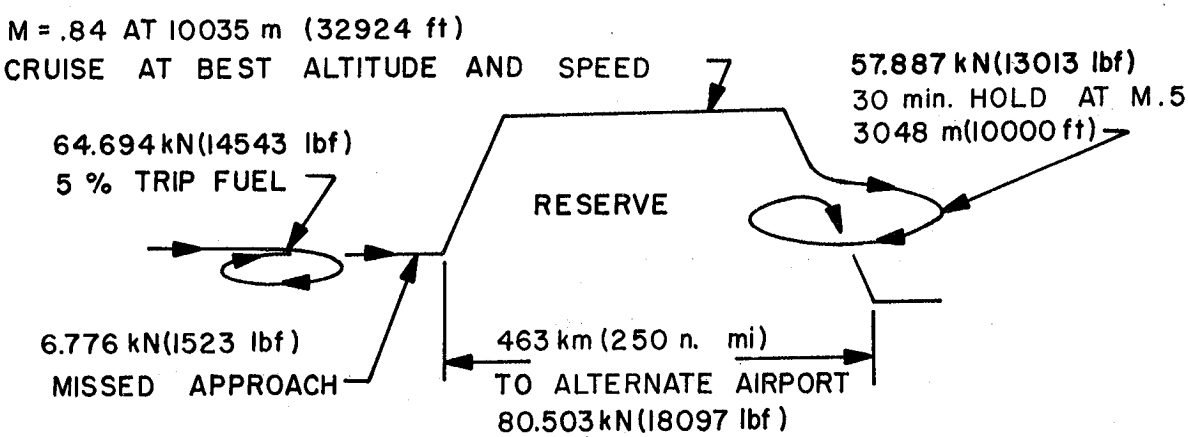


Figure 57.- Mission profile.

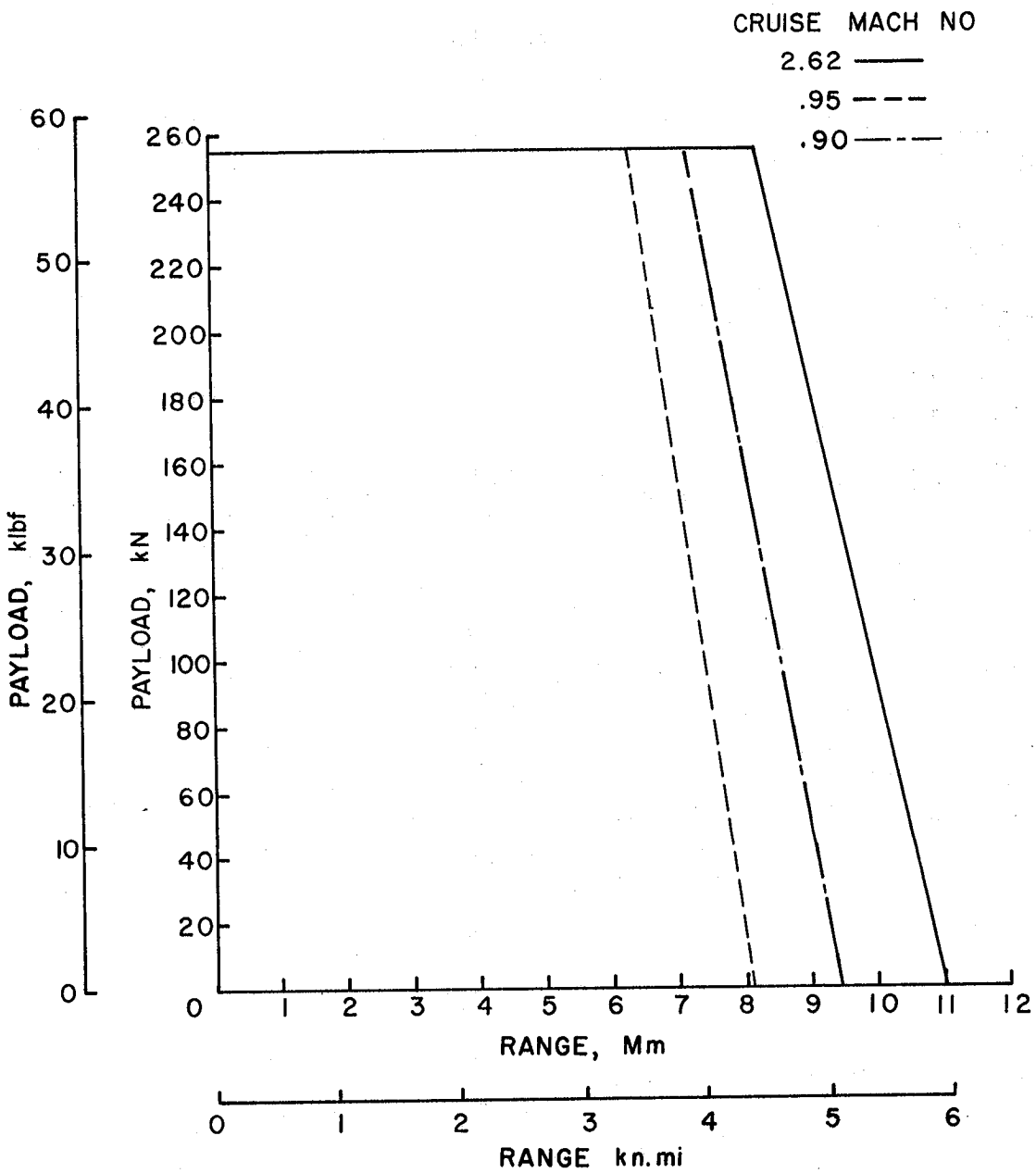


Figure 58.- Payload-range capability variation with cruise Mach number.

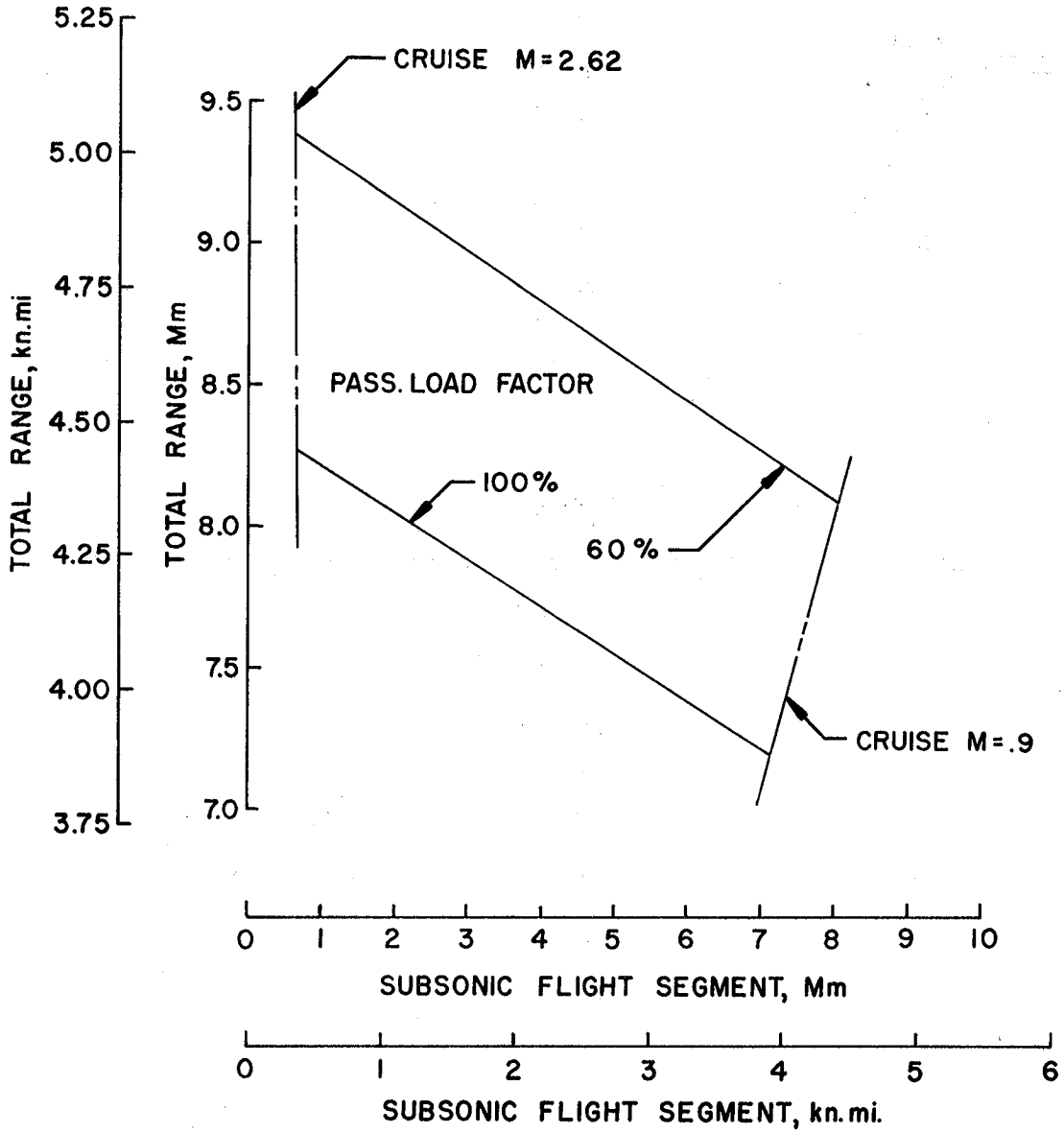


Figure 59.- Total range as a function of subsonic flight segment and passenger load factor.

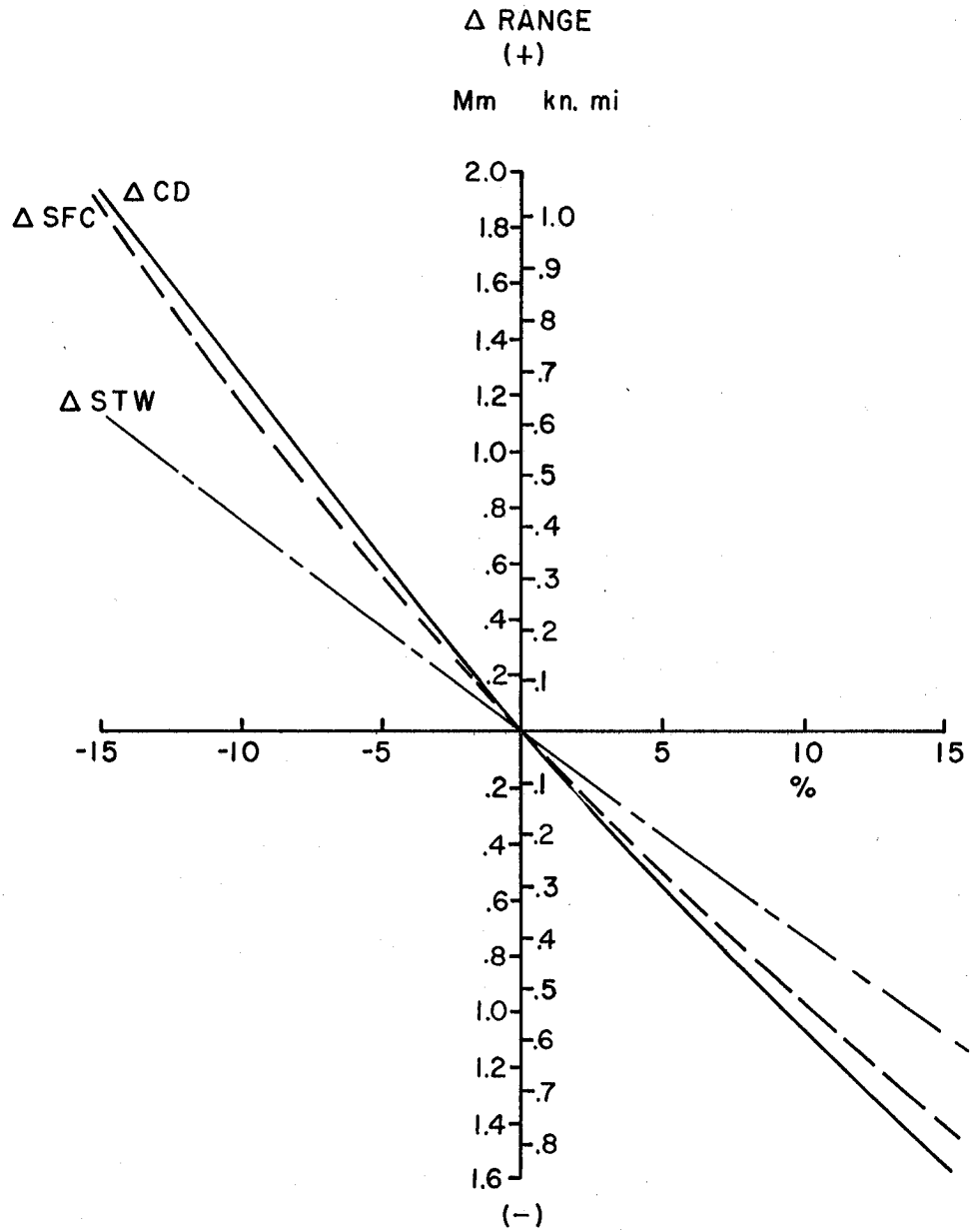


Figure 60.- Range sensitivity to changes in drag, structural weight and specific fuel consumption.

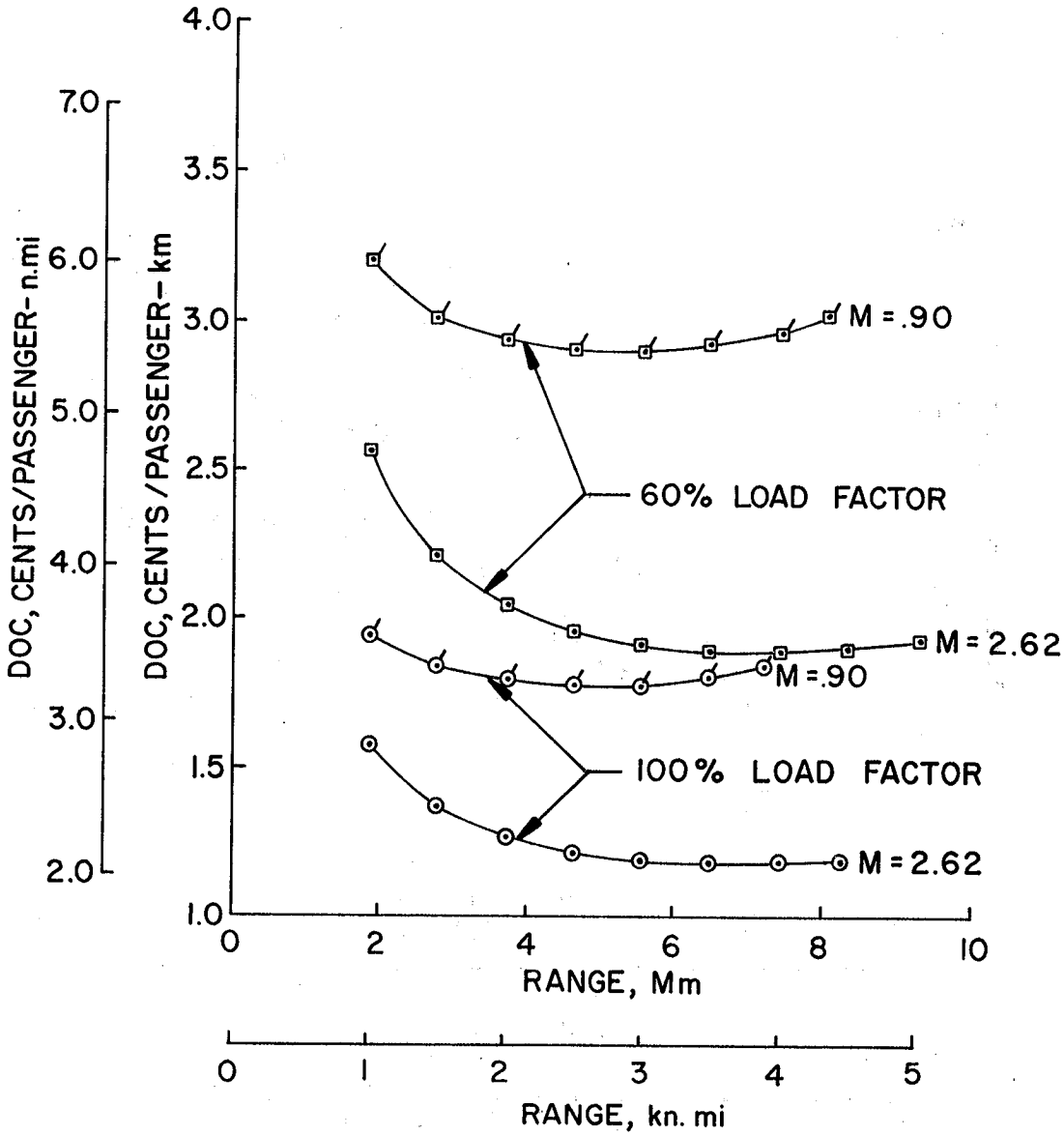


Figure 61.- Effect of passenger load factor and cruise speed on direct operating cost (DOC).

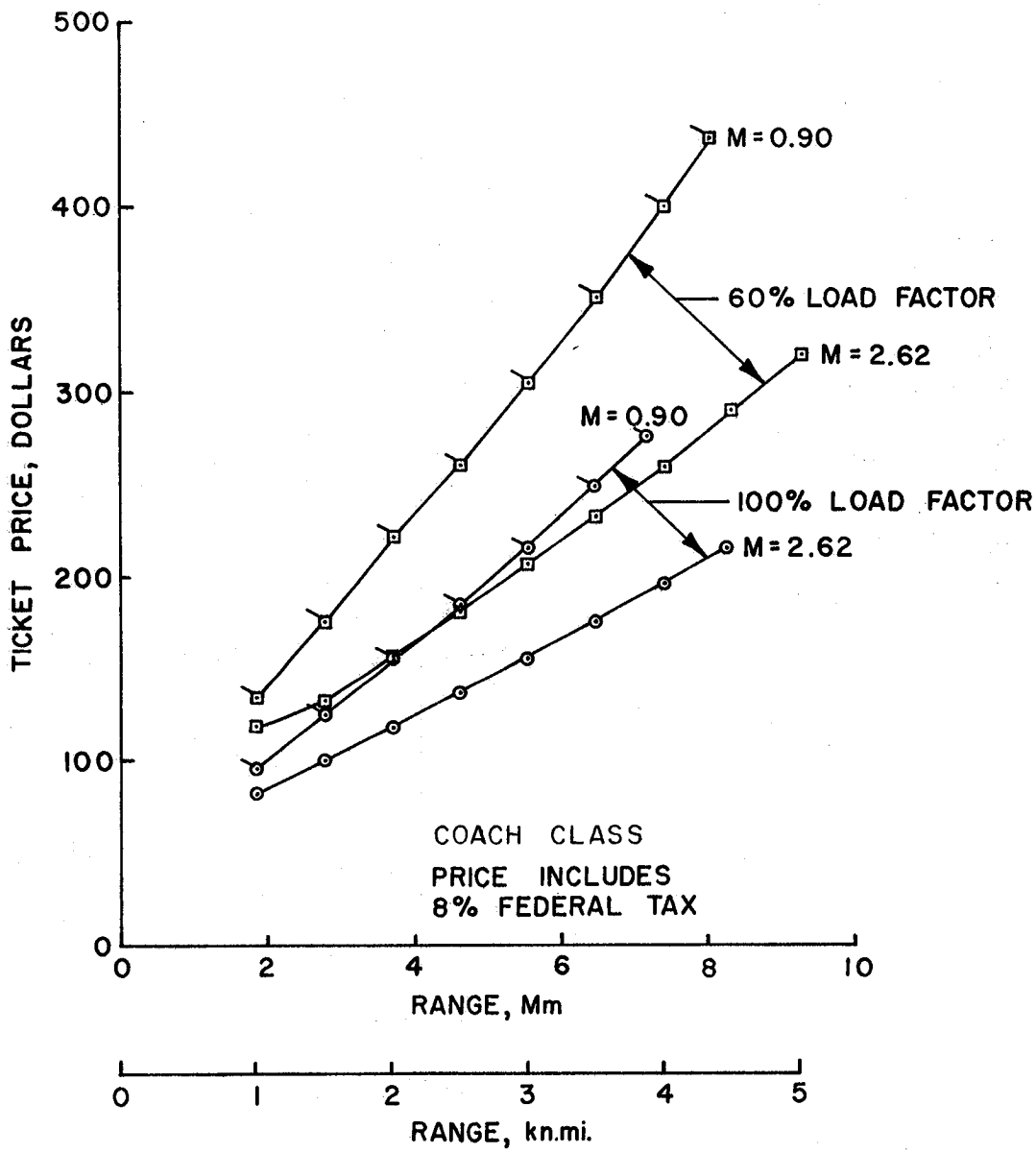


Figure 62.- Ticket price sensitivity to passenger load factor and cruise speed.

| 1. Report No. | 2. Government Accession No. | 3. Recipient's Catalog No. |
|---|---|---|
| TM 78818 | | |

| 4. Title and Subtitle | 5. Report Date |
|---|---|
| Characteristics of the Advanced Supersonic Technology AST-105-1 Configured for Transpacific Range With Pratt and Whitney Aircraft Variable Stream Control Engines | March 1979 |
| | 6. Performing Organization Code |
| 7. Author(s) | 8. Performing Organization Report No. |
| Hal T. Baber, Jr. | |
| 9. Performing Organization Name and Address | 10. Work Unit No. |
| NASA Langley Research Center<br>Hampton, Virginia 23665 | 517-53-43-01 |
| | 11. Contract or Grant No. |
| | 13. Type of Report and Period Covered |
| 12. Sponsoring Agency Name and Address | Technical Memorandum |
| National Aeronautics and Space Administration<br>Washington, DC 20546 | 14. Sponsoring Agency Code |

15. Supplementary Notes

Analytical support is acknowledged as follows: Configuration Development, E. E. Swanson; Low Speed Aerodynamics and Stability and Control, P. M. Smith; High Speed Aerodynamics, K. B. Walkley; Mass Characteristics and Mission Analysis, G. J. Espil; Propulsion, W. A. Lovell; Noise, J. W. Russell (all of HTC*); Aircraft Sizing and Sonic Boom, D. E. Fetterman, Jr.; Takeoff and Landing Procedures, W. E. Foss, Jr.; Propulsion, E. Boxer; Economics, M. J. Neubauer, Jr. (all of VIB**)

16. Abstract

Characteristics of an Advanced Supersonic Technology reference configuration designated AST-105-1 have been generated as part of a continuing technology development and assessment activity. This detailed systems integration study supports the Langley Research Center noise trade-off study (1978) performed for the FAA/ICAO by giving credence to systems weights and assurance that the noise study AST concept can be balanced. Current titanium structural technology is assumed. The AST-105-1 is the first of several AST's to be configured with an aircraft propulsion company engine concept; a Pratt and Whitney Aircraft duct-burning turbofan variable stream control engine (VSCE), with noise reduction potential through use of a coannular nozzle. With 273 passengers, range of the AST-105-1 for a cruise Mach number of 2.62 is essentially transpacific. Lift-to-drag ratio is slightly higher than for previous AST configurations. It is trimmable over a center-of-gravity range of 4.7m (15.5 ft). Inherent high positive effective dihedral, typical of arrow-wing configurations in high-lift approach, would limit AST-105-1 to operating in crosswinds of 11.6 m/sec (22.4 kt), or less, with 75 percent of available lateral control. Normal power takeoff with cutback results in noise in excess of Federal Aviation Regulation Part 36 but less than for conventional procedure takeoff. Results from preliminary studies of advanced (noncertificated) programmed throttle takeoff and approach procedures, not yet optimized, indicate that such can be an important additional method of noise reduction.

| 17. Key Words (Suggested by Author(s)) | 18. Distribution Statement |
|---|---|
| Aerodynamics; Aircraft Design, Testing, and Performance; Aircraft Propulsion and Power; Aircraft Stability and Control; Advanced Supersonic Transport; Aircraft Noise; Sonic Boom | UNCLASSIFIED - UNLIMITED<br>STAR CATEGORY 01 |

*Kentron International, Hampton Technical Center
**Langley Research Center, Vehicle Integration Branch

| 19. Security Classif. (of this report) | 20. Security Classif. (of this page) | 21. No. of Pages | 22. Price* |
|---|---|---|---|
| Unclassified | Unclassified | 134 | $7.25 |

* For sale by the National Technical Information Service, Springfield, Virginia 22161